

# **Fabrication and characterization of polymer optical fibers for photonic device applications**



**M Sheeba**

**International School of Photonics  
Cochin University of Science and Technology  
Cochin-682022, India**

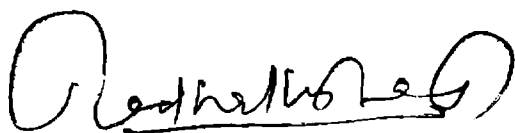
**PhD Thesis submitted to Cochin University of Science and  
Technology in partial fulfillment of the requirements for the  
award of the Degree of Doctor of Philosophy**

**May 2008**

*Dedicated  
To my  
Eleppan, loving parents and brother*

## CERTIFICATE

Certified that the research work presented in the thesis entitled *“Fabrication and characterization of polymer optical fibers for photonic device applications”* is based on the original work done by Mrs. M Sheeba under my guidance and supervision at the International School of Photonics, Cochin University of Science and Technology, Cochin – 22, India and has not been included in any other thesis submitted previously for the award of any degree.



Dr. P Radhakrishnan

(Supervising Guide)

Cochin 682 022

22 May, 2008

## DECLARATION

Certified that the work presented in the thesis entitled ***“Fabrication and characterization of polymer optical fibers for photonic device applications”*** is based on the original work done by me under the guidance and supervision of Dr. P.Radhakrishnan, Professor, International School of Photonics, Cochin University of Science and Technology, Cochin – 22, India and has not been included in any other thesis submitted previously for the award of any degree.

Cochin 682 022

22 May, 2008



M Sheeba

न चोरहार्यं न च राजहार्यं न  
भ्रातृभ्राज्यं न च भारकारि।  
व्यये कृते वर्धत एव नित्यं  
विद्याधनं सर्वधनप्रधानम्॥

## **Preface**

Optical fiber-based communication networks have been the enabling factor in the shift of modern information technology from the electronics regime to the photonics regime. Even though silica glass fibers have been the enabling factor for the current advancement of information technology, the plastic optical fibers (POFs) are of great commercial interest because they can maintain flexibility at thicker fiber sizes making them more easy to handle and install when the communication systems make their way from the local loop (premise networks, local area networks) closer towards, and into, the home.

Implementation of optical communication in the visible region demands the development of suitable optical amplifiers and lasers working in this region. POF doped with dyes or rare earth elements are potential candidates for this purpose. Laser dyes, which act as highly efficient media for lasing and amplification have a wide range of tunability in the visible region. The range of tunability of laser dyes like rhodamine B and rhodamine 6G usually comes between 570nm to 640nm. The advantage of incorporating laser dyes in solid matrices such as POF is that it is easier and safer to handle them than when they are in liquid form.

Compact, lightweight and inexpensive lasers operating in the short wavelength visible region are desired for use in such diverse applications

as medical diagnostics, surgery, high-capacity optical storage and high-resolution scanning and printing. Methods of generating these shorter wavelengths include optical harmonic generation and sum frequency mixing techniques that require phase matching in expensive inorganic crystals. An excellent alternative to generate these shorter wavelengths is the frequency upconversion by two-photon absorption of IR photons. Upconversion lasers based on dye doped polymer fiber and dye doped polymer waveguide is an important area of research and has become more interesting and promising in recent years.

Although the main application of optical fibers are in the field of telecommunication, optical fiber based sensors of various designs are becoming valuable devices for wide industrial applications. The advantages of optical fiber-based sensors include high sensitivity, insensitivity to electromagnetic radiation; spark free, light weight and minimal intrusiveness due to their relatively small size and deployment in harsh and hostile environments. It has been proved that POF based sensors can be employed to detect a great variety of parameters including temperature, humidity, pressure, refractive index etc.

The proposed thesis presented in six chapters deals with the work carried on dye doped and undoped POF for photonic device applications such as amplifier, laser and sensor.

**Chapter 1:** First chapter discusses the emergence of polymer fiber optics as an interesting area with its profound application in short distance optical communication such as LAN, DTH, automotive communication and in both industrial and domestic lighting. An overview of the different POF based photonic devices and their applications with emphasis on the development of dye doped POF based amplifiers, lasers and sensors are given. Energy transfer process in dye mixture doped polymer matrix is discussed in the context of its application in extending the tunability of the operating region of fiber amplifiers and lasers. Two photon processes in dye doped POF system and its application for the development of upconversion lasers is also covered in this chapter. Recent trends in POF based systems such as microstructured POF lasers, POF Bragg gratings, etc are also discussed.

**Chapter 2:** First section of this chapter deals with the fabrication of rhodamine 6G and rhodamine B dye mixture doped polymer preforms by bulk polymerisation method, drawing of dye doped POFs using the fiber drawing station developed in our laboratory and the characterisations of the developed fibers such as absorption, fluorescence emission, uniformity in dye concentration etc. Second section covers the development of dye doped POF as an optical amplifier which can be operated in the visible region along with the necessary theoretical background. Performance of single dye doped POF amplifier is compared with dye mixture doped amplifier. Background theory of radiative and non radiative energy



transfer processes in dye mixture system is also discussed. Tunable operation of the amplifier over a broad wavelength region is achieved by mixing different ratios of the dyes. The dye doped POF amplifier (POFA) is pumped axially using 532 nm, 8 ns laser pulses from a frequency doubled Q-switched Nd: YAG laser and the signals are taken from a tunable optical parametric oscillator (OPO). A maximum gain of 22.3dB at 617nm wavelength has been obtained for a 7 cm long dye mixture doped POFA. The effects of pump power, signal power, concentration of dye molecules and length of the fiber on the performance of the fiber amplifier are also studied.

**Chapter 3:** Observation of multimode laser emission from a dye mixture doped POF excited by 532 nm pulsed laser beam from an Nd: YAG laser is considered in this chapter. Tuning of laser emission is achieved by using mixture of dyes utilizing the energy transfer occurring from donor (rhodamine 6G) molecule to acceptor molecule (rhodamine B). As the energy of the pump beam is increased, fluorescence spectrum gets narrowed due to amplified spontaneous emission and at a threshold energy, laser emission with a multimode structure emerges. Serially connected microcavity resonator based model is discussed to explain the multimode laser emission from the POF. The effects of parameters like diameter and length of the POF and the pump power on the multimode laser emission structure are studied.

**Chapter 4:** Two photon excited side illumination fluorescence (SIF) studies in Rh 6G-RhB dye mixture doped POF and the effect of energy transfer on the attenuation coefficient are reported in this chapter. The dye doped POF is pumped sideways using 800nm, 80 femto second laser pulses from a Ti: Sapphire laser and the two photon excited fluorescence emission is collected from the end of the fiber for different propagation distances. One photon and two photon excited fluorescence spectra are compared and the basic theory of two photon absorption is also covered. Two photon excited fluorescence signal is used to characterise the optical attenuation coefficient in dye doped POF. The variation in the attenuation coefficient for different propagation distances and for different wavelengths are examined based on the energy transfer process in the dye doped POF.

**Chapter 5:** Sensitive and versatile side polished polymer optical fiber based refractive index sensor developed for the detection of trace amounts of adulterants in coconut oil sample, which is one of the most commonly used edible oils in south Asia, is discussed in this chapter. The sensing head is basically a multimode side-polished polymer fiber and the adulterants used for the present study are paraffin oil and palm oil. The observed sensitivity is almost linear and the detection limit is 2 % (by volume) paraffin oil /palm oil in coconut oil. The proposed sensor is user-friendly and repeatable allowing instantaneous determination of the

presence of adulterant in a coconut oil sample without involving any chemical analysis.

Summary and conclusions of the work carried out are given in **Chapter 6**. Future prospects are also discussed in this chapter.

Some of the results have been published in standard journals and presented at various national and international conferences, the details of which are given below.

### **RESEARCH PUBLICATIONS**

#### **INTERNATIONAL JOURNAL**

1. **M Sheeba**, M Rajesh, K Geetha, C P G Vallabhan ,V P N Nampoori, P Radhakrishnan, “Fiber optic sensor for the detection of adulterant traces in coconut oil”, *Meas. Sci. Technol.* **16**, 2247–2250 (2005).
2. **M Sheeba**, K J Thomas, M Rajesh, V P N Nampoori, C P G Vallabhan, P Radhakrishnan, “Multimode laser emission from dye doped polymer optical fiber”, *Applied Optics* **46**, 8089-8094 (2007).
3. **M Sheeba**, Thomas Kannampuzha Jhony, Rajesh Mandamparambil, Nitish Kumar, Praveen Ashok Cheriyan, Nampoori P N Vadakkedathu, Radhakrishnan Padmanabhan , “Laser emission from dye mixture doped polymer optical fiber”, *SPIE –Proceedings, Photonic Fiber and Crystal Devices*, 6698 (2007).
4. **M Sheeba**, M Rajesh, S Mathew, V P N Nampoori, C P G Vallabhan and P Radhakrishnan, “Fluorescence emission characteristics from a dye

- doped POF under two photon excitation”, *Applied Optics* **47**,1913-1921(2008).
5. **M Sheeba**, M Rajesh, V P N Nampoore and P Radhakrishnan, “Fabrication and characterisation of dye mixture doped POF as a broad wavelength light amplifier”, *Applied Optics* **47**, 1907-1912 (2008).
  6. M Rajesh, K Geetha, **M Sheeba**, P Radhakrishnan P G Vallabhan & V P N Nampoore, “A fiber optic smart sensor for studying the setting characteristics of various grades of cement”, *Optics and Lasers in Engineering* **44**, 486-493 (2006).
  7. M Rajesh, K Geetha, **M Sheeba**, P Radhakrishnan P G Vallabhan & V P N Nampoore, “Characterization of Rhodamine 6G doped polymer optical fiber by side illumination fluorescence”, *Optical Engineering* **45**, 075003-075007 (2006.)
  8. M Rajesh, **M Sheeba**, K Geetha, C P G Vallabhan, P Radhakrishnan and V P N Nampoore, “Fabrication and characterisation of dye doped polymer optical fiber as light amplifier”, *Appl. Opt.* **46**, 106-112 (2007).
  9. M Rajesh, **M Sheeba**, K Geetha, C P G Vallabhan, P Radhakrishnan and V P N Nampoore “Design and fabrication of dye-doped polymer optical fiber for optical amplification.” *Proceedings of SPIE -- Volume 6289, Novel Optical Systems Design and Optimization IX*, 628919 (Sep. 5, 2006).

## **INTERNATIONAL CONFERENCE**

1. **M Sheeba** , M Rajesh, K Geetha , P Radhakrishnan, C P G Vallabhan & V P N Nampoori, “Fibre optic sensor for the detection of paraffin oil traces in coconut oil”, Photonics 2004 ,9-11 December, cochin India.
2. **M Sheeba**, M Rajesh, C P G Vallabhan, V P N Nampoori, and P Radhakrishnan, “Polymer optical fibre based temperature sensor”, ICOL-2005,12-15 December, IRDE -Dehradun, India.
3. **M Sheeba** , M Rajesh , K Nitish,P Radhakrishnan, C P G Vallabhan & V P N Nampoori, “Dye mixture doped polymer optical fiber amplifier” Photonics 2006 ,13-16 December, Hyderabad, India
4. M Rajesh, **M Sheeba**, K Geetha, P Radhakrishnan, C P G Vallabhan & V P N Nampoori, “A Fibre optic distributed sensor to characterize the properties of concrete mix” Photonics 2004 ,9-11 December, cochin India.
5. M Rajesh, **M Sheeba**, K Geetha, C P G Vallabhan, P Radhakrishnan and V P N Nampoori, “Fabrication of Polymer Optical Fibre based amplifiers” , ICOL-2005,12-15 December, IRDE -Dehradun, India.
6. M. Rajesh, **M Sheeba** and V P N Nampoori, “POF based smart sensor for studying the setting dynamics of cement paste”, Third International Conference on Optical and Laser Diagnostics –ICLOAD, City University, London, May 2007.
7. Jibi John, M Rajesh, **M Sheeba**, P Radhakrishnan, V P N Nampoori & Hema Ramachandran, “Optical diode using dye doped polymer”, Photonics 2006 ,13-16 December, Hyderabad,India.

## **NATIONAL CONFERENCE**

1. **M Sheeba**, K J Thomas, M Rajesh, V P N Nampoori, & P Radhakrishnan, "Two photon fluorescence study of dye doped polymer optical fiber", NLS 2006, RRCAT, Indore, India
2. **M Sheeba**, K J Thomas, K T Mathew, VPN Nampoori, CPG Vallabhan, P Radhakrishnan, "Fluorescence lifetime calculation of rhodamine 6g dye using femto second laser", NLS-2007, RRCAT, Indore, India
3. M Rajesh, K Geetha, **M Sheeba**, C P G Vallabhan, P Radhakrishnan and V P N Nampoori, "Side Illumination Fluorescence Technique for Loss Characterization of Dye Doped POF", NLS-2005, Vellore Institute of Technology-Vellore, Tamilnadu, India.

## **Acknowledgments**

The printed pages of this dissertation hold far more than the culmination of years of study. These pages also reflect the relationships with many generous and inspiring people I have met since the beginning of my research work. The list is long and I cherish each one's contribution to my development as a scholar.

I would like to express my deepest gratitude to my advisor, Prof P Radhakrishnan, for his excellent guidance, care and patience through out my research period. He provided me with an excellent research atmosphere, patiently corrected my writing and supported my research.

Prof. V P N Nampoori, a gracious mentor who demonstrates that rigorous scholarship can and must be accessible to everyone, that social change is central to intellectual work and, as such, scholars have a responsibility to use the privileges of academia to imagine and create a better world. He is a person to whom I am immensely indebted for giving proper advice and channeling me in the right direction to fulfill my dream and passion.

I would like to thank Prof C P G Vallabhan, who let me experience the research of optics and photonics in the field and practical issues beyond the textbooks.

Prof V M Nandakumaran is always a great inspiration for me and mentally supported me during my desperate hours. I also remember with thanks Mr. M Kailasnath.

The financial assistance from UGC and CELOS,CUSAT is greatly acknowledged.

To my colleagues for sharing their enthusiasm and comments on my work: Thomas, Lyjo Litty, Dann, Sajeev ,Prabhath, Manu, Jijo, Parvathy, Jinesh, Linesh, Sudheesh, Murali, Sony, Tintu, Nithyaja, Sithara, Vasuja and Jayasree. I would like to express special thanks to Sandeep and Mathew who showed keen interest in discussing with me during the final year of my research period. I remember the happy days in ISP with Dr Geetha, Dr Sr.Ritty, Dr Sajan, Dr Deepthy and Dr Pramod.

To the ISP and CELOS staffs for assisting me with the administrative tasks necessary for completing my doctoral program.

To my invaluable network of supportive, forgiving, generous and loving friends without whom I could not have survived the up and downs in my research life: Sini, Mangala, Ragitha, Chithra, Chithra R Nayak, Jisha C P, Sherin Binoy, Jisha, Gleeja and Shahina.

To my amma, achan and Shibu, nothing in this world is above their love and care. To my Guruvayur amma, achan, malu, chechi and sunilettan, who are making my days the most joyful and colourful events than ever before.

And finally, to my ettan for creating a safe space where I could dig deep into the muck and find the gems of my existence.

Sheeba



## Contents

<b>1. Polymer fiber optics: An overview</b>	<b>1</b>
1.1. An introduction to optical fibers	2
1.2. Theory governing light propagation through optical fibers	3
1.3. Types of optical fibers	6
1.4. Advantages of Polymer Optical Fibers	8
1.5. Application of Polymer Optical Fibers	8
1.6. Materials used for POF	9
1.7. Fabrication of polymer optical fibers	10
1.7.1. Continuous extrusion method	10
1.7.2. Preform method	11
1.8. Dye doped polymer optical fibers	14
1.9. Application of dye doped polymer optical fiber	15
1.9.1. Dye doped fiber amplifier	15
1.9.2. Dye doped fiber laser	19
1.9.3. Two photon processes in dye doped POF	21
1.9.4. POF based sensors	22
1.10. Conclusions	25
<b>2. Fabrication and characterization of dye mixture doped polymer optical fiber as a broad wavelength optical amplifier</b>	<b>31</b>
2.1. Introduction	32

2.2. Part I: Fabrication and characterization of dye mixture doped polymer optical fibers	33
2.2.1. Materials	33
2.2.1.1. Host material: Polymethylmethacrylate (PMMA)	33
2.2.1.2. Dyes : Rhodamine 6G and Rhodamine B	35
2.2.2. Energy level structure of a dye molecule	36
2.2.3. Fabrication of dye doped polymer optical fibers	37
2.2.4. Characterization	39
2.2.4.1. Absorption spectrum	39
2.2.4.2. Spectral overlap between absorption and emission bands	40
2.2.4.3. Spectral overlap between Rh 6G emission and Rh B absorption bands	42
2.2.4.4. Redshift in fluorescence peak emission	44
2.2.4.5. Uniformity in dye concentration	45
2.3. Part II : Development of dye mixture doped POF as a broad wavelength optical amplifier	46
2.3.1. Theoretical background: Rate equation approach	46
2.3.2. Experiment	50
2.3.3. Results and discussions	51
2.3.3.1. Energy transfer in dye doped POF	51
2.3.3.2. Amplification of a weak signal	54
2.3.3.3. Tuning range analysis of the amplifier gain	56
2.3.3.4. Gain variation with input pump energy	57

2.3.3.5. Optimum length of amplifier	58
2.3.3.6. Gain variation with input signal energy	60
2.3.3.7. Photostability of dye doped POFA	61
2.4. Conclusions	62
<b>3. Multimode laser emission from dye doped polymer optical fiber</b>	<b>67</b>
3.1. Introduction	68
3.2. Theoretical background	69
3.2.1. Fabry-Perot optical resonator	69
3.2.2. Microcavity resonator model	69
3.3. Experiment	71
3.4. Results and Discussions	72
3.4.1. Energy transfer in dye doped POF	72
3.4.2. Emission spectra with pump energy	74
3.4.3. Mode competition with pump energy	75
3.4.4. Wavelength tuning of multimode laser emission peak	77
3.4.5. Mode spacing dependence on diameter of the fiber	79
3.4.6. Length dependent wavelength tuning of multimode laser emission peak	81
3.5. Conclusions	86

<b>4. Two photon excited fluorescence studies in dye doped polymer optical fibers</b>	<b>91</b>
4.1. Introduction	92
4.2. Two photon absorption (TPA)	94
4.3. Single beam two-photon absorption	95
4.4. Jablonski diagram	95
4.5. One photon and two photon excited fluorescence spectra	96
4.6. Square- law dependence of fluorescence intensity	97
4.7. Side illumination fluorescence (SIF) measurement technique	98
4.8. Experiment	99
4.9. Results and Discussion	100
4.9.1. Energy Transfer	100
4.9.2. SIF spectra with propagation distance	104
4.9.3. Attenuation coefficient	111
4.10. Conclusions	119
<b>5. Fiber optic sensor for the detection of adulterant traces in coconut oil</b>	<b>123</b>
5.1. Introduction	124
5.2. Theory of operation	126
5.3. Experimental setup	128
5.4. Fabrication of the sensor head	129

5.5. Results and discussion	130
5.6. Conclusion	134
<b>6. General Conclusions and future prospects</b>	<b>138</b>
6.1. General Conclusions	139
6.2. Future prospects	141

## *Polymer fiber optics: An Overview*

*Optical information and data transmission has been an integral part of the economic life for many years. The demand for ever increasing transmission rates and a high horizon of expectations led to a boom in glass fiber technologies. Polymer optical fiber (POF) has emerged as another interesting, viable and economical transmission element especially in short distance communications. Historical development of undoped and dye doped POF, its advantages, fabrication and applications in different fields are discussed.*

## **1.1 An introduction to optical fibers**

Communication using optical means has evolved to an unimaginable degree of sophistication over the past century. There are a number of undisputed evidences both recorded and unrecorded that light was one of the effective mode of communication from prehistoric times. Simple signals using fires, reflecting mirrors and more recently signaling lamps have successfully provided limited information transfers. These communication techniques were crude and were rather cumbersome and are often prone to errors.

In the past few decades the explosion of information technology and the related fields have contributed to the development of radio waves leading to radio from fixed wire systems. With the exponential growth of bandwidth requirements, new avenues in optical communication techniques were envisaged using optical fiber which boasts of having a definite edge over the conventional fixed wire communication systems [1-7]. Since photons are considered to be chargeless particles they have a high immunity to internal noise, cross talk, electrical noise, ringing, echoes or electromagnetic interferences. It is also highly immune to lightning, and thus immune from lightning caused hazards. The transmitted signal through the fibers does not radiate. Further the signal cannot be tapped from a fiber in an easy manner. Optical fibers are developed with small radii, and they are flexible, compact and lightweight. Fibers can be bent or twisted without damage to a certain extent. Further, the optical fiber cables are superior to the copper cables in terms of storage, handling, installation and transportation, maintaining comparable strength and durability, low risk of fire, explosion, and ignition.

Furthermore, advances in the technology to date have surpassed even more optimistic predictions, creating additional advantages. It's often worth to

consider the merits and special features offered by optical fiber communication over more conventional electrical communication.

The information carrying capacity of a transmission system is directly proportional to the carrier frequency of the transmitted signals. The optical fiber yields greater transmission bandwidth than the conventional communication systems and the data rate or number of bits per second is increased to a greater extent in the optical fiber communication system. Further, the wavelength division multiplexing operation enhances the data rate or information carrying capacity of optical fibers to many orders of magnitude.

Due to the usage of the ultra low loss fibers and the erbium doped silica fibers as optical amplifiers, one can achieve almost lossless transmission. In the modern optical fiber telecommunication systems, the fibers having a transmission loss of 0.2 dB/km are used. Further, using erbium doped silica fibers over a short length in the transmission path at selective points, appropriate optical amplification can be achieved. Since the amplification is done in the optical domain itself, the distortion produced during the strengthening of the signal is almost negligible [6-7].

## 1.2 Theory governing light propagation through optical fibers

In its simplest form, an optical fiber consists of a central core surrounded by a cladding layer for which the refractive index  $n_2$  is slightly lower than the core refractive index  $n_1$ . Such fibers are generally referred to as step-index fibers to distinguish them from graded-index fibers in which the refractive index of the core decreases gradually from centre to core boundary. Fig 1.1



shows schematically the cross section and refractive index profile of a step index fiber.

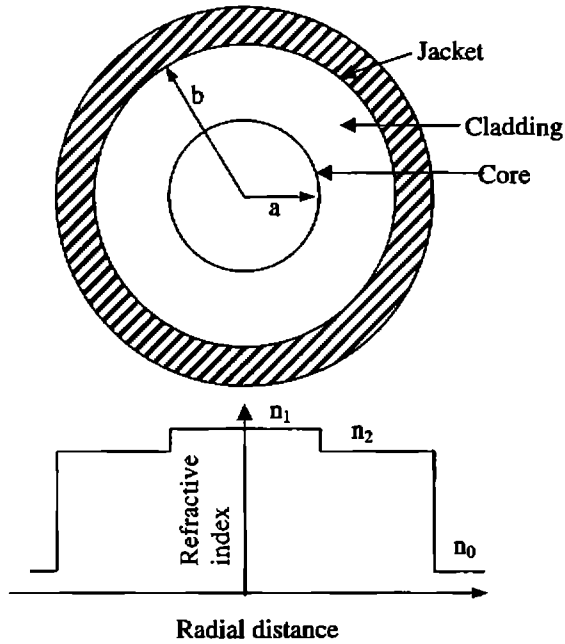


Fig 1.1: Cross section and refractive index profile of a step index fiber

Total internal reflection-the basic phenomenon responsible for guiding of light in optical fibers-is known from the nineteenth century. To ensure that a light ray that has entered the fiber can be guided along it, the following must hold true:  $n_1 > n_2$ , (Fig 1.2), so that below a certain angle  $\theta_{max}$ , total internal reflection takes place at the boundary between the core and the cladding. The surrounding medium is air with refractive index  $n_0=1$ . Rays that strike the end face of the fiber at an angle greater than  $\theta_{max}$ , are no longer completely reflected at the core/cladding boundary; instead they are partly refracted into the cladding so that they are no longer completely available for transmitting a signal [1-7].

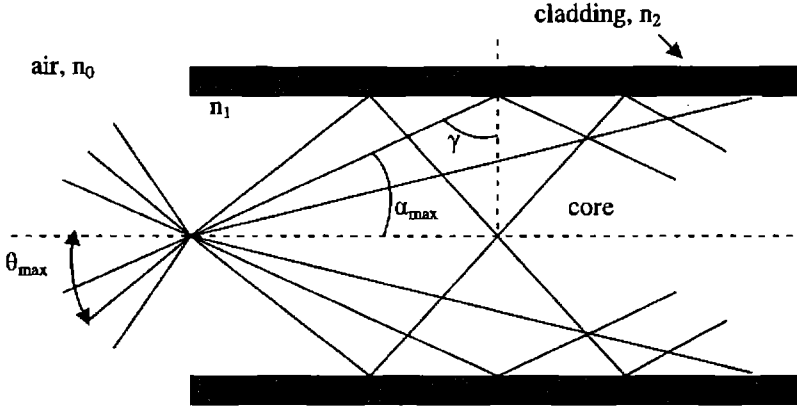


Fig 1.2: Light propagation through optical fiber

The sine of the maximum incident-ray angle  $\theta_{\max}$  is defined as the numerical aperture of the fiber,

$$NA = \sin \theta_{\max} = \sqrt{n_1^2 - n_2^2} \quad (1.1)$$

Two parameters that characterize an optical fiber are the relative core-cladding index difference

$$\Delta = \frac{n_1 - n_2}{n_1}, \quad (1.2)$$

and the so-called  $V$  parameter defined as

$$V = k_0 a \sqrt{n_1^2 - n_2^2} \quad (1.3)$$

where  $k_0 = \frac{2\pi}{\lambda}$ ,  $a$  is the core radius and  $\lambda$  is the wavelength of light.

The  $V$  parameter determines the number of modes supported by the fiber. A step-index fiber supports a single mode if  $V < 2.405$ . Optical fibers designed

to satisfy this condition are called single mode fibers. The main difference between the single mode and multimode fibers is the core size. The core radius  $a$  is typically 25-30  $\mu m$  for multimode fibers and they support a large number of modes. However, single mode fibers with  $\Delta \approx 0.003$  require  $a$  to be  $< 5 \mu m$ .

Another important fiber parameter is fiber loss during transmission of optical signals inside the fiber. If  $P_0$  is the power launched at the input of a fiber of length  $L$ , the transmitted power  $P_T$  is given by

$$P_T = P_0 \exp(-\alpha L), \quad (1.4)$$

where the attenuation constant  $\alpha$  is a measure of the total fiber losses from all sources. It is customary to express  $\alpha$  in units of dB/km using the relation

$$\alpha = -\frac{10}{L} \log \frac{P_T}{P_0} \quad [1-7] \quad (1.5)$$

### 1.3 Types of optical fibers

#### a) Glass optical fibers

Glass fibers are mostly made from silica or silicates. Glass fibers are low loss fibers compared to polymer fibers and are widely used in long distance communication purposes. There are a number of glass fibers available, some among them are silica glass fibers made of silica ( $\text{SiO}_2$ ), fluoride glass fibers which have extremely low transmission losses at mid IR wavelength region with the minimum loss being at around 2.55  $\mu m$ , active glass fibers in which rare-earth elements are doped into a normally passive glass to give new optical and magnetic properties and chalcogenide glass fibers which is doped with chalcogen elements (Se, Te) to impart high nonlinear optical properties.

**b) Polymer optical fibers:**

Polymer optical fibers (POF) are large diameter, flexible and durable multimode fibers made from polymers, including polymethylmethacrylate (PMMA), polystyrene, polycarbonates and perfluorinated materials. Typically POF has a core diameter of 1 mm and a cladding thickness of 20  $\mu\text{m}$ ; it can be cut with a scapel or hot knife, and polished using abrasive papers or metal polish [3-5].

POF was developed in 1968 by the US Company Dupont, who sold the patents to Mitsubishi Rayon, and since then, POF technology has developed in Japan, with rapid advances being made in reducing attenuation and increasing bandwidth for telecommunications applications. Key developments are listed as follows: Y Koike in 1992 developed graded index POF(GIPOF), and demonstrated a 1 Gbit/s capability over 30 m using a light emitting diode(LED), and 2.5 Gbit/s transmission over 100 m using a laser diode [8].

Researchers at Keio University in Japan developed a deuterinated PMMA fiber with losses of 20 dB/km and predicted a theoretical attenuation limit at 1.3  $\mu\text{m}$  and 1.5  $\mu\text{m}$  of 0.25 and 0.2 dB/km respectively, comparable to that of silica fiber [9]. In 2000, Koike developed perfluorinated GIPOF using a Teflon -type fluoropolymer called CYTOP, with low absorption from visible wavelength to 1300 nm (50 dB/km), enabling light sources and detectors developed for silica fiber to be used with perfluorinated POF [10]. Such improvements in the POF performances in the telecommunication sector enhance sales and reduce the cost of POF components and enable it to be commercially viable for sensing applications as well.

#### **1.4 Advantages of polymer optical fibers**

POF is very flexible in contrast to silica fiber, which is very brittle. This property is important for the fiber interface within the opto-electronic systems where space is usually limited. Commercial POF has a typical diameter of 1 mm with only a thin cladding, making it a multimode fiber. The large core diameter and flexibility allow ease of handling, large alignment tolerance and less connection cost. Because larger diameter makes splicing optical fibers much easier and allows the use of lower cost light sources and connectors, the economic advantage is very significant. Low processing temperature (200 °C to 250 °C) of POF allows organic nonlinear optical materials to be incorporated into the POF which is otherwise impossible in silica fibers because of its high processing temperature (1000 °C to 1500 °C). The low loss transmission windows of POF are distributed throughout the visible wavelength range. The utilization of these windows will allow very convenient and low cost deployment of POF systems [11-15].

#### **1.5 Application of polymer optical fibers**

POFs are in great demand for the transmission and processing of optical communication compatible with the Internet, which is one of the fastest growing industries of modern times. POFs also have potential applications in telecommunication and high capacity transmission systems, WDM systems, gigabit Ethernet, power splitters and couplers, amplifiers, sensors, filters, lenses, scramblers, integrated optical devices, frequency up-conversion, etc. POF is emerging as the new standard for LAN (Local Area Network) cabling because the installation cost of POF is less than either copper or glass, although its material cost falls directly between the cost of high-speed copper and glass. The real growth market will continue to be simple point-to-point links in a wide range of applications across all industries. Data links for PCs and workstations, Local Area Networks, industrial data links, consumer

digital data links, optical computing, optical interconnects, automobile networks and links are some of the other applications [11-15].

## 1.6 Materials used for POF

The material most frequently used for the fabrication of POF is PMMA (Polymethylmethacrylate), better known as Plexiglas. Each MMA monomer has a total of eight C-H bonds. The vibrations of this compound are the main cause for the losses encountered in PMMA-POF. From the beginning of 80's, the available PMMA-POF were found to have an attenuation of around 150 dB/km. PMMA-SI-POF has a theoretical minimum attenuation of 106 dB/km at 650 nm which is due to the Rayleigh scattering and absorption of C-H bonds. Polystyrene is another suitable candidate for making POFs. The initial PS-POF had an attenuation of over 1,000 dB/km, later it was possible to reduce this to 114 dB/km at 670 nm. Polycarbonate based POF is used for high temperature application fields like automotive technology and automation technology [4].

A typical characteristic for all materials used at temperatures over +100 °C is the higher attenuation compared to the PMMA fiber. For achieving a significant reduction in the absorption loss of polymers one has to substitute the hydrogen with heavy atoms which will result in lower vibration frequency, thus moving the attenuation bands to a longer wavelength. One method is to replace it with deuterium. This isotope has twice the atomic mass compared to hydrogen. Chemically, deuterium behaves the same way as hydrogen so that heavy water (D<sub>2</sub>O) can be used as a base material for synthesis. The first deuterinated SI-POF was produced by Dupont in 1977 [12]. In 1983, NTT produced a SI-POF in deuterinated material with a minimum attenuation of 20 dB/km at 680 nm [16]. Deuterinated polymers have a number of advantages associated with them. Chemically these

materials behave identically to the substances made from normal hydrogen. The attenuation is approximately one order of magnitude less than the values achieved for PMMA fibers.

The decisive disadvantage of deuterated POF is that water vapor present in the atmosphere will be absorbed by these fibers leading to absorption losses. The atomic mass of fluorine is many times greater than that of hydrogen so that absorption bands are moved significantly further into the infra-red zone. The theoretical minimum values are less than 0.2 dB/km [17], which is comparable to silica fibers in the wavelength range of about 1,500 nm. However, practical experience shows that these impressive theoretical values are in fact difficult to achieve. Another important aspect is that it is very difficult to process a fluorinated polymer into a fiber in its amorphous state. To date the best results in producing low attenuation (~15 dB/km at 1300 nm) POF have been achieved with the material CYTOP (cyclic transparent optical polymer) developed at Asahi Glass in Japan. This material no longer contains hydrogen [10,17].

## **1.7 Fabrication of polymer optical fibers**

Continuous extrusion and preform techniques are the common methods used for fabricating polymer optical fibers [3,5]

### **1.7.1 Continuous extrusion method**

Perhaps the most economical method for making polymer optical fiber that is also amenable to high-volume processing is the extrusion process. This method was successfully developed by Mitsubishi rayon [3, 4], and is one of the well-developed methods for producing step index polymer optical fibers (SIPOF). In this method, a purified monomer (methylmethacrylate), an initiator and a chain transfer agent are fed into a reaction chamber where the monomer is polymerized. The material is partially polymerized into a thick

fluid, which is typically 80% polymer and 20% monomer. The temperature of the reactor chamber is typically 180 °C. This concentrated solution is directed to a screw extruder, which pushes the material through a nozzle that creates the fiber. Remaining monomer is evaporated in the core extruder and recovered for further use. Subsequently, the core of the fiber runs into a second chamber and then through a nozzle where the cladding is also coated onto the fiber using an extrusion process. This leads to the formation of a continuous fiber. Effectively, material is fed into one end and the fiber comes out at the other end.

The most important advantage of continuous extrusion is high production rate. The drawback is that this cannot be operated continuously since the materials used for extruding SI-POF gets thermally degraded as time progresses. This will, in turn, have adverse effect on the optical properties of the fiber.

### **1.7.2 Preform method:**

The preform drawing process is important because it can be used to make single mode step index fiber, multimode fiber and graded index fiber. Fabrication of POFs by preform method involves two stages. In the first stage a cylindrical preform of required diameter and length is made. In the second stage, the preform is drawn into fiber by the heat-drawing process.

#### **a) Preform fabrication process:**

The most important part of fabrication of a POF is to start with a high optical quality polymer preform with low levels of impurities. The fiber drawing process relies on the smooth flow of softened polymer. Since thermoplastics are polymers that flow at an elevated temperature, they are well suited as fiber materials. An important property of the polymer is its molecular weight, which is a measure of the average chain length. If the molecular weight is too



low, the polymer turns into a liquid and due to surface tension breaks apart into drops. If the molecular weight is too high, the chains are too long to permit them to slip and flow. The result is that the polymer remains rubbery even at temperatures that are high enough to cause the material to decompose. The ideal molecular weight allows the material to flow without dripping. In making the polymer, a chain transfer agent is used to control the molecular weight.

A cylindrical tube, which serves as the cladding layer, is made by polymerizing a cladding material inside a rotating cylindrical reactor. Materials that can be polymerized by the radical polymerization reaction are used and the reaction is induced thermally or by UV radiation using photoinitiator. Due to the fast rotational speed of the reactor about its axis, a tube of uniform thickness is formed once the reaction is complete. This tube is then removed from the reactor and filled with a core material mixed with an initiator and a chain transfer agent. The core material is then polymerized to make a preform that is drawn to a fiber by heat-drawing process.

There are three other commonly used methods for preform fabrication [3,5]. First is the rod-in-tube method, in which a pre-fabricated polymer core rod is inserted into a pre-fabricated polymer cladding tube with a tight-fitting. The disadvantage of this method is that the rod diameter is usually too large for the drawn fiber to achieve a single -mode operation. Also bubbles may be trapped at the core-cladding interface. The second method is the hole-in-rod technique where a hole is drilled into a cladding polymer rod followed by pouring in core monomer. A polymerization process is then initiated to obtain a composite core-cladding polymer preform. The core-cladding interface of this preform may not be smooth because of drilling. This could lead to excessive loss.

'Teflon technique' is another most successful technique for the fabrication of the preform. In this technique a thin teflon string is properly fixed in the center of a glass tube. The thermal polymerization of the filled tube is carried out in a temperature controlled oil bath. After the monomers are fully polymerized and heat treated, the teflon string is removed and we obtain a polymer tube (polymer rod with a small hole in its center). The bottom side of the core is sealed and the hole is then filled with the initiated monomers for the core. Again it is kept in an oil bath for further polymerization.

**b) Heat drawing process:**

The heat drawing process is shown schematically in Fig 1.3.

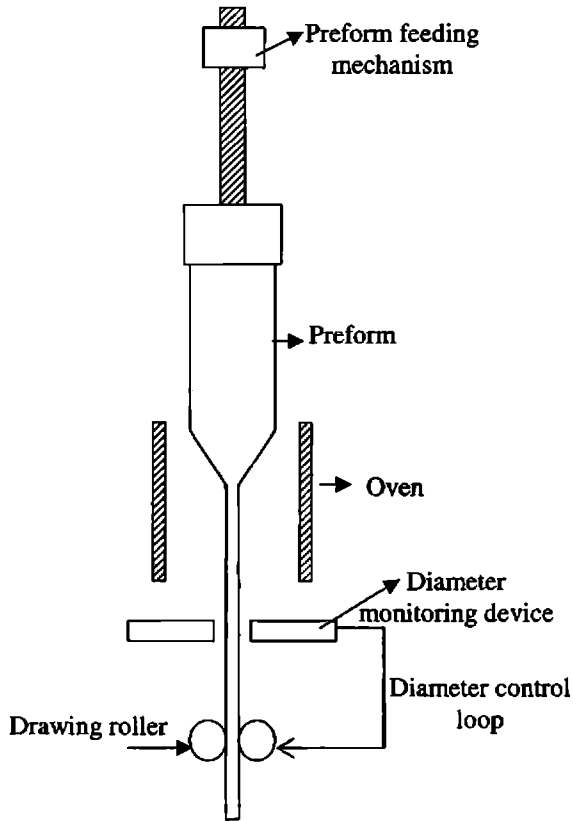


**Fig 1.3:** Schematic diagram of heat drawing process

The preform is positioned vertically in the middle of the oven where its lower portion is heated locally to the drawing temperature. Both convective and radiative heat transfer mechanisms are important in heating the preform in the oven. When the lower part of the preform reaches a temperature beyond its softening point, it necks downward by its own weight due to gravity [3, 5]. Once this initiation of the drawing process is achieved, tension is applied to the fiber by drawing rollers and the fiber is drawn continuously while the preform is fed at a predetermined rate.

The fiber diameter is continuously measured and the desired value is maintained by controlling the preform feed speed and the drawing roller speed. Another design of the fiber drawing system is the horizontal drawing rig. The only difference in this case from the conventional drawing system is that the whole drawing procedure is horizontal. GD Peng et al have widely used this type of configuration and has observed no fiber sagging during drawing and the fiber diameter was kept at an acceptable tolerance. The horizontal machine offers an additional advantage of avoiding the climbing up and down the ladder during the draw initiation phase.

### **1.8 Dye doped polymer optical fibers**

In recent years, the incorporation of dyes into solid state materials has enabled development of various opto-electronic devices ranging from tunable lasers and amplifiers to nonlinear devices such as switches and modulators. These devices have applications in optical communications, photonics, material science, medicine and optical spectroscopy. Usually organic laser dyes are used which have the advantages of high quantum efficiency, high non linearity and broad spectral range.

PMMA doped with such dyes has advantages over its silica based counterparts in that it has better efficiency, beam quality and superior optical homogeneity than ORMOSIL (dye doped organically modified silicates). Further advantages of dye doped POF include the fact that a wide range of organic materials can be incorporated as dye molecules due to POFs low processing temperature. Silica fibers are manufactured at temperatures in the range 1800-2100 °C, making it impossible to dope organics into them. Optical nonlinear organic dyes begin to deteriorate at 300-500 °C, but these temperatures are above the manufacturing temperature range of POF, enabling the incorporation of such dyes into POF during manufacture. Dye doped polymeric devices formed into POF have advantages over their waveguide or bulk optic counterpart, in that useful and usually weak effects can accumulate over long distances to build up a total effect, due to the confined core area and long interacting lengths[18-28]

## **1.9 Application of dye doped polymer optical fiber**

Availability of laser sources in the visible region has increased the utilization of POF in data communication over LAN systems . Implementation of optical communication in the visible region demands the development of suitable optical amplifiers working in this region. Given the great flexibility in controlling the optical properties of a dye-doped polymer, it is possible to make polymer fiber sources and amplifiers that act over a broad range of wavelengths.

### **1.9.1 Dye doped fiber amplifier**

Optical fibers attenuate light like any other material. In the case of silica fibers, losses are relatively small, especially in the wavelength region near 1.55  $\mu\text{m}$  ( $\alpha \approx 0.2\text{dB} / \text{km}$ ) whereas for PMMA based POF the losses are high in the wavelength region near 650 nm ( $\alpha \approx 120\text{dB} / \text{km}$ ) [4]. In the case

of long-haul fiber-optic communication systems, transmission distances may exceed thousands of kilometers. Fiber amplifiers are commonly used to overcome transmission losses and restore the optical signal in such systems. Fiber amplifiers amplify incident light through stimulated emission, the same mechanism used by lasers. Indeed, an optical amplifier is just a laser without feedback. Its main ingredient is the optical gain, occurring when the amplifier is pumped optically to realize population inversion.

Laser dyes are highly efficient media either for laser source with narrow pulse width and wide tunable range or for optical amplifier with high gain, high power conversion and broad spectral bandwidth. Dyes have a wide range of tunability in the visible region. For example the range of tunability of laser dyes like Rhodamine B and Rhodamine 6G lies between 570 nm to 640 nm. The dye molecules, most commonly dissolved in solgels or polymers, have large absorption and emission cross sections due to allowed pi-pi transitions and are ideal active dopants for the generation and amplification of light pulses. Solid state dye matrices offer practical advantages such as compactness as well as alleviating some disadvantages associated with the flammable and volatile organic solvents used in liquid dye media. From recent studies it is found that the dye doped polymer materials have better efficiency, beam quality and superior optical homogeneity when compared to other solid matrices [18-28].

In 1995, Akihiro Tagaya and co-workers, achieved the first optical amplification in dye doped polymer optical fiber. In their experiment ,using a dye-doped gradient index (GI) POF, maximum gain of 27 dB was achieved at 591 nm wavelength with a pump power of 11 kW [20]. Subsequently, G D Peng etal have achieved high gain and high efficiency optical amplification in a rhodamine B doped POF with a low pump power of 1 kW[19] and Karimi

et al have reported a high gain of 30 dB in Rh B doped POF [24]. Argyros et al have reported the first demonstration of microstructured POF based amplifier with a high gain of 30 dB [28]. Reilly et al have achieved 14 dB signal gain at the polymer optical fiber low-loss window of 650 nm in a polymer waveguide with dye doped cladding [29].

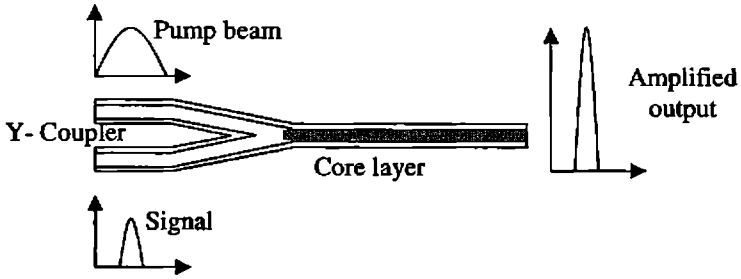


Fig 1.4: A general dye doped fiber amplifier configuration

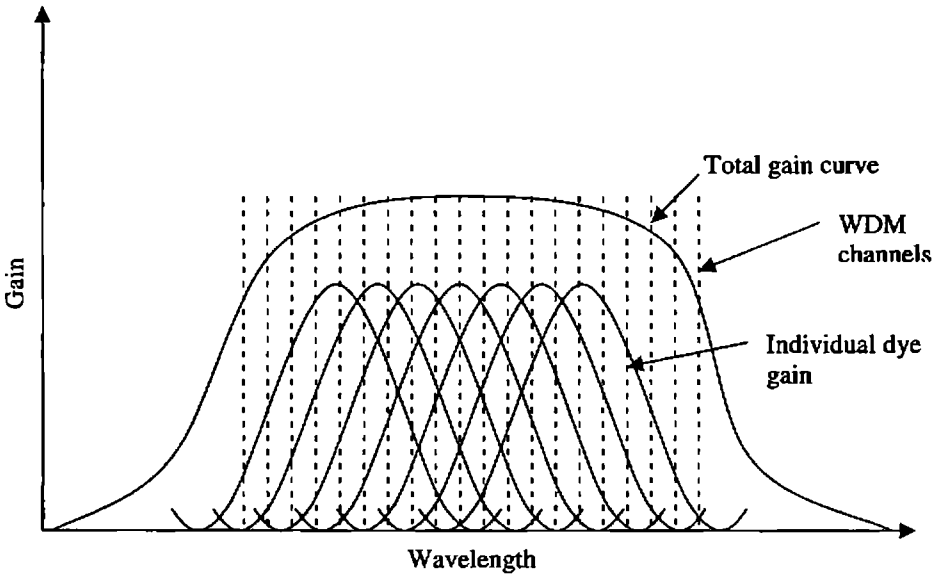


Fig.1.5: Several individual gain curves of different molecules add to yield a broader gain curve.

In dye doped optical fiber amplifiers the pump power can be limited to a very low level and utilized in a most efficient manner since the power is well confined to the core region and is propagated with less diffraction. The most important aspect of reducing the pump power is that it reduces the bleaching effects thereby increasing the stability of the medium. A general dye doped amplifier configuration is shown in the Fig 1.4.

Wavelength-division-multiplexed (WDM) optical communication systems make use of optical fiber amplifiers which operate in a broad wavelength region. The unique advantage of a dye-doped polymer is the fact that it can be doped with several different dyes simultaneously to make a broad-band amplifier [3]. Thus, dye mixture doped polymers are potential candidates for realizing broad wavelength amplifiers suitable for WDM systems.

Fig 1.5 shows an example where the gain peaks of each dye overlap. The net gain is then given by the broader curve. The vertical dashed lines show the position of the wavelength division multiplexed channels. As such, a much broader range of wavelengths can be amplified. In making a multiple-dye amplifier, the choice of dyes used and their concentrations need to each be carefully adjusted to make the gain curve flat over the wavelength range of operation. Given the broad range of dyes available, controlling the gain profile should be, in principle, straightforward.

Rare earth doped POF is also a potential candidate for the development of optical amplifiers [30-31]. Rare-earth-doped inorganic glass fibers are commonly used for making commercial optical amplifiers viz Erbium Doped Fiber Amplifier (EDFA). The concentration that is attainable with such rare-earth ions in glass is relatively low compared with the concentration that is possible with dye molecules that are dissolved into a polymer. As such, the

higher concentrations can lead to higher gain. Unfortunately, lanthanide atoms can interact with the surrounding polymer, quenching the fluorescence. One approach for protecting the rare earth molecule from the polymer is to incorporate it into a structure of several ligands. Such ligand structures are called chelates, where the rare-earth atom is held in place with ligands in the shape of pincers. Liang and co-workers reported on optical amplification of a Europium ion surrounded by ligands designated as  $\text{Eu}(\text{DBM})_3\text{Phen}$  [tris(dibenzoyl methanido)(*O*-phenanthroline)Europium III], doped in a step index PMMA POF[3].

### 1.9.2 Dye doped fiber laser

A fiber amplifier can be converted into a laser by placing it inside a cavity to provide optical feedback. Such lasers are called fiber lasers. Fiber lasers can be designed with a variety of choices for the laser cavity. The most common type of laser cavity is called a Fabry-Perot cavity [32], which is made by placing the gain medium between two high reflecting mirrors. Stimulated emission and the development of laser from organic dye molecules in solution by laser excitation was first reported by Sorokin and Lankard [33] and was subsequently studied by Schafer et al. They observed a decrease in luminescence decay time with increasing flash lamp intensity which they cited as evidence for stimulated emission.

Dye lasers can oscillate at wavelengths from the ultraviolet to infrared region by changing the dyes or pigments. Later Soffer and McFarland reported continuously tunable dye lasers over larger bandwidths by use of diffraction gratings as cavity mirrors. In 1967, Soffer and McFarland, first demonstrated a solid-state dye laser using a polymethylmethacrylate (PMMA) sample containing rhodamine 6G dye [34] and then by Peterson and Snively in 1968 using dye doped polymer rods. Since then organic dye doped polymers have been widely investigated as gain media in solid state dye lasers. In 1984,



## *Polymer fiber optics*

---

Avnir et al reported the application of a dye doped silica gel as the laser medium synthesized by the sol-gel method [35]. Solid state dye lasers have great advantages over liquid dye lasers by being nonvolatile, nonflammable, nontoxic, compact and mechanically stable.

The potential of fiber media in laser systems is well established for organic amplifying materials. The merits of optical fibers as a laser medium include long gain length, flexibility in designs suitable for optoelectronics and single mode or multimode operation. Prasad et al reported lasing action in rhodamine 6G doped sol-gel glass fiber [36]. The photostability of dye doped sol-gel fiber is increased compared to a dye doped bulk, due to a larger ratio of surface area to volume allowing for better heat relaxation. Muto et al. investigated a dye doped step index polymer fiber laser. Also, Ken Kuriki et al have reported lasing action of graded index polymer optical fibers containing dyes such as rhodamine B, rhodamine 6G and perylene orange [37]. Again, photo-pumped narrow line laser emission is demonstrated using cylindrical micro cavities formed by conjugated polymer thin films, dye doped polymers and dendrimer doped polymers.

A kristensen et al have reported the first observation of lasing action in a levitated, Rh 6G dye dissolved ethylene glycol micro droplets [38]. Micro cavities ( $\mu$  cavities) have been shown to furnish an excellent quality factor Q and optimal coupling between emission and cavity modes which results in low laser thresholds [39]. Planar  $\mu$  cavities suffer from unavoidable losses due to imperfect reflections and emission leakage to the sides of the  $\mu$  cavity plane. Cylindrical  $\mu$  cavities of ring or disc type, on the other hand, provide superior two dimensional optical confinement

resulting in Q values in excess of  $10^6$  and thus are much more advantageous for obtaining low laser thresholds.

As in the case of fiber amplifier, a fiber laser which can be operated in a broader wavelength region can be achieved by doping several different dyes in the POF. In the dye mixture system, the excitation of dye lasers through energy transfer processes provides one of the means of extending the lasing wavelength region. Both radiative and non-radiative energy transfer is possible in the dye mixture system.

### 1.9.3 Two-photon processes in dye doped POF

Since the first observation of a two-photon absorption process in  $\text{CaF}_2: \text{Eu}^{2+}$  by Kaiser and Garrett, this effect, postulated a long time ago by M. Gappert-Meyer, has been the subject of numerous investigations [40]. It has been recognized early that large organic molecules like dyes are especially suited to the study of this process due to their large number of energy levels implying relatively large cross sections for double-quantum transitions.

Fluorescence by one-photon absorption involves the excitation of dye molecules to higher energy state by absorbing a single photon from the exciting radiation field and the subsequent emission of fluorescence. If the exciting laser intensity is high, a fluorophore can simultaneously absorb two long wavelength photons to reach the first singlet state by the process called two-photon absorption (TPA) and then the usual fluorescence emission can occur. Two-photon excited (TPE) frequency upconversion lasing and two-photon fluorescence imaging are important areas of research and have become more interesting and promising in recent years.

Lasers operating in the short wavelength visible region are desired for use in such diverse applications as medical diagnostics, surgery, high-capacity optical storage and high-resolution scanning and printing. Compared to other coherent frequency upconversion techniques, such as optical harmonic generation or sum frequency mixing based on second or third order nonlinear optical processes, the main advantages of upconversion lasing by two-photon absorption are (i) elimination of phase-matching requirement, (ii) feasibility of using semiconductor lasers as pump sources and (iii) capability of adopting waveguide and fiber configurations. There have been two important technical approaches to achieve frequency upconversion lasing. 1) Simultaneous absorption of two photons by the gain medium (two-photon pumped). 2) Sequential stepwise multi-photon excitation (multistep one-photon pumped) [40].

As a result of the quadratic dependence of the two-photon absorption probability on intensity, the two-photon absorption cross section is much smaller than the corresponding one-photon cross section. Therefore a higher pump intensity and longer gain length are required for TPE lasing purposes. The prospect of using waveguide or fiber configurations to achieve upconversion lasing are (i) a higher local pump intensity and (ii) much longer effective gain length. G S He et al have reported two-photon pumped frequency upconversion cavity lasing at 610 nm in an ASPI dye(trans-4-[p-(N-hydroxyethyl -N-methylamino)styryl]-N-methylpyridinium iodide) doped POF system pumped with 1.06  $\mu\text{m}$  IR laser pulses and in ASPT dye(trans-4-[p-(N-ethyl-N-hydroxyethylamino)styryl]-N-methylpyridinium tetraphenyl borate) doped bulk polymer rods [41]

#### **1.9.4 POF based sensors**

Although many of the applications of optical fibers are based on their capacity to transmit optical signals with low losses, it can also be desirable

for the optical fiber to be strongly affected by certain physical parameters of the environment. In this way, it can be used as a sensor of such a parameter. Optical fiber based sensors have got wide spectra of applications. They can be employed in hostile or corrosive environments due to its chemical and electrical passivity. They are immune to electromagnetic interference and are biocompatible owing to inertness to biological systems [1, 2]. There are many strong arguments for the use of POF as sensors. POF sensors have been developed based on the ideas already used in silica optical fiber sensors, but exploiting the rugged and inexpensive nature of POF for harsh environments and sensors which can be reused. In addition to their easiness to handle and low price, they present the advantages common to all multimode optical fibers. Moreover, it has been proved that POF can be employed to detect a great variety of parameters, including temperature, humidity, pressure, presence of organic and inorganic compounds, wind speed, refractive index, to name a few [42-44].

Enabling technologies that allow POF to be sensitized to various measurands have been developed. POF can easily be sensitized to bending or deflection by cutting grooves in the radial fiber surface, to form an optical fiber strain sensor. Perturbing the surface of POF fiber by cutting radial grooves into its surface enhances the bending loss when the fiber is curved, so that light transmitted through the fiber is attenuated as a function of the deflection of the fiber. Thus an optical fiber strain gauge is formed where the deflection or extension of the fiber is related to the opening of each groove [45]. A respiratory plethysmograph for use in a Magnetic Resonance (MR) scanner exploits the well known modulation mechanism of microbending by measuring the intensity changes when a loop of POF is caused to expand and contract in sympathy with the ribcage [46]. Microstructured POF has also been proved as a potential candidate for developing POF based sensors [47].

## *Polymer fiber optics*

---

Again, fluorescent dye doped POF has been used for various sensor applications [48].

Removing the cladding from an optical fiber and replacing with the measurand is a well known technique used with optical fibers to form evanescent field sensors. The evanescent portion of the electric field travelling within the core of the fiber, penetrates into the cladding layer. Changes in the absorption or refractive index of the cladding perturb the evanescent field, thus affecting the intensity of the guided modes within the fiber core. The cladding can be removed in a polymer optical fiber by chemical method using suitable solvents or by side polishing technique [42-44].

Tapering is a technique well developed in silica fibers and optical fiber sensors and devices based on fiber tapers are used in diverse fields of application. Replacing the cladding with a measurand, and exploiting the increased penetration of the evanescent field with decreased fiber diameter, causes an enhanced interaction with measurands or analytes present at the core-cladding interface. Fibers can be reduced to diameters of 1  $\mu\text{m}$ , enabling them to penetrate into single cells [49]. Such configurations have been extended to POF to take advantage of its ease of coupling and termination, and low cost. Silica fibers are traditionally tapered using heat and pull techniques, but for POF tapers, an alternative technique of chemical etching, has been developed using organic solvents [50].

The technology of FBG (Fiber Bragg Grating) and LPG (Long Period Grating), formed in silica optical fibers using UV laser light to create photoinduced refractive index changes, is well established and has found numerous applications in communications and metrology [51]. FBG and LPG

have also been successfully photoinduced into core and sides of doped and undoped polymer optical fibers and preforms and sensors based on these devices have great application value for smart materials and structures. For silica optical fiber gratings, the change in Bragg wavelength due to the changes in temperature and strain is small, typically a few nanometers. This is because silica glass has small thermal effect and large Young's modulus. In the case of polymer optical fibers, its Young's modulus is more than 70 times smaller than that of glass and the refractive changes that can be induced by photo-reaction are relatively high. Therefore POF based Bragg gratings are tunable over a wide wavelength range and this nature of POF gratings can be exploited to make sensors which are highly sensitive to strain and temperature [52-53].

### **1.10 Conclusions**

An overview of optical fiber based communication systems, types of optical fibers giving emphasis to undoped and dye doped polymer optical fibers, historical development and fabrication of POFs, advantages over silica fibers and applications in different fields such as fiber amplifiers, fiber lasers, and sensors have been described in this chapter.

## References

1. J M Lopez-Higuera ed, *Handbook of optical fiber sensing technology* (John Wiley & Sons, 2002).
2. B.P.Pal ed, *Fundamentals of fiber optics in telecommunication and sensor systems* (John Wiley & Sons, New York, 1992).
3. Mark G Kuzyk, *Polymer fiber optics-Materials, Physics and Applications* (Taylor & Francis group, 2007).
4. W Daum, J Krauser, P E Zamzow and O Ziemann, *POF-Polymer Optical Fibers for Data Communication* (Springer, New York 2002).
5. H S Nalwa, *Polymer optical fibers* (American scientific publishers, 2004).
6. A Ghatak and K Thyagarajan, *Introduction to fiber optics* (Cambridge University press, 1999).
7. G P Agrawal, *Fiber- Optic Communication systems* (Wiley Interscience, 2002).
8. Y Koike, "High bandwidth and low loss polymer optical fiber", POF-92, Paris, 15-19(1992).
9. Y Koike, "POF from the past to the future", 7<sup>th</sup> international plastic optical fibers conference, Berlin, 1-8(1998).
10. Y koike, "Progress in GI-POF – Status of high speed plastic optical fiber and its future prospect", POF -2000, Boston, 1-5(2000).
11. T Ishigure, E Nihei and Y koike "Graded-index polymer optical fiber for high speed data communication", *Appl. Opt.* **33**, 4261-4264(1994).
12. Y Koike, T Ishigure and E Nihei "High bandwidth, high numerical aperture graded index polymer optical fiber", *Journal of lightwave technology* **13**, 1475-1489(1995).
13. D W Garvey, K Zimmerman, P Young, J Tostenrude and M G Kuzyk "Single mode nonlinear-optical polymer fibers", *J. Opt. Soc. Am. B* **13**, 2017-2022(1996).
14. M A van Eijkelenborg, A Argyrosa, G bartonc and J Zagari "Recent progress in microstructured polymer optical fiber fabrication and characterisation", *Optical fiber technology* **9**, 199-209(2003).

15. C Koeppen, R F Shi, W D Chen and A F Garito "Properties of plastic optical fibers", *J. Opt. Soc. Am. B* **15**, 727-738(1998).
16. Y koike, "Status of POF in Japan", POF- 96, Paris 1-8(1996).
17. M Murofushi , "Low loss perfluorinated POF", POF-96, Paris17-23(1996).
18. K H Drexhage and F P Schafer, *Dye lasers* (Springer Verlag, 1977).
19. G D Peng,P K Chu, Z Xiong, T W Whitbread and R P Chaplin, "Dye-doped step- index polymer optical fiber for broadband optical amplification", *Journal of Lightwave Technology* **14**, 2215-2223 (1996).
20. A Tagaya,Y Koike,E Nihei,S Teramoto,K Fujii,T Yamamoto and K Sasaki, "Basic performance of an organic dye-doped polymer optical fiber amplifier", *Appl.Opt* **34**, 988-991(1995).
21. A Tagaya,Y Koike,T Kinoshita,E Nihei, T Yamamoto and K Sasaki, "Polymer optical fiber amplifier", *Appl.Phys.Lett* **63**,883-884(1993).
22. A Tagaya, S Teramoto, E Nihei, K Sasaki and Y Koike, "High-power and high-gain organic dye-doped polymer optical fiber amplifiers :novel techniques for preparation and spectral investigation", *Appl.Opt* **36**,572-578(1997).
23. A Tagaya, S Teramoto,T Yamamoto, K Fujii, E Nihei,Y Koike and K Sasaki,"Theoretical and experimental investigation of rhodamine B doped polymer optical fiber amplifiers", *Journal of Quantum electronics* **31**, 2215-2220(1995).
24. M Karimi,N Granpayeh,M K Morraveghfarshi, "Analysis and design of a dye doped polymer optical fiber amplifier", *Appl.Phys.B* **78**,387-396(2004).
25. H Liang,Z Zheng,Z Li,J Xu,B Chen,H Zhao,Q Zhang and H Ming, "Fabrication and Amplification of Rhodamine B doped Step-Index polymer optical fiber", *Journal of Applied Polymer Science* **93**,681-685(2004).
26. M Rajesh, M Sheeba, K Geetha, C P G Vallabhan,P Radhakrishnan and V P N Nampoori, "Fabrication and characterization of dye doped polymer optical fiber as a light amplifier", *Appl. Opt* **46**,106-112 (2007).
27. M Rajesh, K Geetha, M Sheeba, C P G Vallabhan, P Radhakrishnan and V P N Nampoori, "Characterisation of rhodamine 6G doped polymer optical



- fiber by side illumination fluorescence”, *Optical Engineering* **45**, 075003-075007(2006).
28. A Argyros, M A van Eijkelenborg, S D Jackson and R P Mildren, “Microstructured polymer fiber laser”, *Opt.Lett* **29**, 1882-1884(2004).
  29. M A Reilly, B Coleman, E Y B Pun, R V Penty and I H White, “Optical gain at 650nm from a polymer waveguide with dye doped cladding”, *Appl. Phys.Lett.* **87**, 231116-231119(2005).
  30. E Desurvire, *Erbium-Doped fiber amplifiers :Principles and Applications* (John Wiley & Sons Inc,New york 1994 p- 382).
  31. X Xu, “Properties of Nd<sup>3+</sup> -doped polymer optical fiber amplifiers”, *Opt.Commun* **225**, 55-59(2003).
  32. B E A Saleh and M C Tech, *Fundamentals of photonics* (Wiley Interscience, 1991).
  33. P.P. Sorokin and J R Lankard, “Stimulated emission observed from an organic dye chloro-aluminum Phthalocyanine,” *IBM J.of Res. And Dev.* **10**,162-163(1966).
  34. B H Soffer and B B McFarland, “Continuously tunable, narrow band organic dye lasers”, *Appl.Phys.Lett.***10**, 266-267(1967).
  35. D Avnir, D Levy and R Reisfeld, “The nature of the silica cage as reflected by spectral changes and enhanced photostability of trapped Rhodamine 6G”, *J.Phys.Chem* **88**,5956-5959(1984).
  36. R Gvishi, G Ruland and P N Prasad, “New laser medium: dye-doped sol-gel fiber”, *Opt.Commun.***126**, 66-72(1996).
  37. K. Kuriki,T Kobayashi,N Imai,T Tamura,S Nishihara,Y Nishizawa,A Tagaya and Y Koike, “High efficiency organic dye doped polymer optical fiber lasers”, *Appl.Phys.Lett.***77**,331-333(2000).
  38. H Azzouz, L Alkhafadiji, S Balslev and A Kristensen “Levitated droplet dye laser”, *Optics Express* **14**,4374-4379(2006).
  39. SV Frolov and Z V Vardeny, “Plastic Microring lasers on fibers and wires”, *Appl Phys Lett* **72**, 1802-1804(1998).
  40. Joseph R Lakowicz, *Principles of fluorescence spectroscopy* (Springer, 2006).

41. G S He, C F Zhao, J D Bhawalkar and P N Prasad, "Two-photon pumped cavity lasing in novel dye doped bulk matrix rods", *Appl.Phys.Lett* **67**, 3703-3705 (1995).
42. R M Ribeiro, J L canedo, M M Werneck and L R Kawase, "An evanescent-coupling plastic optical fiber refractometer and absorptionmeter based on surface light scattering", *Sensors and Actuators A: Physical* **101**, 69-76(2002).
43. J Zubia, G Garitaonandia and J Arrue "Passive device based on plastic optical fibers to determine the indices of refraction of liquids", *Appl.Opt* **39**, 941-946 (2000).
44. R J Bartlett, R P Chandy, P Eldridge, D F Merchant, R Morgan and P J Scully "Plastic optical fiber sensors and devices", *Transactions of the institute of measurement and control* **22**, 431-457(2000).
45. R Chandy, P J Scully and R Morgan "Elastic beam deflection flowmeter using optical and conventional strain gauges", *Proceedings of the conference Applied Optics & Opto-Electronics, University of Reading*, 299-304(1996).
46. A Raza and A T Augousti "Optical measurement of respiration rates", *Proceedings of the seventh conference on sensors and their applications Dublin*. 325-330(1995).
47. J B Jensen, P E Hoiby, L H Pedersen and A Bjarklev, "Selective detection of antibodies in microstructured polymer optical fibers", *Opt. Express* **13**, 5883-5889(2005).
48. S Muto, H Sato and T Hosaka "Optical humidity sensor using fluorescent plastic fiber and its applications to breathing condition monitor", *Japanese Journal of Applied Physics*. **33**, 6060-6064(1994).
49. B D Macraith, C M McDonagh, A K McEvoy, T Butler and F R Sheridan "Sol-gel coatings for optical chemical sensors and biosensors", *Sensors and Actuators B***29**, 51-57(1995).
50. D Uttamchandani and S McCulloch "Optical nano sensors-towards the development of intracellular monitoring", *Advanced Drug Delivery Reviews* **21**, 239-247(1996).

51. Raman Kashyap *Fiber Bragg Gratings* (Academic Press, 1999).
52. Z Xiong, G D Peng, B Wu and P L Chu "Highly tunable Bragg gratings in single mode polymer optical fibers", *Photonics Tech. Lett* **11**, 352-354(1999).
53. G D Peng and P L Chu "Polymer optical fiber photosensitivities and highly tunable fiber gratings", *Fiber and Integrated optics* **19**, 277-293(2000).

*Fabrication and characterization of dye mixture doped polymer optical fiber as a broad wavelength optical amplifier*

*Rhodamine 6G and rhodamine B dye mixture doped polymer optical fiber amplifier which can operate in a broad wavelength region (60nm) is successfully fabricated and tested. Tunable operation of the amplifier over a broad wavelength region is achieved by mixing different ratios of the dyes. The effect of pump energy, signal energy, length of the fiber and the concentration of the dyes on the performance of the fiber amplifier is studied.*

### **2.1 Introduction**

Polymer optical fibers (POF) have attracted much attention during the past two decades for short distance communication because of their unique characteristics, such as flexibility, easiness in handling and relative low cost in coupling [1-7]. Although higher loss factor is a major handicap for POF, recently developed techniques for decreasing losses in polymethylmethacrylate based POF have raised much interest in this field [8]. Implementation of optical communication in the visible region demands the development of suitable optical amplifiers working in this region. POFs doped with dyes or rare earth elements are potential candidates for this purpose [9-19]. Laser dyes, which act as highly efficient media for lasing and amplification, have a wide range of tunability in the visible region.

Dye molecules that have large absorption and induced emission cross sections due to allowed pi-pi transitions are ideal active dopants for the generation and amplification of light pulses. The advantage of incorporating laser dyes in solid matrices such as POF is that it is easier and safer to handle them than when they are in liquid form. The first optical amplification in dye doped polymer optical fiber was demonstrated by researchers in Japan [10, 11]. In their experiment using a dye-doped gradient index (GI) POF, maximum gain of 27 dB was achieved at 591 nm wavelength with a pump power of 11kW. Also, G D Peng et al have achieved high gain and high efficiency optical amplification in a rhodamine B doped POF with a low pump power of 1kW [12] and Karimi et al have reported a high gain of 30 dB in Rh B doped POF [16]. Microstructured POF fiber based amplifier with a high gain of 30 dB has been reported by Argyros et al [20]. Reilly et al have achieved a gain of 14dB in a polymer waveguide with dye doped cladding [21]. Xu et al have reported optical amplification in rare earth doped polymer optical fibers [22].

Perhaps the most unique advantage of a dye doped polymer is the fact that it can be impregnated with several different dyes simultaneously to make a broad-band amplifier [2, 23-25]. Implementation of wavelength-division-multiplexed optical communication system demands the development of optical fiber amplifiers which can be operated in a broad wavelength region. Here comes the application of the dye mixture doped POF amplifiers which is illustrated in this chapter.

This chapter is divided into two sections. Fabrication of dye doped polymer preforms, the drawing of polymer optical fibers using the fiber drawing station developed in our laboratory and the characterization of the fabricated fibers are discussed in the first part. Development of dye mixture doped polymer optical fiber amplifier which can be used for amplifying signals in a broad wavelength region of the visible spectrum is discussed in the second part [24].

## **2.2 Part I : Fabrication and characterization of dye mixture doped polymer optical fibers**

### **2.2.1 Materials**

Rhodamine 6G and rhodamine B dye mixture doped polymethylmethacrylate based polymer optical fiber is used as the gain medium for amplifying optical signals in a broad region of the visible spectrum.

#### **2.2.1.1 Host material: Polymethylmethacrylate (PMMA)**

The material most frequently used for polymer fibers is PMMA ,better known as Plexiglass ,which belongs to the thermoplastics family. PMMA is chosen as the host as it has good optical quality and is compatible with most of the organic dyes used as dopants. Fig 2.1 shows the structure of monomer and its bonding to form polymer chains.

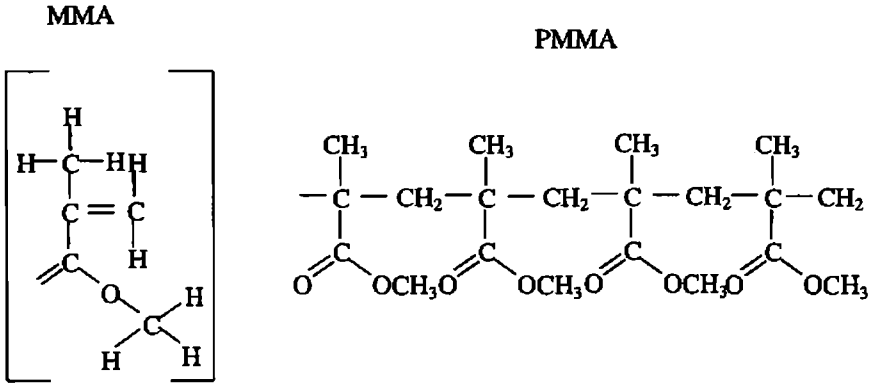


Fig 2.1: Molecular structure of PMMA

PMMA is an organic compound forming long chains with typical molecular weights around  $10^5$ . The refractive index of PMMA is 1.492 and the glass transition temperature,  $T_g$  lies between  $+95\text{ }^\circ\text{C}$  and  $+125\text{ }^\circ\text{C}$ . Each MMA monomer has a total of eight C-H bonds. The vibrations of this compound, or more precisely its harmonic waves, are the main cause for the absorptive losses encountered in PMMA polymer fibers along with the Rayleigh scattering losses which is proportional to  $1/\lambda^4$ . In particular the harmonic waves at 627 nm (6<sup>th</sup> harmonic wave) and 736 nm (5<sup>th</sup> harmonic wave) essentially determine the level of attenuation within the application range of PMMA-POF. The wavelength-dependent attenuation curve of a PMMA-POF (Fig 2.2) shows mainly three attenuation minima at wavelengths 520 nm, 570 nm and 650 nm which can be used for POF based communication systems [3].

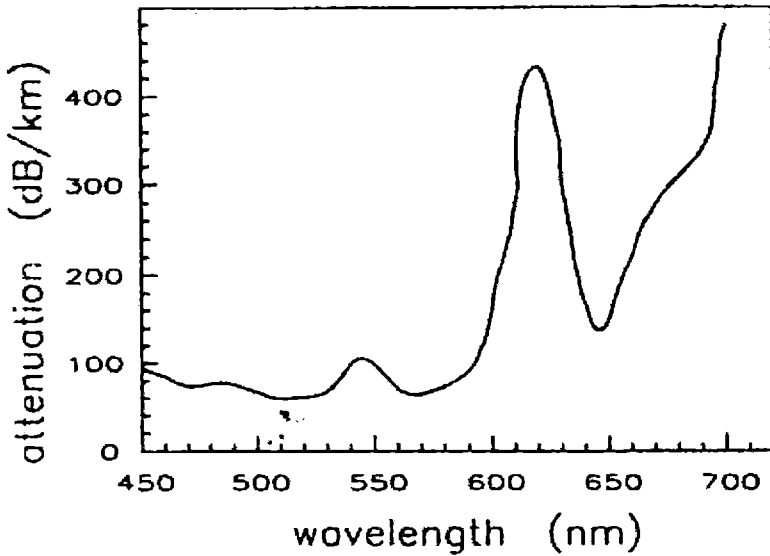


Fig 2.2: Attenuation spectrum of PMMA based POF [3].

### 2.2.1.2 Dyes : Rhodamine 6G and Rhodamine B

Rh 6G and Rh B belong to the family of xanthene dyes and are generally very efficient. They have high quantum yield, low inter system crossing rate, low excited state absorption at both pump and lasing wavelengths and reasonably good photostability [26-28]. Molecular structure of Rh 6G and Rh B is shown in Fig 2.3.

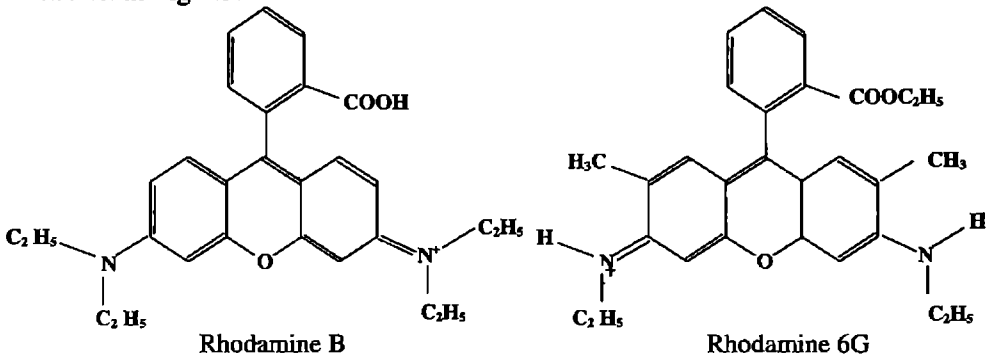


Fig 2.3: Molecular structure of Rh 6G and Rh B [26].



### 2.2.2 Energy level structure of a dye molecule

Organic dye molecules are large and complex and are characterized by a strong absorption band in the visible region of the electromagnetic spectrum. A schematic representation of the energy levels of an organic dye molecule (such as Rh 6G, for example) is shown in Fig 2.4.  $S_0$  is the ground state.  $S_1$ ,  $S_2$ ,  $T_1$  and  $T_2$  are excited electronic states. Typical energy separation, such as  $S_0 - S_1$  is about  $20,000 \text{ cm}^{-1}$ .

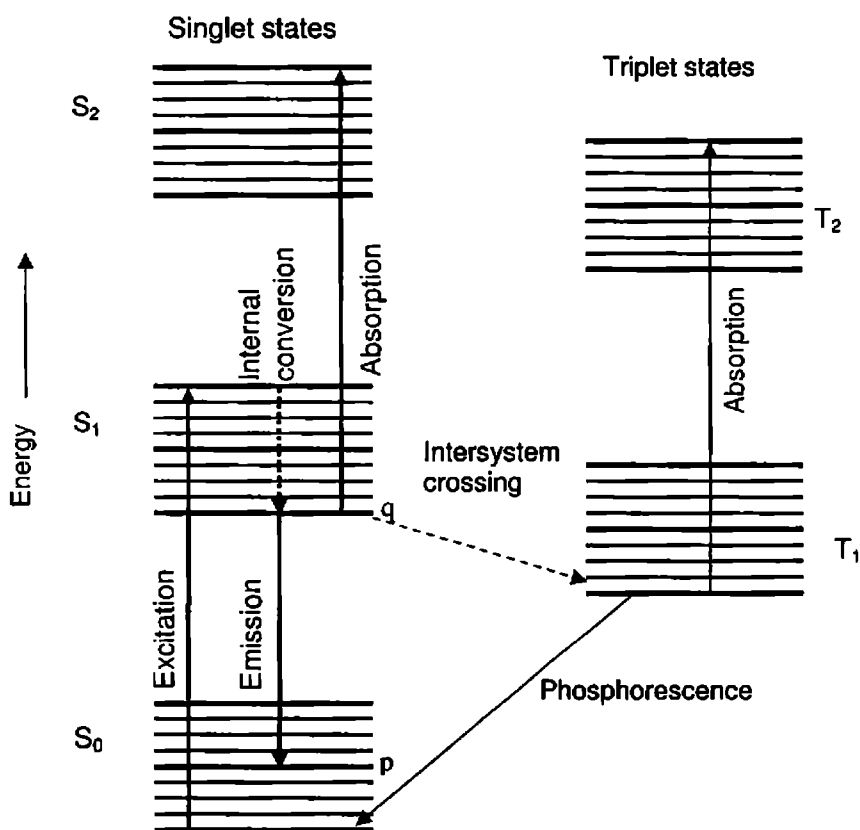


Fig 2.4: Schematic representation of the energy levels of an organic dye molecule.

In a singlet ( $S$ ) state, the magnetic spin of the excited electron is antiparallel to the spin of the electrons in the remaining molecules. In a triplet ( $T$ ) state,

the spins are parallel. Transitions between two singlet states or between two triplet states, which are spin-allowed, give rise to intense absorption and fluorescence. The characteristic color of the organic dyes is due to the  $S_0$ - $S_1$  absorption. The singlet and triplet states are further split into vibrational levels shown as heavy horizontal lines. Typical energy separation between two adjacent vibrational levels within a singlet or triplet state is about  $1500\text{ cm}^{-1}$ . The fine splitting between vibrational levels corresponds to rotational levels for which spacing is about  $15\text{ cm}^{-1}$ . In the process of pumping the dye molecule, it is first excited, by the absorption of a pump photon, into some of the upper rotational-vibrational state within  $S_1$ . This is followed by a very fast decay within picoseconds to the bottom of the  $S_1$  group, level  $q$ , by a process called the internal conversion. Most of the excited molecules will then decay spontaneously with a lifetime of the order of nanoseconds to the level  $p$  of the ground state  $S_0$  by emitting a photon of frequency  $\nu = (E_q - E_p)/h$ . This transition  $S_1 - S_0$  is responsible for the spontaneous emission known as fluorescence. There is also a small probability that an excited molecule can decay to the triplet state  $T_1$  by a spin-forbidden transition called inter-system crossing. The lifetime for radiative decay of  $T_1$  to the ground state by a process called phosphorescence is relatively long of the order of milliseconds. The absorption of molecules due to  $T_1 - T_2$  transition is spin-allowed and is therefore very strong [26-28].

### 2.2.3 Fabrication of dye doped polymer optical fibers.

A step index polymer optical fiber (SI-POF) has a simple structure of a concentric core and a cladding. The most common methods used for fabricating a SI-POF are a) Continuous extrusion method b) Preform method[1].

## Optical amplifier

Preform method is the conventional method for the manufacture of glass optical fibers and the same process is applied for the manufacture of POFs. This method involves two stages. In the first stage, a high quality cylindrical preform of required diameter and length is fabricated. In the second stage, the preform is drawn into a fiber by the heat-drawing process.

Preform method is adopted in the present case for fabricating dye doped POF [18, 19, 24, 29]. In the first stage, a cylindrical preform of 1.5 cm in diameter and 15 cm in length is fabricated. In the second stage, this preform is drawn into a fiber using the oven of the fiber drawing station at our laboratory. The base material used for the fabrication of polymer preform is methylmethacrylate (MMA) monomer. The refractive index of pure methylmethacrylate is about 1.41 and it will increase upto 1.48 to 1.49 due to volume reduction during phase transition from liquid to solid. Present studies are concentrated primarily on bare core fibers with air acting as cladding.

Commercially available MMA will contain inhibitors like hydroquinons. Inhibitors are used for suppressing polymerization during the transport of MMA. Inhibitors are removed by repeatedly washing the monomer with 5% NaOH solution followed by flushing it with distilled water. The remaining water is removed by adding suitable drying agents like  $\text{CaCl}_2$ . The monomer is then purified by distillation under reduced pressure.

Suitable initiators like benzoyl peroxide or azobisisobutyronitrile (AIBN) can be used to start the polymerization. Benzoyl peroxide is used for the present study as there is no gas evolution during polymerization as in the case of AIBN. This reduces the possibility of air bubble formation in the polymer preforms. Along with the initiator, n-butyl mercaptan is used as the chain transfer agent to regulate and terminate the polymerization process. Addition

of appropriate quantity of chain transfer agent and initiator controls the molecular weight of the polymer. The molecular weight regulation is an important factor that governs the drawability of the polymer preform. An optimum molecular weight (typically between 60000 and 100000) is fixed by adding 0.01 M benzoyl peroxide and 0.06 M mercaptan through numerous trials. To make dye mixture doped fibers, i) 0.25 mM Rh 6G and 0.11 mM Rh B and ii) 0.25 mM Rh 6G and 0.25 mM Rh B are added into two conical flasks containing the monomer and the resulting mixture is stirred well so as to avoid aggregate formation.

The monomer mixed with initiator, dyes and chain transfer agent is poured into a glass test tube of 1.7 cm diameter and 15 cm length. This is then kept in a constant temperature bath at 70 °C for 48 hours and at 90 °C for 18 hours. These steps lead to high quality polymer preforms which can be used for drawing the fiber. The prepared preform can be drawn to fiber in a custom-made fiber drawing tower. By using a preform feeder, the preform is lowered into the oven of the fiber drawing station and fiber is drawn at a temperature of 160 °C. The fiber diameter can be varied by adjusting the feed rate of the preform and the draw rate of the fiber.

#### **2.2.4 Characterization**

The application of dye doped materials and fibers ranges from optical communication devices such as fiber amplifiers and lasers to chemical sensors, radiation sensors, memories and illuminators. Improvement in the performance of these devices requires thorough knowledge of the absorption and emission characteristics of the dye doped fibers.

##### **2.2.4.1 Absorption spectrum**

For our investigations on the dye mixture doped POF amplifier, four fiber samples with a diameter of 510  $\mu\text{m}$  are used having the following dye concentrations. a) Rh 6G (0.25 mM) b) Rh 6G (0.25 mM) & Rh B (0.11 mM)

c) Rh6G (0.25 mM) & Rh B(0.25 mM) d) Rh B(0.25 mM). To select the pump beam for exciting the dye doped fiber, the absorption spectra of the above mentioned four dye doped PMMA bulk samples are recorded using a spectrophotometer (JASCO UV/VIS/NIR V-570), which is shown in Fig 2.5. It is clear from the spectra that the absorption peaks of the samples are in the wavelength range of 530-550 nm.

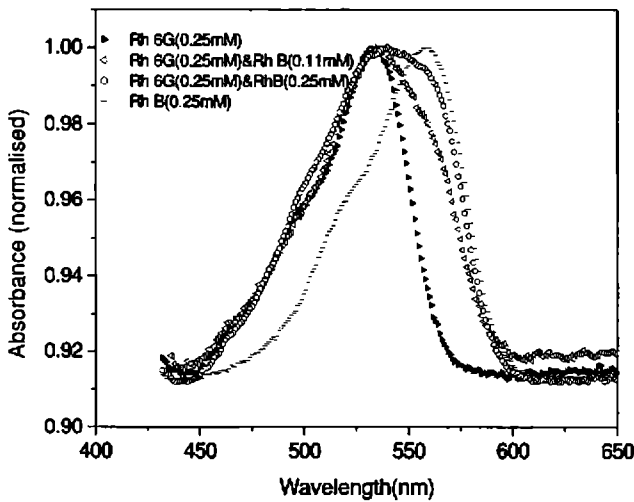
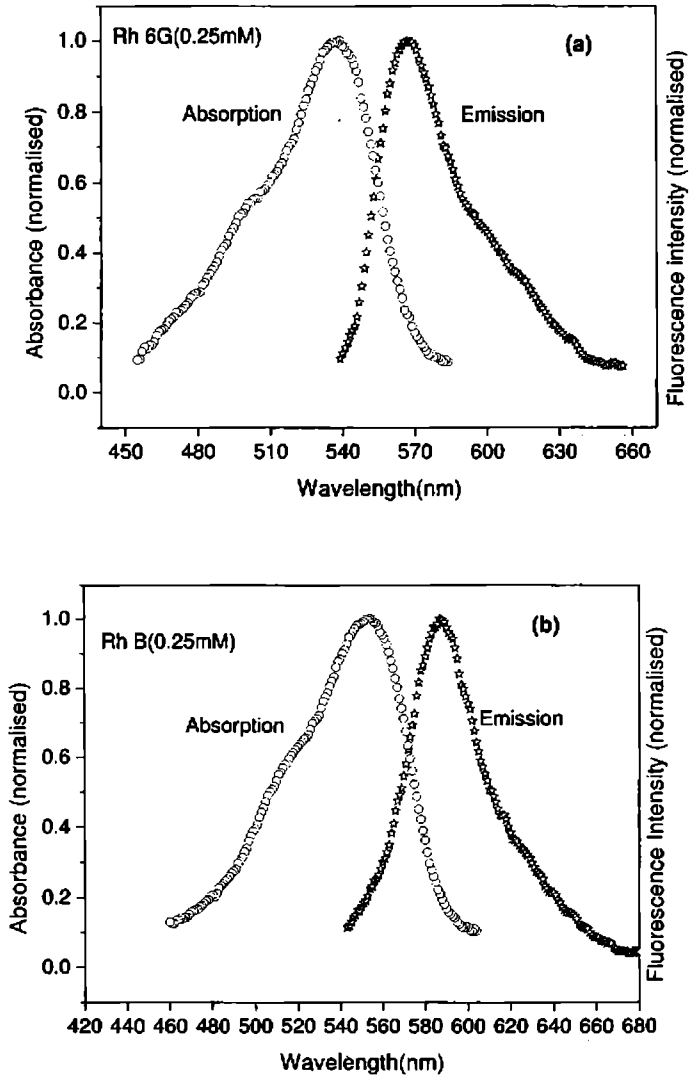


Fig 2.5: Absorption spectra of Rh 6G, Rh B and dye mixture doped PMMA samples.

#### **2.2.4.2 Spectral overlap between absorption and emission bands.**

Fluorescence emission spectra of dye doped PMMA bulk samples are recorded using a spectrofluorimeter (Varian Cary eclipse). Fluorescence peak wavelength is Stoke shifted by about 30nm with respect to the absorption maximum as shown in Fig 2.6 for two typical samples, Rh 6G and Rh B. Also, there is a clear overlap between the shorter wavelength part of the emission band and the longer wavelength tail of the absorption band which indicates that the fluorescence emission can be self absorbed by the dye molecules and re-emitted at a slightly longer wavelength [18,30].



**Fig 2.6:** Spectral overlap between the absorption and emission bands of *a)* Rh 6G (0.25 mM) *b)* Rh B (0.25 mM) doped PMMA samples.

### 2.2.4.3 Spectral overlap between Rh 6G emission and Rh B absorption bands.

There is a clear overlap between the Rh 6G emission and Rh B absorption bands as shown in Fig 2.7 which indicates that energy transfer is possible from Rh 6G (donor) to Rh B (acceptor) in a Rh 6G: Rh B dye mixture system. This energy transfer effect is made use of in Rh6G: Rh B dye mixture doped POF system for developing an optical fiber amplifier which can be operated in a broader wavelength region compared to single dye doped POF system and the same will be discussed in the part II section of this chapter.

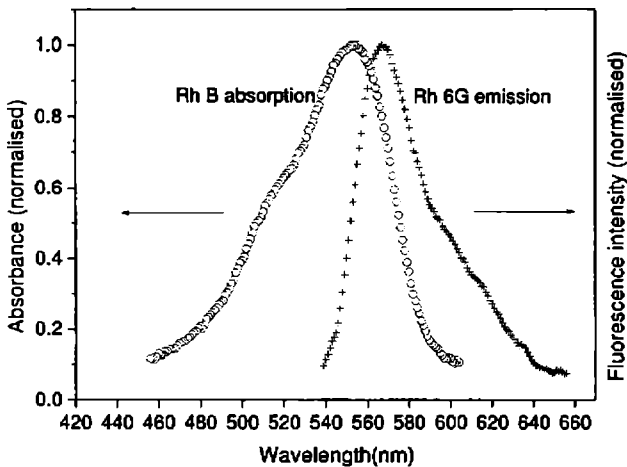


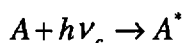
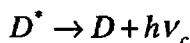
Fig 2.7: Spectral overlap between the absorption bands of Rh B (0.25 mM) doped PMMA and emission bands of Rh 6G (0.25 mM) doped PMMA samples.

Mainly two types of energy transfer can be possible in a Rh 6G: Rh B dye mixture system and is discussed in the following section [31].

#### a) Radiative energy transfer

The radiative energy transfer involves the emission of a photon by the donor molecule and its subsequent absorption by the acceptor, which causes its fluorescence. For this mechanism, the donor emission is affected by the

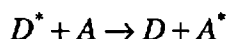
absorption of the acceptor molecule. This energy transfer mechanism can be figured as



where  $D^*$  is the donor molecule in the excited state and  $A$  is the acceptor molecule in the ground state.

**b) Non-radiative energy transfer**

Non-radiative energy transfer occurs because of the interaction between donor and acceptor molecules during the excitation lifetime of the donor, before its emission of a photon. This energy transfer mechanism can be figured as



This is possible in two ways.

**1) Fluorescence resonance energy transfer (FRET)**

FRET is a non-radiative type energy transfer due to long-range dipole-dipole interaction between donor and acceptor molecules. This type of energy transfer is effective when the distance between the donor and the acceptor molecule is in the range of 10-90 Å.

FRET is often interpreted in terms of Forster theory which yields the expression for the rate of energy transfer  $K_T$  as

$$K_T = \frac{1}{\tau_D} \left( \frac{R_0}{R} \right)^6 \quad (2.1)$$

where  $R$  is the donor-acceptor separation,  $\tau_D$  is the decay time of the excited state of the donor in the absence of the acceptor and  $R_0$  is the Forster radius which is the characteristic distance between donor and acceptor molecule at which the energy transfer efficiency is 50%.



**2) Diffusion-controlled collisional energy transfer**

This process is a non-radiative energy transfer process where the excitation energy of the donor is transferred to the acceptor via collisions. This process occurs over intermolecular distances of the order of molecular distances. In many cases, these two mechanisms of energy transfer processes, radiative and non-radiative, act simultaneously and it is difficult to distinguish between them.

**2.2.4.4 Redshift in fluorescence peak emission**

Fig 2.8 shows the peak fluorescence emission wavelength of different lengths of a dye doped POF sample pumped axially by a 532 nm pulsed laser beam from a frequency doubled Nd: YAG laser. A redshift is observed for the peak emission wavelength as the length of the fiber is increased as a result of the spectral overlap between the absorption and emission spectra of dye molecules [19, 29, 30].

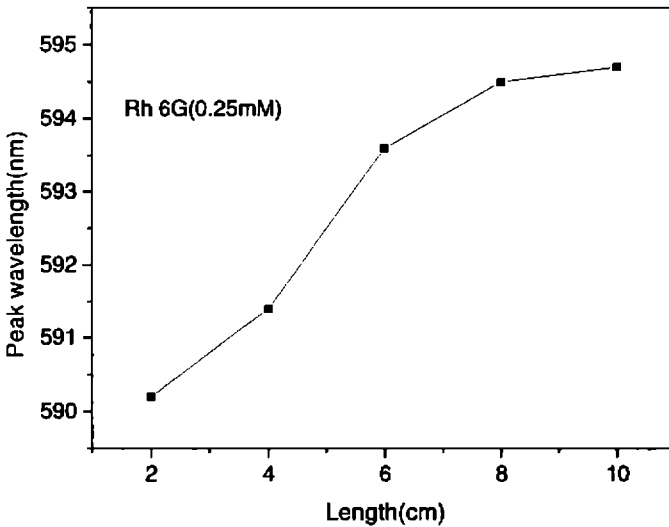


**Fig 2.8: Length dependent red shift in fluorescence peak**

As the fluorescence light is guided through the dye doped POF, interaction with the dye molecules increases the re-absorption and re-emission resulting

in the redshift of the emission spectrum. This redshift is equivalent to the concentration dependent redshift observed in dye molecules [26]. This characteristic elucidates the potentiality of the dye doped POF as a length dependent wavelength tunable device.

#### 2.2.4.5 Uniformity in dye concentration

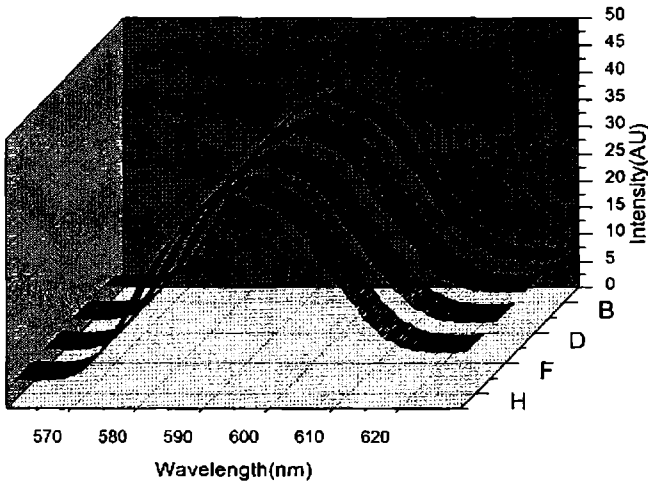


**Fig 2.9:** Fluorescence spectra of four fiber pieces taken from the same fiber.

The uniformity of dye concentration has an important role to play in optical amplification. If the dye concentration is not uniform or if there is aggregate formation of the dye, it will quench the fluorescence propagating through the fiber. This will adversely affect the overall gain of the fiber amplifier. In order to study the uniformity in dye concentration throughout the length of the fiber, a fiber of total length 20 cm is taken. This fiber is then cut into four equal lengths of 5 cm each and the fluorescence spectrum is charted for each of these individual lengths. The plots in Fig 2.9 shows the fluorescence spectra of the four individual fibers cut from the same dye doped POF

sample. The four fiber samples show the same spectral behavior which implies that the dye is uniformly doped along the length of the fiber.

### **2.3 Part II : Development of dye mixture doped POF as a broad wavelength optical amplifier**

As mentioned earlier, dye doped POF is an ideal candidate for amplifying optical signals in the visible region [9-19]. The important difference between spontaneous and stimulated emission is that, although the former is random and incoherent, the latter is phase coherent with the incident radiation. This characteristic is used in the amplification of optical signals and in lasers for the generation of coherent radiation.

The necessary condition for a medium to be an amplifying one is the occurrence of population inversion in the medium. In the case of dye doped POF, this population inversion is achieved by pumping it with high energy laser pulses. Development of dye mixture doped POF as a broad wavelength optical amplifier and the variation of gain with different parameters like pump energy, signal energy, length of the gain medium and concentration of the dyes are discussed in this section.

#### **2.3.1 Theoretical background: Rate equation approach**

In order to analyze the amplification in the dye doped POF, it is assumed that the amplifier is a three level system and that the decay of the vibrational energy in the first excited singlet state  $S_1$  is extremely fast [16]. Thus the population densities of each of these levels are described as follows.

$$N_3(t, z) \cong 0 \quad (2.2)$$

$$N_t = N_1(t, z) + N_2(t, z), \quad (2.3)$$

where  $N_i$  is the population density of level  $i$  at a position  $z$  along the fiber at a time  $t$  and  $N_t$  is the total population density of dyes in the fiber.

The rate equation for level 2 can be written as

$$\frac{\partial N_2(t, z, r)}{\partial t} = \frac{2\pi\sigma_p^a N_1(t, z) I_p(t, z)}{h\nu_p} \eta - \frac{N_2(t, z)}{\tau} - \frac{2\pi(\sigma_s^e N_2(t, z) - \sigma_s^a N_1(t, z) I_s(t, z))}{h\nu_s} \eta \quad (2.4)$$

The signal and pump pulses propagates in the positive direction of the fiber axis, according to

$$\frac{\partial I_s(t, z, r)}{\partial z} = 2\pi(\sigma_s^e N_2(t, z) - \sigma_s^a N_1(t, z)) I_s(t, z) \eta \quad (2.5)$$

$$\frac{\partial I_p(t, z, r)}{\partial z} = -2\pi\sigma_p^a N_1(t, z) I_p(t, z) \eta \quad (2.6)$$

where  $I_p$  and  $I_s$  are the pump and signal intensities, respectively,  $\sigma_a^p$  and  $\sigma_a^s$  are absorption cross sections at the pump and signal wavelengths,  $\sigma_e^s$  is the emission cross section at the signal wavelength,  $\nu_p$  and  $\nu_s$  are frequencies of the pump and the signal,  $h$  is Planks constant,  $\tau$  is the steady state lifetime of the dye in the metastable level,  $z$  is the direction of propagation of light in the fiber and  $\eta$  is the overlap integral which is defined as

$$\eta = \int_0^{a_0} \theta(r) \bar{\psi}(r) r dr \quad (2.7)$$

## Optical amplifier

where  $\theta(r)$  and  $\bar{\psi}(r)$  are the dye and the pump distributions, respectively, and  $a_0$  is the core radius.

In the steady state, the population density of the second level can be assumed to be constant and hence  $((\delta N_2 / \delta t) = 0)$ .

The time independent signal and pump evolutions can be expressed as

$$\frac{\partial I_s(z, r)}{\partial z} = \eta \frac{\left( \frac{\sigma_s^e \sigma_p^a}{h\nu_p} \right) I_p(z) + \frac{\sigma_s^a}{\tau}}{\left( \frac{\sigma_p^a}{h\nu_p} \right) I_p(z) + \left( \frac{\sigma_s^e + \sigma_s^a}{h\nu_s} \right) I_s(z) + \frac{1}{\tau\eta}} I_s(z) N_1 - k_s I_s(z), \quad (2.8)$$

$$\frac{\partial I_p(z, r)}{\partial z} = -\eta \frac{\left( \frac{\sigma_s^e \sigma_p^a}{h\nu_s} \right) I_s(z) + \frac{\sigma_p^a}{\tau}}{\left( \frac{\sigma_p^a}{h\nu_p} \right) I_p(z) + \left( \frac{\sigma_s^e + \sigma_s^a}{h\nu_s} \right) I_s(z) + \frac{1}{\tau\eta}} I_p(z) N_1 - k_p I_p(z), \quad (2.9)$$

where  $k_s$  and  $k_p$  are the fiber loss at signal and pump wavelengths, respectively. The time independent rate equations were solved by the Runge-Kutta method to derive the gain evolution of the amplifier [[16].

The small signal gain coefficient of the amplifier is given by

$$g(z) = \eta \frac{\left( \frac{\sigma_s^e \sigma_p^a}{h\nu_p} \right) I_p(z) + \frac{\sigma_s^a}{\tau}}{\left( \frac{\sigma_p^a}{h\nu_p} \right) I_p(z) + \left( \frac{\sigma_s^e + \sigma_s^a}{h\nu_s} \right) I_s(z) + \frac{1}{\tau\eta}} \times N_1 - k_s \quad (2.10)$$

Since the pump power must be high in dye doped amplifier, the signal power can be ignored.

Then the gain coefficient becomes

$$g_0 = \eta \frac{\left( \frac{\sigma_s^e \sigma_p^a}{h\nu_p} \right) I_p(z) + \frac{\sigma_s^a}{\tau}}{\left( \frac{\sigma_p^a}{h\nu_p} \right) I_p(z) + \frac{1}{\tau\eta}} \times N_t - k_s \quad (2.11)$$

Thus, the signal variation along the length of the fiber can be written as

$$I_s(z) = I_{0s} \exp(g_0 z), \text{ at constant pump power.} \quad (2.12)$$

Equation 2.10 implies that the gain of the amplifier increases with the concentration of the dye molecules,  $N_t$ . At very high concentration, the amplifier gain will reduce because of the quenching effect. As length of the gain medium increases amplifier gain will also increase as a result of the interaction with more number of dye molecules and this is equivalent to increase in concentration. There is an optimum length at a particular pump power at which the amplifier gain will be maximum and after this length the gain decreases due to absorption by the medium. Again, the amplifier gain will increase with increase in pump power and gain saturation will occur at higher pump powers. The amplifier gain doesn't depend strongly on the input signal power at low values and the gain in this case is given by according to equation 2.11. But the gain will reduce at high signal powers according to equation 2.10.

**2.3.2 Experiment**

A schematic of the experimental set up for the amplification studies is shown in Fig 2.10. The pump source is a frequency doubled Q-switched Nd: YAG laser at 532 nm wavelength at which the dye doped POF has high absorption and the signal source is a tunable output from an optical parametric oscillator which is pumped by the third harmonic at 355 nm from the same Nd: YAG laser.

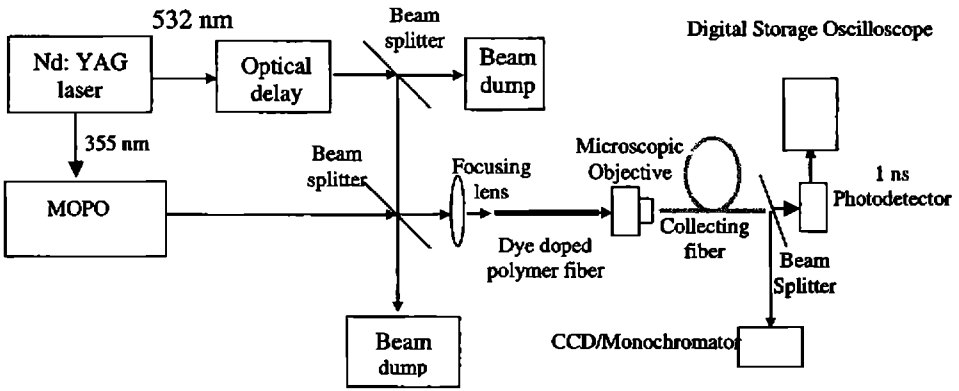


**Fig 2.10:** Experimental set up for the amplification studies in dye doped POF.

The full-width at half maximum of both the signal and the pump pulses is about 10 ns and the repetition rate of the pulses is 10 Hz. The pump beam is combined with the signal beam both temporally as well as spatially by using an appropriate optical delay system and beam splitter and are coaxially launched into the dye doped POF. A convex lens of 7 cm focal length is used to focus the pump and signal beams to the fiber. A photodetector of 1ns response time (Newfocus 1621) along with a 1 GHz digital storage oscilloscope (Tektronix TDS 540) are used to monitor the amplified output. A monochromator–CCD-PC assembly (Acton spectrapro) is used to study the spectral response of the output signal.

For investigating the effect of pump pulse energy and length of the dye doped POF on the gain of the amplifier, pump energy is varied from 0.01 mJ-0.07 mJ/pulse and the fiber length is varied from 3-11cm. The signal pulse energy is kept at  $0.1 \mu\text{J/pulse}$  in these studies.

### 2.3.3 Results and discussions

#### 2.3.3.1 Energy transfer in dye doped POF

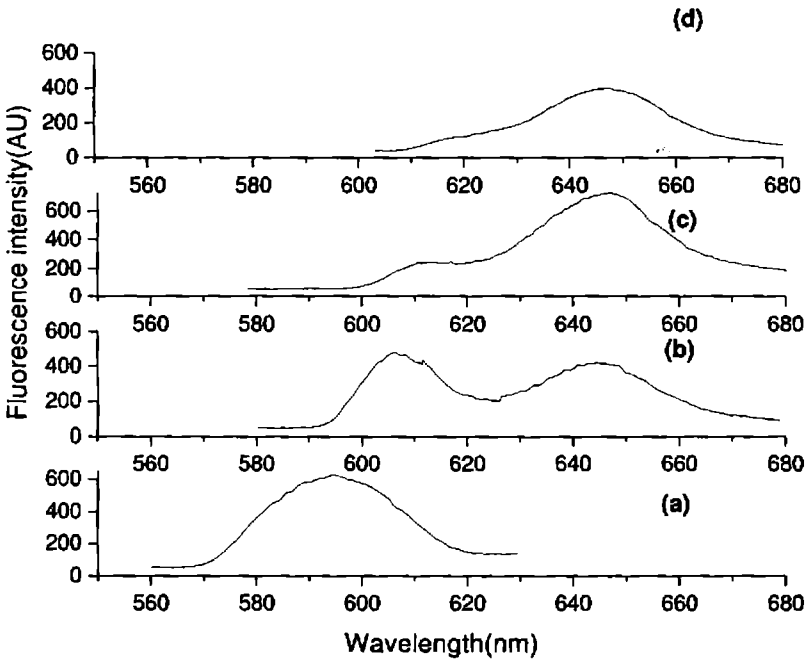


**Fig 2.11:** Shift of the fluorescence emission peak due to energy transfer process in dye mixture doped POF *a)* Rh 6G(0.25mM) *b)* dye mixture Rh 6G(0.25mM) & Rh B(0.11 mM) *c)* dye mixture Rh 6G(0.25 mM) & Rh B(0.25 mM) *d)* Rh B(0.25 mM). Pump energy is 0.06 mJ/pulse and length of the fiber is 7 cm.

Fig 2.11 shows a comparison of the fluorescence emission from POF doped with Rh 6G, Rh 6G- Rh B dye mixture and Rh B. The strong overlap between the emission spectrum of Rh 6G and absorption spectrum of Rh B (Fig 2.7), clearly indicates the possibility of energy transfer from Rh 6G to Rh B.



## Optical amplifier

Energy transfer of Rh 6G: Rh B dye mixtures in a PMMA matrix is well studied and is shown that energy transfer is occurring from Rh 6G to Rh B [32-34]. As discussed in part I section, the main mechanisms that have been reported for such an energy transfer are 1) Radiative transfer i.e, absorption of Rh 6G (donor) emission by Rh B molecule (acceptor) and 2) Non-radiative energy transfer (FRET & collisional transfer) .

In order to have an idea about the non radiative type fluorescence resonance energy transfer (FRET) in the Rh 6G-Rh B dye mixture system, the Forster distance  $R_0$  is evaluated using the equation[31,35-38],

$$(R_0)^6 = \frac{9000 \ln 10 K^2 \phi_d}{128 \pi^5 N n^4} \int F_D(\lambda) \epsilon_A(\lambda) \lambda^4 d\lambda \quad (2.13)$$

where  $R_0$ , known as Forster distance, is the characteristic distance between donor and acceptor molecule at which the energy transfer efficiency is 50%.  $\phi_d$  is the quantum yield of the donor in the absence of the acceptor which is taken as 0.75 in the case of Rh 6G in PMMA matrix [39],  $n$  is the refractive index of the medium which is taken as 1.49 for PMMA [40],  $N$  is Avogadro's number and  $k^2$  is the orientation factor of two dipoles interacting and is usually assumed to be equal to 2/3 for isotropic media [31].  $F_D(\lambda)$  is the corrected fluorescence intensity of the donor in the wavelength range  $\lambda$  to  $\lambda + \Delta \lambda$  with the total intensity normalised to unity.  $\epsilon_A(\lambda)$  is the extinction coefficient of the acceptor at  $\lambda$  which is in units of  $\text{Mol}^{-1}\text{cm}^{-1}$ .

$$\text{The overlap integral, } J(\lambda) = \int F_D(\lambda) \epsilon_A(\lambda) \lambda^4 d\lambda, \quad (2.14)$$

expresses the degree of spectral overlap between the donor emission and the acceptor absorption and is evaluated using a Matlab programme. Thus from equation (2.13),  $R_0$  is evaluated to be 55 Å which is within the limit of 10-90 Å for which FRET can be possible [31, 33, 41-43]. So it can be inferred that the non radiative FRET can be a possible mechanism in the

Rh 6G-Rh B dye mixture system along with the radiative type energy transfer. In the case of Rh 6G (0.25 mM) doped POF, fluorescence emission peak is observed to be at 594 nm (Fig 2.11a). Consider the case of Rh 6G (0.25 mM) and Rh B (0.11 mM) doped POF (Fig 2.11b). It is to be noted that both the dyes Rh 6G and Rh B can get excited by pump absorption and exhibit their own fluorescence in the dye mixture system since the quantum yield of fluorescence is almost equal for both the dyes. But as a result of the strong overlap between Rh 6G emission and Rh B absorption, energy transfer occurs from Rh 6G to Rh B through radiative (shorter wavelength part of the fluorescence emission of Rh 6G gets reabsorbed and reemitted by the Rh B molecules) and non radiative (FRET) paths. Therefore, Rh B molecules in the dye mixture system are excited both by direct pumping at 532 nm and by reabsorbing the energy transferred from the Rh 6G molecules.

Thus, in Fig 2.11b the fluorescence spectral peak is observed to be red shifted to 606 nm because of the energy transfer from Rh 6G to Rh B. Also, a second peak is observed at 647nm which is the characteristic peak from Rh B. In the case of Rh 6G (0.25 mM) and Rh B(0.25 mM) doped POF (Fig 2.11c), intensity of the first peak in the fluorescence emission becomes very less compared to the prominent peak at 647 nm. In this case the energy transfer from Rh 6G to Rh B is maximum and the spectrum looks almost the same as that of Rh B (0.25 mM) doped POF (Fig 2.11d). This is because of the fact that maximum energy transfer occurs when both dyes are taken in equal concentration [34]. Fig 2.11d represents the fluorescence spectrum corresponding to RhB (0.25 mM) alone.

Again, consider the fluorescence intensity of the three samples *b*, *c* and *d* in Fig 2.11. Compared to Rh B (0.25 mM) doped sample, the fluorescence intensity (for example at 647 nm) is slightly more in the case of

## Optical amplifier

Rh 6G(0.25 mM) and Rh B(0.11 mM) doped mixture sample as a result of the energy transfer from Rh 6G to Rh B. For Rh 6G (0.25 mM) and Rh B (0.25 mM) doped sample, the fluorescence intensity is enhanced more than that of the samples *b* and *d* because of the maximum energy transfer in this case. Table 2.1 summarises the above observations.

Concentration of samples.	Fluorescence intensity ( at 647nm) A.U
Rh B(0.25mM)	399
Rh6G(0.25mM) &RhB(0.11mM)	411
Rh 6G(0.25mM)& Rh B(0.25mM)	728

**Table 2.1:** Enhancement in Rh B fluorescence intensity as a result of the energy transfer from Rh6G to Rh B

Fig 2.11b also shows an enhancement of spectral width upto 60 nm compared to the 40 nm spectral width of Rh 6G doped POF (Fig 2.11a). This indicates the potentiality of the dye mixture doped POF as a medium for broad wavelength optical amplifier. In addition to the increase in the spectral width, central wavelength is shifted, and hence the amplification region needed for a particular application can be precisely determined by fine tuning the dye mixture.

### **2.3.3.2 Amplification of a weak signal**

To check the efficiency of the dye doped POF as an optical amplifier, experiments are carried out to measure the gain by injecting a weak signal (at 602 nm) and measuring the output intensity with and without the pump beam. Pump pulse energy is 0.06 mJ and the length of the POFA is always

selected as 7 cm. As can be seen from Fig 2.12, there is a clear signal amplification in the presence of pump source which proves beyond doubt that dye doped optical fiber can be used effectively as an amplifier in a communication link in the visible spectral region.

Gain of the amplifier is evaluated using the expression,

$$Gain_{dB} = 10 \log \frac{S_{output}}{S_{input}} \quad (2.15)$$

where  $S_{output}$  is the amplified output signal in the presence of the pump pulse and  $S_{input}$  is the input signal pulse.

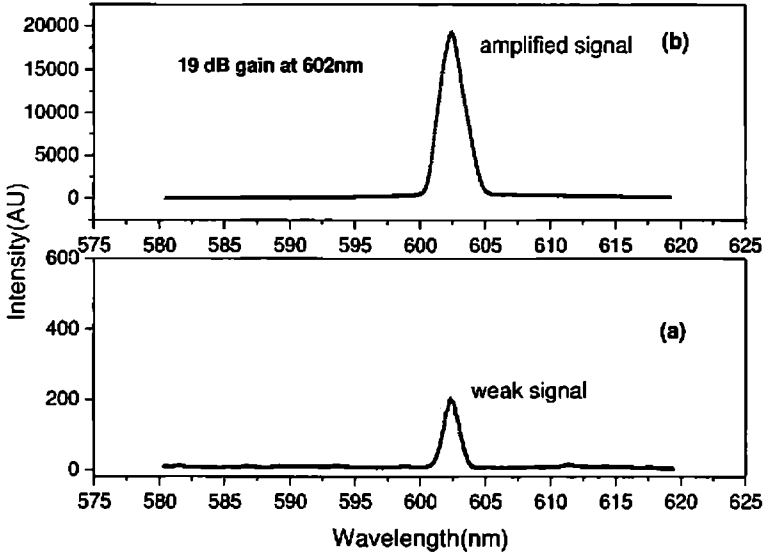


**Fig 2.12:** Amplification of a weak signal at 602 nm in a 7 cm long dye mixture doped POF amplifier {Rh 6G (0.25 mM) & Rh B(0.11 mM)}. Pump energy is 0.06 mJ/pulse and pump wavelength is 532 nm.

**2.3.3.3 Tuning range analysis of the amplifier gain**

Fig 2.13 depicts the gain for different signal wavelengths in the case of the above mentioned four dye doped POF samples under study. Maximum gain of 18 dB at 592 nm and a gain bandwidth of 40 nm (574-614 nm) is achieved in the case of Rh6G (0.25 mM) doped POF amplifier (Fig 2.13a). In the case of Rh6G (0.25 mM) and Rh B (0.11 mM) doped POF amplifier a maximum gain of 20dB is achieved at a redshifted wavelength of 608 nm (Fig 2.13b).

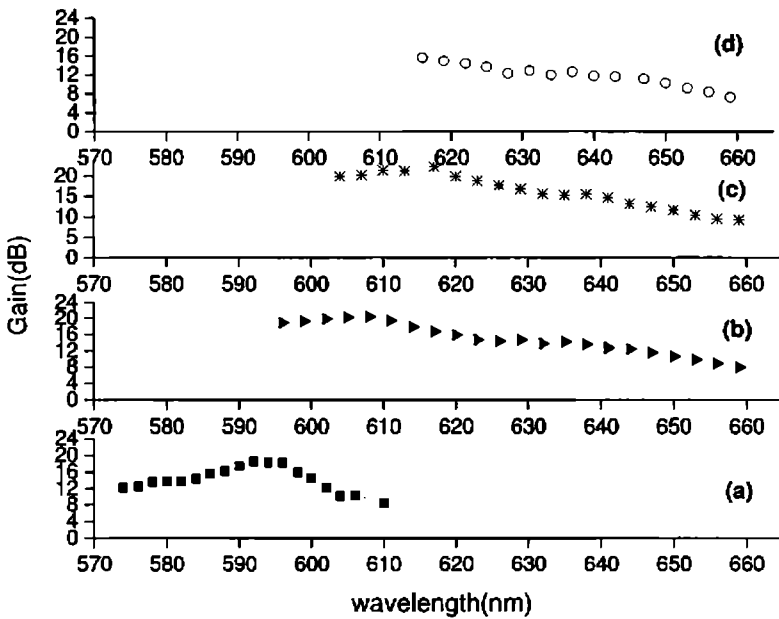


**Fig 2.13:** The gain for different signal wavelengths in a 7 cm long dye doped POF amplifier at pump wavelength 532 nm and pump energy 0.06 mJ/pulse. a) Rh 6G(0.25mM) b) dye mixture Rh 6G(0.25 mM) & Rh B(0.11 mM) c) dye mixture Rh 6G(0.25 mM) & Rh B(0.25 mM) d) Rh B(0.25mM).

Redshift of the maximum gain wavelength is due to the shift in fluorescence emission peak resulting from the energy transfer process in Rh 6G- RhB dye mixture system. The enhancement in the gain (20 dB) is the result of the increase in total dye molecules. In the case of dye mixture system, as

mentioned earlier, Rh B molecules are excited both by direct pumping at 532 nm and by reabsorbing the energy transferred from the Rh 6G molecules. Thus, the fluorescence intensity and gain is higher in this case.

Also, an increased gain bandwidth of about 60 nm (596-660 nm) is obtained in this case. In the case of Rh 6G (0.25 mM) and Rh B(0.25 mM) doped POFA amplifier, a maximum gain of 22 dB is observed at 617 nm which is higher than the previous two values because of the presence of more number of dye molecules and maximum energy transfer (Fig 2.13c). Here also, the gain bandwidth is about 60 nm. In RhB (0.25 mM) doped POFA amplifier a maximum gain of 15 dB is observed at 616 nm (Fig 2.13d). In addition to the increase in gain bandwidth, the amplification region needed for a particular application can also be controlled by selecting specific ratios of the dyes.

#### 2.3.3.4 Gain variation with input pump energy

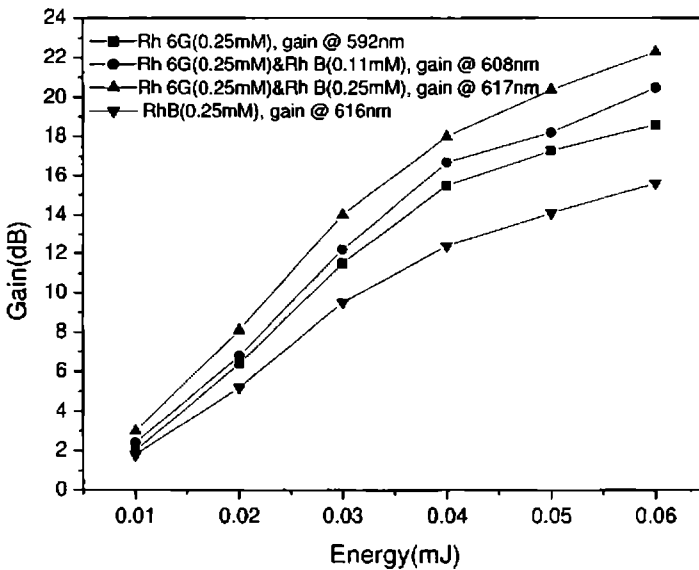


Fig 2.14: Gain dependence on the input pump energy of the dye doped POFA .Fiber length is 7cm.

## Optical amplifier

Fig 2.14 shows the variation in gain with the input pump energy for the four fiber samples under study. A linear dependence between the gain and the launching pump energy is observed upto 0.03 mJ/pulse. Above 0.03 mJ, the relationship deviates from linearity showing a tendency of gain saturation. The saturation behavior is essentially due to the fact that as the pump energy is increased, more and more dye molecules get inverted and for large pump energies almost the entire dye molecules are inverted. Once the saturation is reached, there will be no more increase in inversion and, hence, gain. [9-18].

### 2.3.3.5 Optimum length of amplifier

Fig 2.15 shows the variation in gain with length of the dye doped POFA amplifier at a pump energy of 0.06 mJ/pulse.

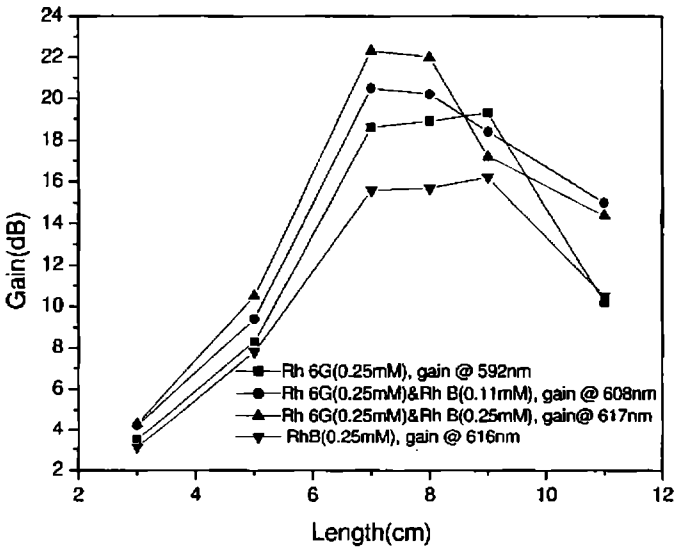
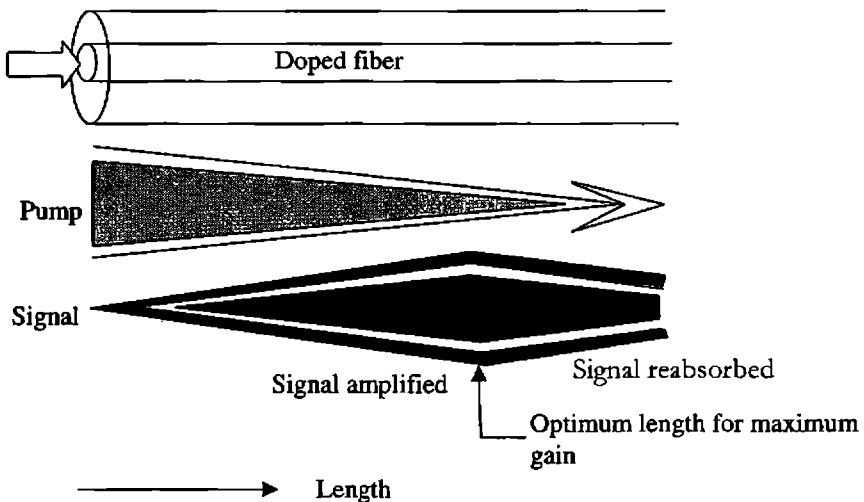


Fig 2.15: Gain dependence on the length of the POFA. Here the pump energy is 0.06 mJ/pulse.

It is clear from the plot that the gain increases with length upto an optimum length ( $L_z$ ) for which the amplifier gain is maximum and after this length the

gain reduces [9-18]. Signal gain increases upto this optimum length due to the stimulated emission in the inverted medium. Intensity of the pump beam gets reduced along the POFA as length increases due to absorption by the dye molecules. This results in a decrease of the population inversion of the medium as length increases. Thus, the signal absorption along the fiber medium dominates the stimulated emission beyond a certain length and the signal gain reduces.

In the case of Rh6G (0.25 mM) doped POFA and Rh B(0.25 mM) doped POFA, the optimum length for maximum gain is 9 cm at signal wavelengths 592 nm and 616 nm respectively and further increase in the length reduces the gain of the amplifier. In the case of the two dye mixture doped POFA, optimum length occurs at a shorter distance of 7 cm. This is because of the fact that with an increase in dye density, the optimum length of the amplifier becomes shorter. This optimum length actually depends on the input pump energy, because a longer length of inverted medium can be achieved by a higher pump energy [44, 45].



**Fig 2.16:** Schematic diagram showing variation of pump and signal powers with distance along the dye doped fiber.



## Optical amplifier

Fig 2.16 shows a schematic of the variation of pump and signal powers along the length of the dye doped POF. Near the input end, the pump power is high, leading to the population inversion and, hence, signal amplification. As the propagation distance increases, pump power reduces and, beyond the optimum length, the pump power is insufficient to create an inversion and, hence, the signal starts to get attenuated.

### 2.3.3.6 Gain variation with input signal energy

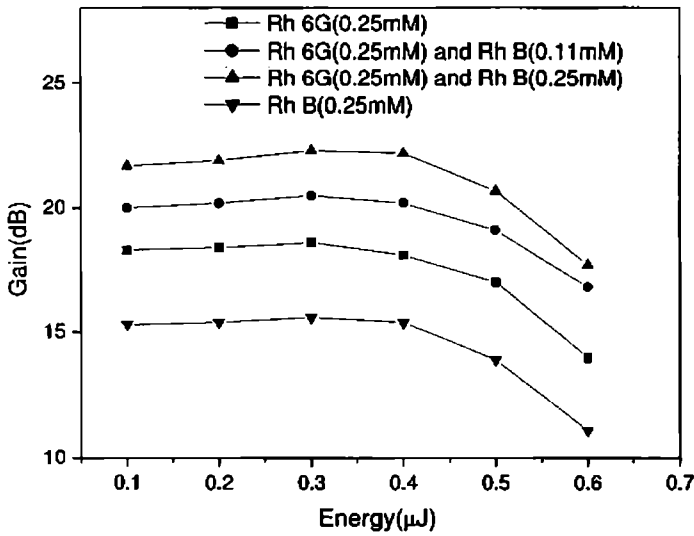
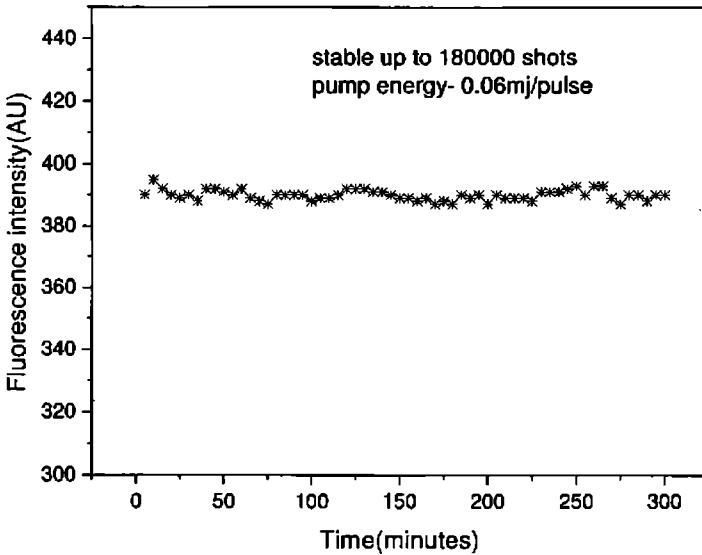


Fig 2.17: Gain dependence on the input signal energy. Here the pump energy is 0.06 mj/pulse

Fig 2.17 shows the variation of gain with the input signal pulse energy for the four fiber samples under study at constant pump energy. It is clear from the plot that the amplifier gain is independent of signal energy at low values and the same will be proportional to the small signal gain coefficient (Eq. 2.11). At higher signal energy, the gain decreases from the small signal gain value. This observation is in accordance with the theory discussed above (Eq.2.10) [45].

### 2.3.3.7 Photostability of dye doped POFA

One of the main concerns in developing solid-state dye doped gain media is their photostability. In order to investigate the photostability of the dye doped POF, a typical sample, Rh 6G(0.25 mM) and Rh B (0.11 mM) doped POF, is continuously pumped by the laser pulses of energy 0.06 mJ at which the amplification experiment is carried out and the fluorescence spectrum is recorded as a function of time for 300 minutes at intervals of 5 minutes. The fluorescence emission intensity at a typical wavelength (605 nm) is plotted against the time of exposure of the pump and is shown in Fig 2.18. The Fig shows that the fluorescence intensity is unaltered up to 180000 shots of pump pulse which indicates the stability of POFA within the duration of the optical amplification experiment. It should be noted that in order to identify any bleaching effect, study on the variation in fluorescence intensity with time of excitation is sufficient.



**Fig 2.18:** Graph showing the fluorescence intensity of the dye doped POF {sample doped with Rh6G (0.25mM) & Rh B (0.11mM) at 605 nm} versus the time of exposure of the pump pulse of energy 0.06 mJ at 532 nm.

## **2.4 Conclusions**

Dye doped polymer optical fiber is drawn successfully using the POF drawing station and absorption and emission characterizations of these fibers are investigated. A broad wavelength optical amplifier is successfully fabricated from Rh 6G: Rh B dye mixture doped POF. An increased gain bandwidth of about 60nm is obtained in Rh 6G: Rh B dye mixture doped POF amplifier compared to the 40nm gain bandwidth of Rh 6G doped POFA. Tunable operation of amplifier in different wavelength region is achieved by mixing different ratio of dyes. A high gain of 22 dB is achieved at 617 nm from a 7cm long dye mixture doped POFA. There exists an optimum length for the amplifier at which the gain is maximum. It is observed that the gain increases with pump energy and a tendency of gain saturation occurs at higher pump energies. The amplifier gain doesn't depend strongly on the input signal energy at low values and the gain reduces at high signal energies. The dye doped POFA is found to be stable up to 180000 shots of pump pulse.

---

**References**

1. H S Nalwa, *Polymer optical fibers* (American scientific publishers, 2004).
2. Mark G Kuzyk, *Polymer fiber optics-Materials, Physics and Applications*(Taylor &Francis group,2007).
3. W Daum, J Krauser,P E Zamzow and O Ziemann, *POF-Polymer Optical Fibers for Data Communication* (Springer, New York 2002).
4. Y Koike, T Ishigure and E Nihei, "High -bandwidth graded- index polymer optical fiber," *Journal of Lightwave Technology* **13**, 1475-1489(1995).
5. H Y Liu, G D Peng and P L Chu, "Thermal tuning of polymer optical fiber Bragg gratings," *Photonics Technology Letters* **13**,824-826(2001).
6. Martijin A.van Eijkelenborg, A Argyros,G Barton, I M Bassett,M Fellow,G Henry,N A Issa,M C J Large,S Manos,W Padden,L Poladian and Joseph Zagari, "Recent progress in microstructured polymer optical fiber fabrication and characterisation,"*Optical Fiber Technology* **9**, 199-209(2003).
7. F M Cox, A Argyros and M C J Large, "Liquid- filled hollow core microstructured polymer optical fiber," *Opt. Express* **14**, 4135-4140 (2006).
8. T Ishigure,Y Koike and J W Fleming, "Optimum index profile of the perfluorinated polymer based GI polymer optical fiber and its dispersion properties," *Journal of Lightwave Technology* **18**, 178-184(2000).
9. K Kuriki and Y Koike, "Plastic optical fiber lasers and amplifiers containing lanthanide complexes,"*Chem.Rev.* **102**, 2347-2356(2002).
10. A Tagaya,Y Koike,E Nihei,S Teramoto,K Fujii,T Yamamoto and K Sasaki, "Basic performance of an organic dye-doped polymer optical fiber amplifier,"*Appl.Opt* **34** 988-992(1995).
11. A Tagaya,Y Koike,T Kinoshita,E Nihei, T Yamamoto and K Sasaki, "Polymer optical fiber amplifier, " *Appl.Phys.Lett* **63**,883-884(1993).
12. G D Peng,P K Chu, Z Xiong, T W Whitbread and R P Chaplin, "Dye- doped step- index polymer optical fiber for broadband optical amplification," *Journal of Lightwave Technology* **14**, 2215-2223 (1996).

13. A Tagaya, S Teramoto, E Nihei, K Sasaki and Y Koike, "High-power and high-gain organic dye-doped polymer optical fiber amplifiers :novel techniques for preparation and spectral investigation," *Appl.Opt* **36**,572-578(1997).
14. A Tagaya, S Teramoto,T Yamamoto, K Fujii, E Nihei,Y Koike and K Sasaki,"Theoretical and experimental investigation of rhodamine B doped polymer optical fiber amplifiers,"*Journal of Quantum electronics* **31**, 2215-2220(1995).
15. H Liang,Q Zhang,Z Zheng,H Ming,Z Li,J Xu,B Chen and H Zhao,"Optical amplification of Eu(DBM)<sub>3</sub> phen-doped polymer optical fiber,"*Opt.Lett.* **29**,477-479(2004).
16. M Karimi,N Granpayeh,M K Morravegfarshi, "Analysis and design of a dye doped polymer optical fiber amplifier",*Appl.Phys.B* **78**,387-396(2004).
17. H Liang,Z Zheng,Z Li,J Xu,B Chen,H Zhao,Q Zhang and H Ming," Fabrication and Amplification of Rhodamine B doped Step-Index polymer optical fiber," *Journal of Applied Polymer Science* **93**,681-685(2004).
18. M Rajesh,M Sheeba, K Geetha,C P G Vallabhan,P Radhakrishnan and V P N Nampoori, "Fabrication and characterization of dye doped polymer optical fiber as a light amplifier," *Appl. Opt.* **46**,106-112 (2007).
19. M Rajesh, K Geetha, M Sheeba, C P G Vallabhan, P Radhakrishnan and V P N Nampoori, "Characterisation of rhodamine 6G doped polymer optical fiber by side illumination fluorescence," *Optical Engineering*, **45**, 075003-075004(2006).
20. A Argyros, M A van Eijkelenborg, S D Jackson and R P Mildren , "Microstructured polymer fiber laser" *Opt.Lett* **29**, 1882-1884(2004).
21. M A Reilly, B Coleman, E Y B Pun, R V Penty and I H White, "Optical gain at 650nm from a polymer waveguide with dye doped cladding" *Appl. Phys.Lett.* **87**, 231116-231119(2005).
22. X Xu, "Properties of Nd<sup>3+</sup> -doped polymer optical fiber amplifiers, " *Opt.Commun* **225**, 55-59(2003).

23. Y Yang, J Zou, H Rong, G D Qian, Z Y Wang and M Q Wang, "Influence of various coumarin dyes on the laser performance of laser dyes co-doped in to ORMOSILs," *Appl. Phys. B* **86**, 309-313 (2006).
24. M Sheeba, M Rajesh, V P N Nampoore and P Radhakrishnan "Fabrication and characterization of dye-mixture-doped polymer optical fiber as a broad wavelength light amplifier," *Appl. Opt.* **47**,1907-1912 (2008).
25. B J Scott, M H Bartl, G Wirnsberger and G D Stucky, "Energy transfer in dye-doped mesostructured composites," *J.Phys.Chem. A* **107**, 5499-5502(2003).
26. K H Drexhage and F P Schafer, *dye lasers*(Springer Verlag, 1977).
27. B E A Saleh and M C Tech, *Fundamentals of photonics* (Wiley Interscience, 1991).
28. A Yariv, *Optical electronics* (Saunders college publishing, 1971).
29. M Sheeba, K J Thomas, M Rajesh, V P N Nampoore, C P G Vallabhan and P Radhakrishnan, "Multimode laser emission from dye doped polymer optical fiber," *Appl.Opt* **46**, 8089-8094(2007).
30. K Geetha, M Rajesh, V P N Nampoore, C P G Vallabhan and P Radhakrishnan, "Loss characterisation in rhodamine 6G doped polymer film waveguide by side illumination fluorescence," *J.Opt. A, Pure. Appl.Opt* **6**, 379-383(2004).
31. Joseph R Lakowicz, *Principles of fluorescence spectroscopy* (Springer, 2006).
32. G A Kumar, Vinoy Thomas, Gijo Thomas, N V Unnikrishnan, and V P N Nampoore "Energy Transfer in Rh 6G: Rh B system in PMMA matrix under CW laser excitation," *J.Photochem.Photobiol A: Chemistry* **153**,145-151(2002).
33. N V Unnikrishnan, H S Bhatti and R D Singh, "Energy transfer in dye mixtures studied by laser fluorimetry," *Journal of Modern Optics*.**31**, 983-987(1984).
34. P J Sebastian and K Sathianandan , "Donor concentration dependence of the emission peak in rhodamine 6G-rhodamine B energy transfer dye laser," *Opt. Commun.***35**,113-114(1980).

35. Forster T, "Transfer mechanisms of electronic excitations," Discuss .Faraday Soc 27, 7-17(1959).
36. D Seth, D Chakrabarty, A Chakraborty and N Sarkar, " Study of energy transfer from 7-amino coumarin donors to rhodamine 6G acceptor in non-aqueous reverse micelles, " Chem.Phy.Lett. 401,546-552(2005).
37. Ch. Scharf, K Peter,P Bauer,Ch.Jung,M Thelakkat and J Kohler, "Towards the characterisation of energy-transfer processes in organic donor-acceptor dyads based on triphenyldiamine and perylenebisimides, " Chem.Phy. 328, 403-409(2006).
38. G Cerulla, S Stagira, M Zavelani-Rossi, S D Silvestri, T Virgili, D G Lidzey and D D C Bradley, " Ultrafast Forster transfer dynamics in tetraphenylporphyrin doped poly(9,9-dioctylfluorene) ," Chem.Phys.Lett. 335, 27-33(2001).
39. AV Deshpande and E B Namdas, "Correlation between lasing and photo physical performance of dyes in polymethylmethacrylate," Journal of Luminescence 91, 25-31(2000).
40. J Brandrup, E H Immergut and E S Grulke "Refractive indices of polymers" in *Polymer Handbook* ( Wiley, 4<sup>th</sup> edition,Newyork,1999) VI/571.
41. Paul R Selvin, "The renaissance of fluorescence resonance energy transfer," Nature structural biology 7, 730-734(2000).
42. J N Miller, "Fluorescence energy transfer methods in bio analysis," Analyst 130, 265-270 (2005).
43. R D Singh, A K Sharman, N V Unnikrishnan and D Mohan, " Energy transfer study on Coumarin 30-Rhodamine 6G dye mixture using a laser fluorimeter," J.Mod.Opt. 37, 419-425 (1990).
44. E Desurvire, *Erbium-Doped fiber amplifiers :Principles and Applications* (John Wiley & Sons Inc,New york 1994 p- 382).
45. A Ghatak and K Thyagarajan, *Introduction to fiber optics* (Cambridge University press, 1999).

## *Multimode laser emission from dye doped polymer optical fiber*

*Multimode laser emission is observed in Rh 6G, Rh B and dye mixture doped polymer optical fiber when excited by 532 nm pulsed laser beam from an Nd: YAG laser. Wavelength tuning of laser emission is achieved by using a mixture of dyes utilizing the energy transfer occurring from donor (Rh 6G) molecule to acceptor molecule (Rh B). The effect of pump energy, length of the fiber, diameter of the fiber and concentration of the dyes on the performance of the multimode laser emission is studied.*



### **3.1 Introduction**

Stimulated emission from organic dye molecules in solution by laser excitation was first reported by Sorokin and Lankard [1,2] and was subsequently studied by Schafer et al [3] , Spaeth and Bortfeld [4] and by McFarland [5]. Solid-state dye lasers first demonstrated by Soffer and McFarland [6] in 1967 and then by Peterson and Snavelly [7] in 1968, have great advantages over liquid dye lasers by being nonvolatile, nonflammable, nontoxic, compact and mechanically stable. Organic dye doped polymers have been widely investigated as gain media in solid state dye lasers [8-13]. Dye molecules that have large absorption and induced emission cross sections due to allowed pi-pi transitions are ideal active dopants for the generation and amplification of light pulses [14].

Polymer optical fibers (POF) have attracted much attention during the past two decades because of their unique characteristics, such as flexibility, easiness in handling and relative low cost in coupling [14-15]. With the development of POF, increasing research activities have also been carried out in the field of active polymer optical fiber amplifiers and lasers [14-17]. Muto et al. investigated a dye doped step index polymer fiber laser [18] and Prasad et al reported lasing action in rhodamine 6G doped sol-gel glass fiber [19]. Also, Ken Kuriki et al have reported lasing action of graded index polymer optical fibers containing dyes such as rhodamine B, rhodamine 6G and perylene orange [20-21]. Again, photo-pumped narrow line laser emission is demonstrated using free standing polymer films [22] and cylindrical micro-cavities formed by conjugated polymer thin films, dye doped polymers and dendrimer doped polymers [23-25].

This chapter deals with the multimode laser emission from an axially pumped polymer optical fiber made of polymethylmethacrylate doped with Rh6G,

---

RhB and mixture of Rh6G and RhB dyes. When high pump energy is applied to the dye doped fiber, stimulated emission occurs and the cylindrical surface of the fiber acts as a Fabry-Perot like resonator cavity by providing the optical feedback for the fiber gain medium. Stimulated emission, optical feedback from the resonator cavity and propagation through the fiber gain medium result in intense multimode laser emission from the dye doped POF. Here, dye mixture doped POF is used to study the extended tunable laser emission from the mixed dye system. The excitation of dye lasers through energy transfer processes provides one of the means of extending the lasing wavelength region [26-27].

### 3.2 Theoretical background

#### 3.2.1 Fabry-Perot optical resonator

Optical resonators, which are the major components of lasers, surrounding the gain medium and providing feedback of the laser light, confine and store light at certain resonance frequencies. The simplest of these is called a Fabry-Perot cavity which consists of two plane parallel highly reflective mirrors separated by a distance,  $L$ . The wavelength spacing between adjacent

resonator modes in this cavity is given by  $\Delta\lambda = \frac{\lambda^2}{2nL}$  [28-29], (3.1)

where  $n$  is the refractive index of the medium.

#### 3.2.2 Microcavity resonator model

Microcavity lasers are of interest for both fundamental studies of cavity quantum electrodynamics and for applications as integrated optical elements. In order to realize low threshold lasers, it is necessary to utilize a high Q cavity to confine the light in a gain region. In lasers with micro-cylindrical resonators, the light in their symmetrical structures is highly confined by total internal reflection, resulting in a high Q factor. Several types of micro-

## Multimode laser emission

cavities such as spheres, rings and discs made by semiconductors, organic dye solutions and dye doped polymers have been reported [30-37].

In the present case, the dye doped fiber can be modeled as a number of serially connected micro-disc type cavities as shown in Fig 3.1.

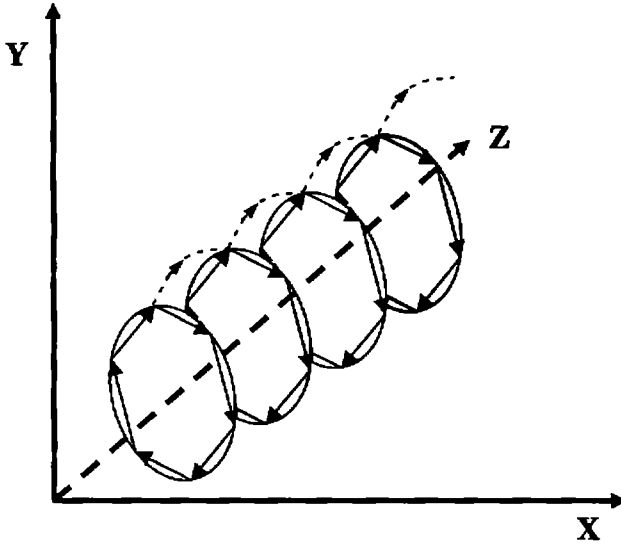


**Fig 3.1:** Schematic representation of micro disc cavity resonator model of dye doped POF. Fiber axis is in the z direction.

The resonant frequencies  $\nu_m$  for the waveguided laser modes are given by [30-32]

$$\nu_m = \frac{mc}{\pi n D} \quad (3.2)$$

where  $m$  is an integer,  $c$  is the speed of light in vacuum,  $n$  is the refractive index of the medium and  $D$  is the diameter of the fiber.

The intermodal spectral spacing,  $\Delta\nu = \nu_m - \nu_{m-1}$

$$\begin{aligned} &= \frac{mc}{\pi n D} - \frac{(m-1)c}{\pi n D} \\ &= \frac{c}{\pi n D} \end{aligned}$$

We have  $\Delta\lambda = \frac{\lambda^2}{c} \Delta\nu$

substituting for  $\Delta\nu$ ,

$$\Delta\lambda = \frac{\lambda^2}{\pi D} \quad (3.3)$$

where  $\lambda$  is the wavelength of the strongest emission mode.

### 3.3 Experiment

The dye doped bare core polymer fibers used for the present studies are based on polymethylmethacrylate and are fabricated as described in chapter 2. For our investigations of the multimode laser emission from dye mixture doped POF, four fiber samples are fabricated having the following dye concentrations. *a)* Rh 6G (0.25 mM) *b)* Rh 6G (0.25 mM) and Rh B (0.11 mM) *c)* Rh6G (0.25 mM) and RhB(0.25 mM) *d)* Rh B(0.25 mM). For the present study, we have used fibers with diameters 335  $\mu\text{m}$ , 405  $\mu\text{m}$  and 510  $\mu\text{m}$ . The maximum variation observed in the measurement of fiber diameter is  $\pm 2 \mu\text{m}$ . For investigating the effect of the length of the dye doped fiber on the multimode laser emission, fiber length is varied from 2-12 cm.

A schematic of the experimental set up for the laser emission studies from the dye doped POF is shown in Fig 3.2. Dye doped POF is mounted on a five - axis fiber aligner. The fiber is axially pumped using 10 ns pulses from a frequency doubled Nd: YAG laser (532 nm, 10 Hz). A set of calibrated neutral density filters is used for varying the pump energy. Pump beam is focused at the tip of the fiber using a convex lens of 10 cm focal length. The emission is collected from the other end of the dye doped fiber using a collecting optical fiber coupled to a monochromator-CCD system (Acton-Spectrapro).

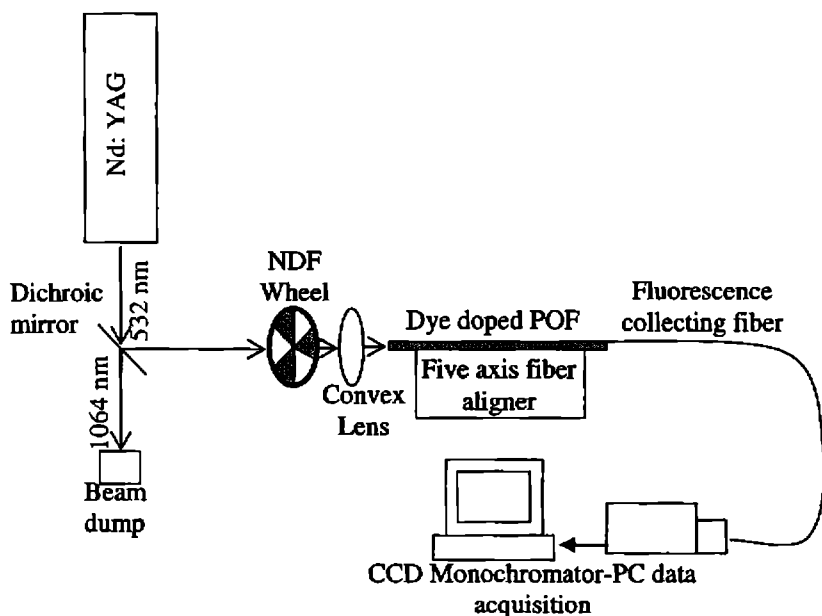


Fig 3.2: Experimental set up to record the fluorescence emission from the fiber end. Pumping is done axially.

### 3.4 Results and Discussions

#### 3.4.1 Energy transfer in dye doped POF

Fig 3.3 shows a comparison of the fluorescence emission from POF doped with Rh 6G, Rh 6G- Rh B dye mixture system and Rh B at a pump energy of 0.12 mJ/pulse. As explained in chapter 2, the fluorescence spectrum from the POF doped with Rh 6G(0.25 mM) and Rh B(0.11 mM), shows a red shift in comparison with Rh6G(0.25 mM) doped POF (Fig 3.3 a) confirming that energy transfer occurs from Rh6G(donor) to RhB(acceptor). A detailed description of energy transfer process and its implications have been discussed in chapter 2. Fig 3.3 b shows an enhancement of spectral width upto 60 nm compared to the 30 nm spectral width of Rh 6G doped POF (Fig 3.3 a) which indicates the potentiality of the dye mixture doped POF as a

medium for extended wavelength tunable laser emission. Spectral width is measured in terms of FWHM, ie, the wavelength separation between the two points in the spectrum which has got half of the maximum intensity value.

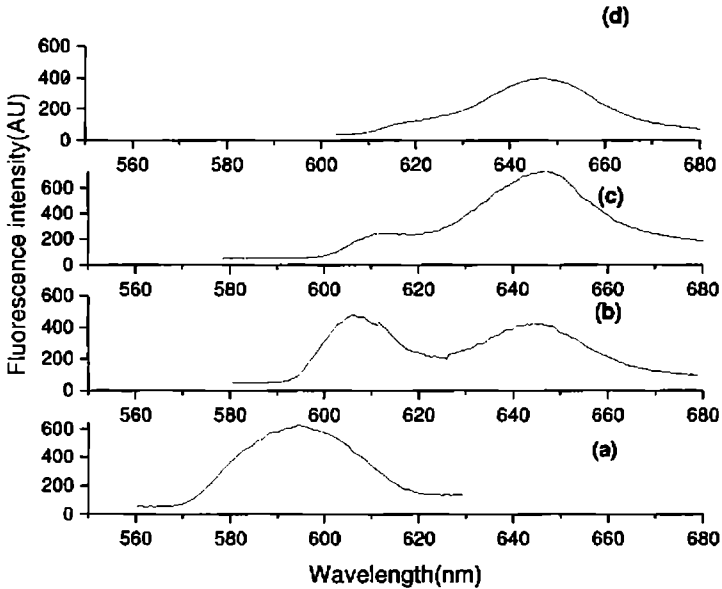


**Fig 3.3:** Shift of the fluorescence emission peak as a result of the energy transfer process in dye mixture doped POF. *a)* Rh 6G (0.25 mM) *b)* Rh 6G (0.25 mM) and Rh B(0.11 mM) *c)* Rh 6G(0.25 mM) and Rh B(0.25 mM) *d)* Rh B(0.25 mM). Pump energy is 0.12 mJ/pulse. Length of the POF is 7 cm and diameter is 510  $\mu\text{m}$ .

In addition to the increase in the spectral width, an interesting aspect of the tuning bands resulting from the shift in the central wavelength in the dye mixture system is that the multimode laser emission region required for a particular application can be precisely determined by fine tuning the concentration of the dye mixture.

## Multimode laser emission

### 3.4.2 Emission spectra with pump energy.

If the pump energy is increased further, more and more dye molecules get excited to higher energy state and population inversion in the medium increases and the medium can start lasing if proper cavity mirror arrangement is provided.

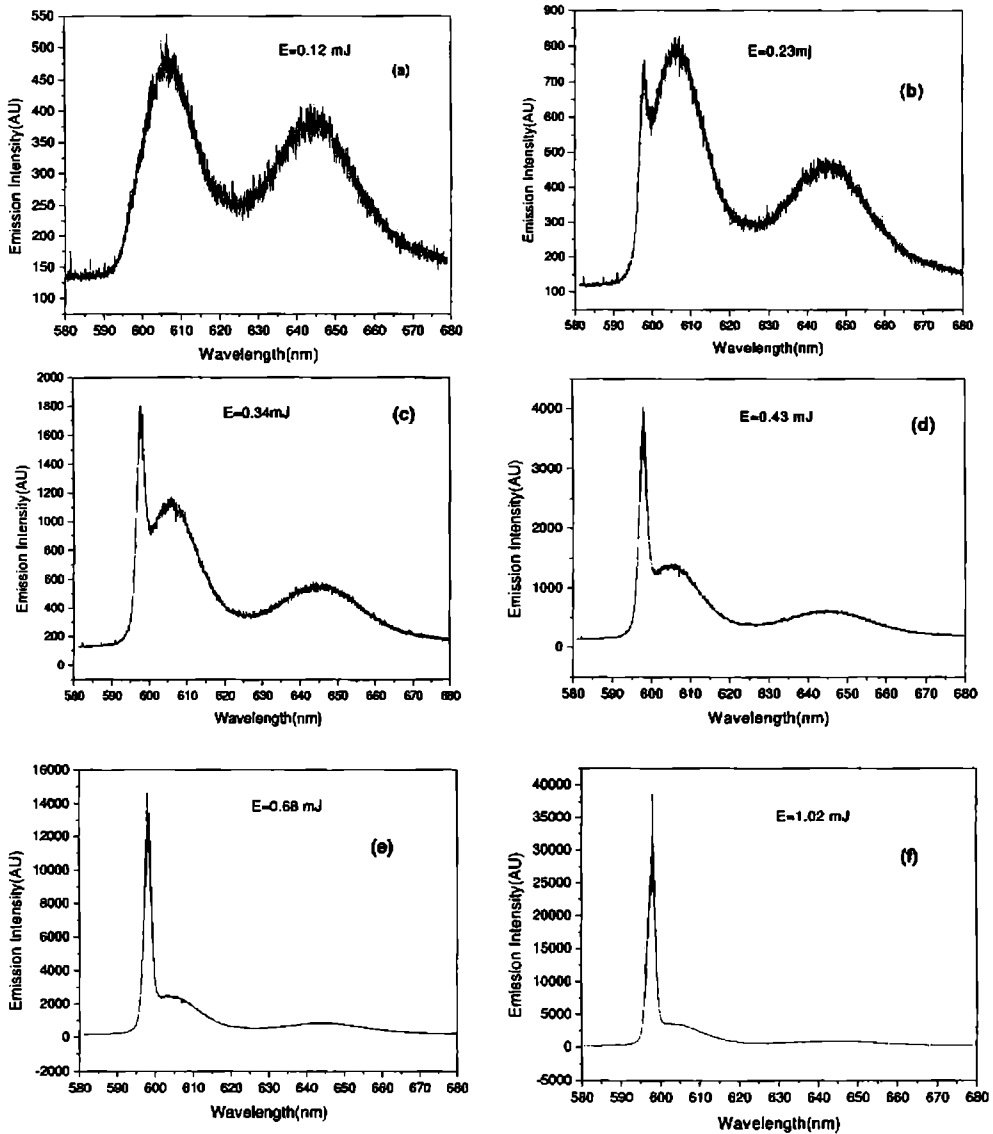


Fig 3.4: Emission from 510  $\mu\text{m}$  diameter and 7 cm long dye doped POF at a pump energy of a) E=0.12 mJ b) E=0.23 mJ, c) E=0.34 mJ, d) E=0.43 mJ, e) E=0.68 mJ, f) 1.02 mJ.

In order to study the multimode laser emission process in the dye doped POF gain medium, higher pump energy is applied and the fluorescence emission intensity is noted. Fig 3.4 shows the emission spectra of Rh 6G (0.25 mM) and Rh B (0.11 mM) dye mixture doped polymer optical fiber with variation in pump energy. Fig 3.4a shows a typical fluorescence emission spectrum from the dye mixture doped polymer optical fiber when pumped using the 532 nm laser pulse of energy 0.12 mJ.

As the pump energy is increased further, fluorescence spectrum gets narrowed due to amplified spontaneous emission (ASE) [28-29] and at a threshold pump energy, laser emission with a multimode structure emerges (Fig 3.4 c). For a fiber with a diameter of 510  $\mu$ m and a length 7 cm the threshold energy for multimode emission is observed to be 0.34 mJ/pulse. The expanded modes are clearly shown in Fig 3.5.

### 3.4.3 Mode competition with pump energy

Fig 3.5 shows the behavior of different modes as the pumping energy is increased from 0.43 mJ to 1.02 mJ. A particular mode at  $\lambda = 598\text{nm}$ , which is at the centre of the spectrum, acquires maximum energy and becomes very prominent compared to other modes as the pumping energy is increased to 1.02 mJ. This is because of the selective excitation of that mode at the centre of the spectrum which has got higher stimulated emission cross section. Also, this particular high energy mode becomes very narrow with an FWHM of 0.1 nm at a pump pulse energy of 1.02 mJ, which is a significant feature of laser emission modes.



*Multimode laser emission*

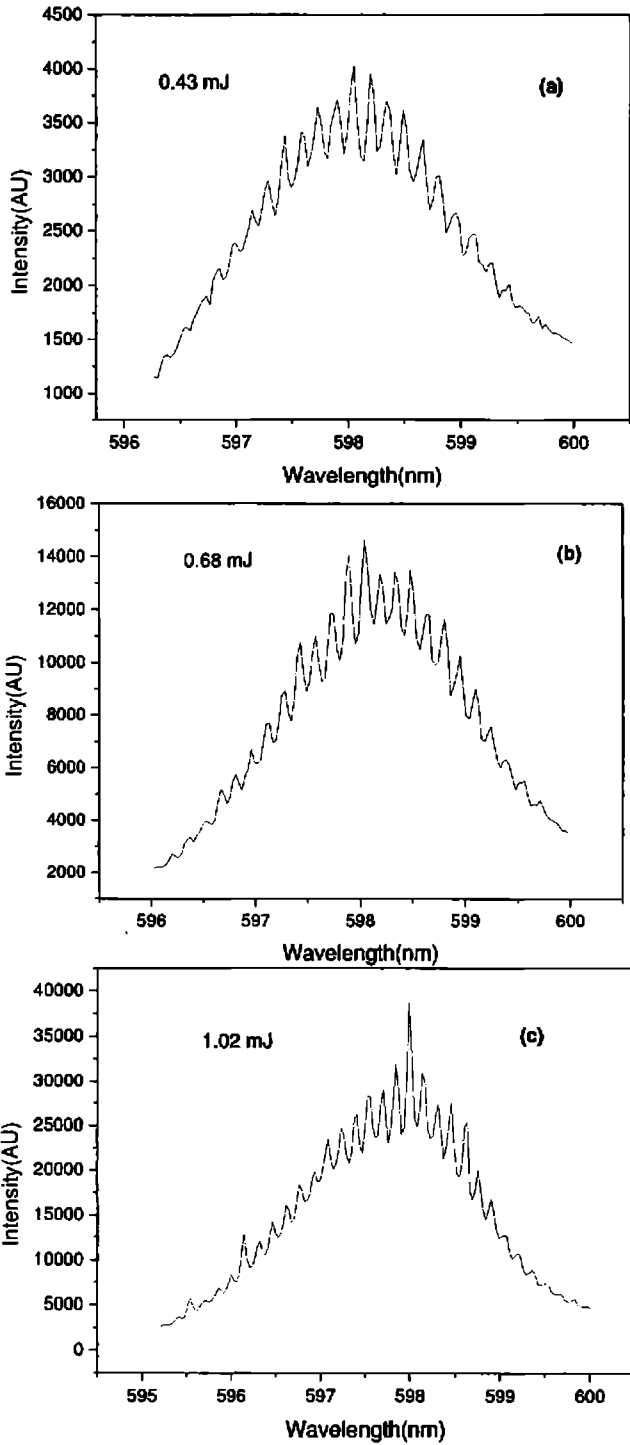


**Fig 3. 5:** Multimode emission structures from dye doped POF. a) 0.43 mJ b) 0.68 mJ c) 1.02 mJ.

### 3.4.4 Wavelength tuning of multimode laser emission peak

Similar type of multimode laser emission is observed in all other samples corresponding to Fig 3.3 a, Fig 3.3 c and Fig 3.3 d. Fig 3.6 shows the wavelength tuning of the multimode laser emission peak with variation in RhB dye concentration in the mixture.

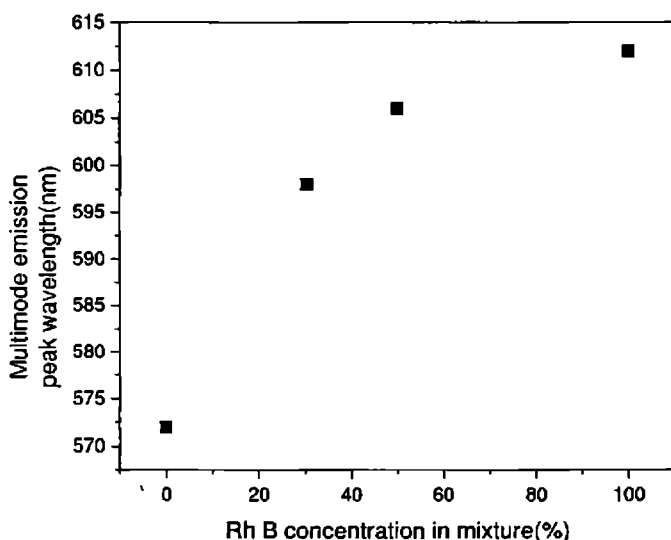


**Fig 3.6:** Tuning of multimode laser emission peak with different dye concentration. Pump energy is 1.37 mJ/pulse. L=7 cm and D=510  $\mu\text{m}$ .

The multimode laser emission peak wavelength of Rh 6G (0.25 mM) doped POF is found to be at 572 nm. When a mixture of Rh 6G (0.25 mM) and Rh B (0.11 mM) is used, the lasing wavelength peak shows a clear red shift towards 598 nm (Fig 3.6). When Rh B concentration in the dye mixture system is increased to 0.25 mM, the lasing wavelength peak shifts to 606 nm. The lasing wavelength of Rh B (0.25 mM) is found to be at 612 nm. Since there is a clear overlap between the emission spectrum of Rh 6G and absorption spectrum of Rh B, the energy transfer occurs from Rh 6G to Rh B and the lasing wavelength also shifts towards the emission region of Rh B.

### Multimode laser emission

Thus, it is clear from these observations that multimode laser emission region needed for a particular application can be precisely determined by fine tuning the concentration of the dye mixture.

A typical multimode laser emission spectrum at a pump energy of 1.37 mJ/pulse from a POF doped with Rh 6G (0.25 mM) and Rh B (0.25mM) is shown in Fig 3. 7.

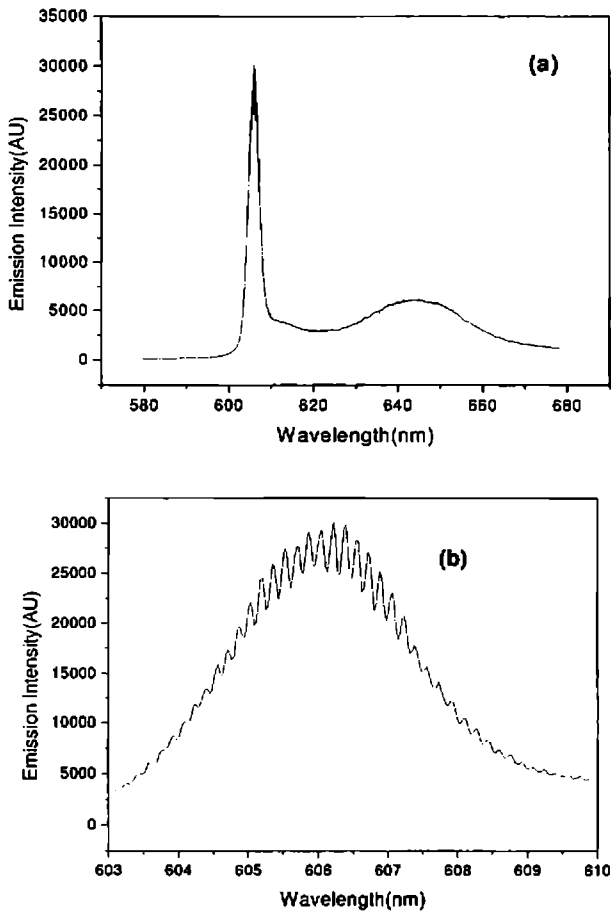


**Fig 3.7:** a) A typical multimode laser emission spectrum at a pump energy of 1.37 mJ/pulse from a POF doped with Rh 6G (0.25mM) and Rh B (0.25mM) . b) Expanded modes of Fig 3.7a.

A similar multimode laser emission phenomenon is observed by K Geetha et al and Ritty J et al [22, 38] in dye doped free standing polymer films and Yokoyama et al [39] in dye doped dendrimer solution. The observed resonant modes in our case can also be compared with the multimode lasing in plastic micro-ring lasers on fibers and wires [30-32].

External feedback is necessary to obtain laser emission. In this case there are no external mirrors to give feedback to the gain medium. The optical feedback for the gain medium is provided by the cylindrical surface of the optical fiber which acts as the micro-disc type optical cavity. Though the reflections from these cylindrical surfaces are weak compared to the conventional laser cavity mirrors, the stimulated emission along with its propagation through the gain medium resulted in intense laser emission with a multimode structure. Thus, the fine structure pattern in the emission spectrum of dye doped fiber can be attributed to the resonator modes of the micro-disc type cavity. These modes are guided through the optical fiber.

#### 3.4.5 Mode spacing dependence on diameter of the fiber.

To check the validity of the proposition of dye doped POF as a number of serially connected micro-disc type cavities, multimode laser emission is recorded for different diameter fiber samples and the mode spacing is evaluated according to the equation 3.3. Fig 3.8 shows the emission spectra recorded in the case of Rh 6G(0.25 mM) and Rh B(0.11 mM) doped POF for different diameters of dye doped polymer optical fiber at a pump energy of 1.37 mJ/pulse. Fiber length is 7 cm. The spectrum shown in Fig 3.8 a is a clear indication of the existence of resonant modes. The observed value of the average mode spacing is 0.23 nm. The strongest mode at 595.3 nm has an FWHM of 0.1 nm. In the case of Fig 3.8 a, substituting the values for  $\lambda$ ,  $n$  and  $D$  as 595.3 nm, 1.49 and 335  $\mu\text{m}$  respectively, we get the mode spacing as 0.23 nm which is the same as the observed mode spacing value.

**Multimode laser emission**

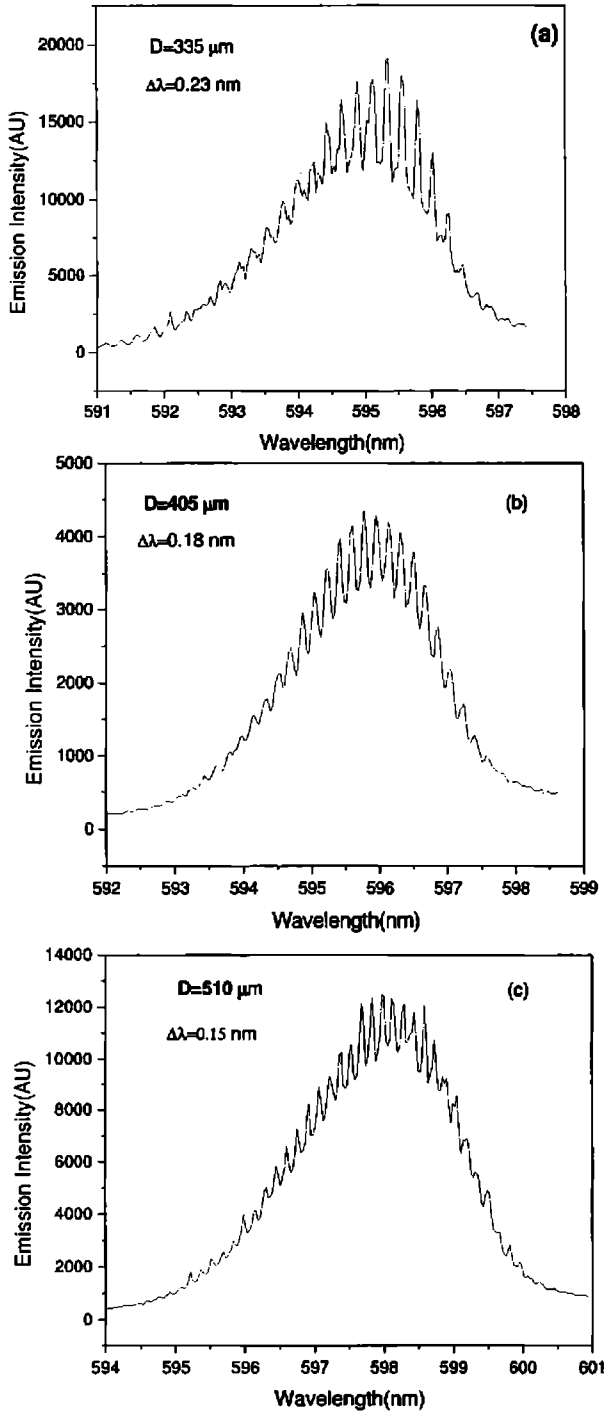


**Fig 3.8:** Multimode laser emission from 7 cm long dye doped fiber at a pump energy of 1.37 mJ /pulse. (a)  $D=335 \mu\text{m}$ , (b)  $D=405 \mu\text{m}$ , (c)  $D=510 \mu\text{m}$ .

Table 3.1 shows the observed and calculated mode spacing values for fibers having different diameters and the maximum variation observed in the measurement of mode spacing is  $\pm 1\%$ . There is a close agreement between the observed mode spacing and calculated values. As the diameter of the fiber increases, the mode spacing decreases accordingly. This observation is a clear evidence of the fact that the observed fine structures in the emission spectra are resonant modes of the cavity formed by the cylindrical surfaces of the dye doped polymer optical fiber.

Diameter, D ( $\mu\text{m}$ )	Calculated mode spacing, $\Delta\lambda = \frac{\lambda^2}{\pi n D}$ (nm)	Observed mode spacing, $\Delta\lambda$ (nm)
335	0.23	0.23
405	0.19	0.18
510	0.15	0.15

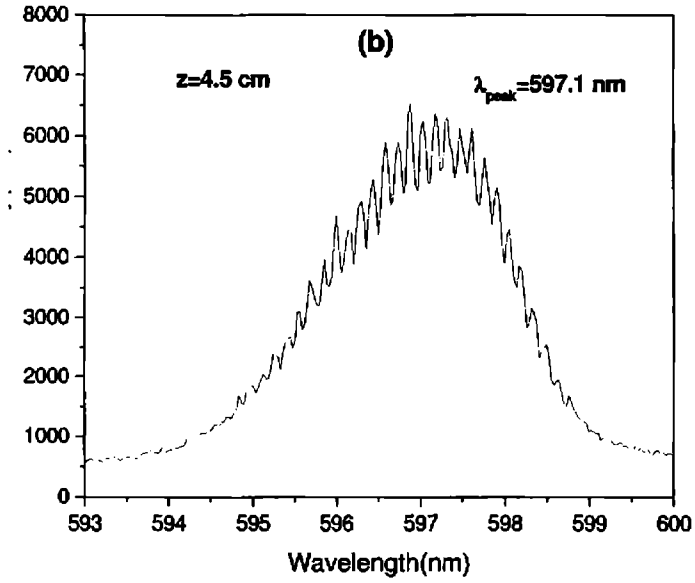
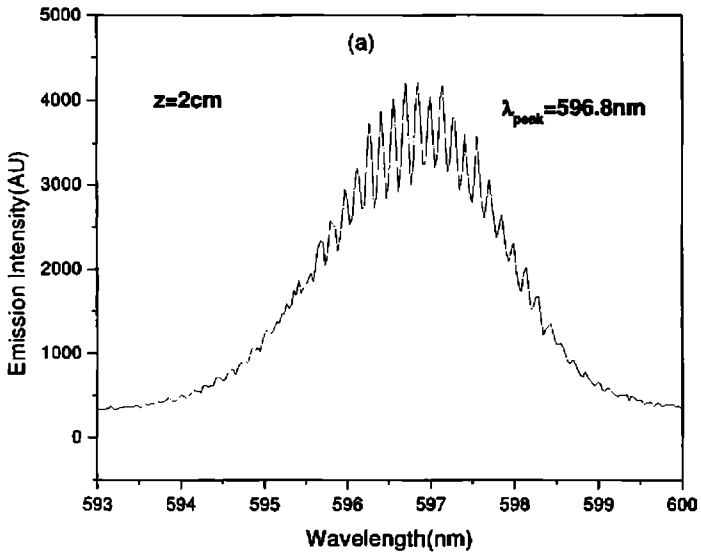
**Table 3.1:** Mode spacing dependence on diameter of fiber based on micro-disc resonator model. Fiber length is 7 cm and pump energy is 1.37 mJ/pulse.

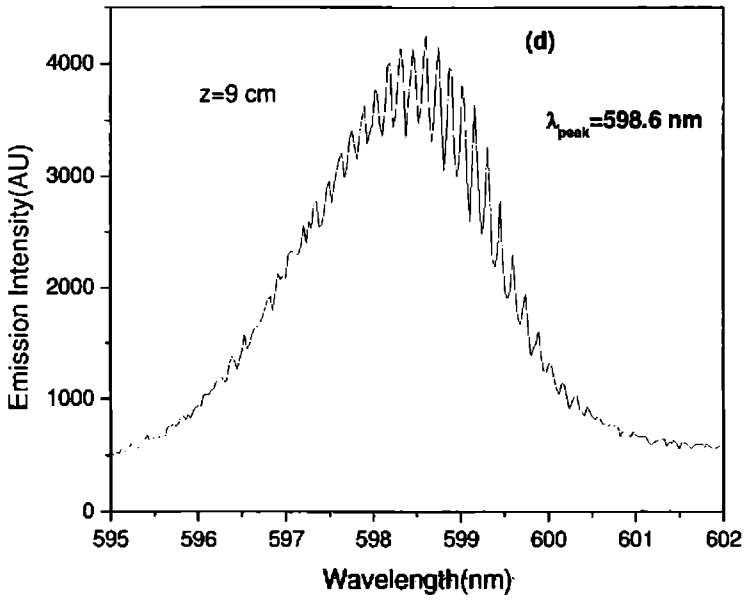
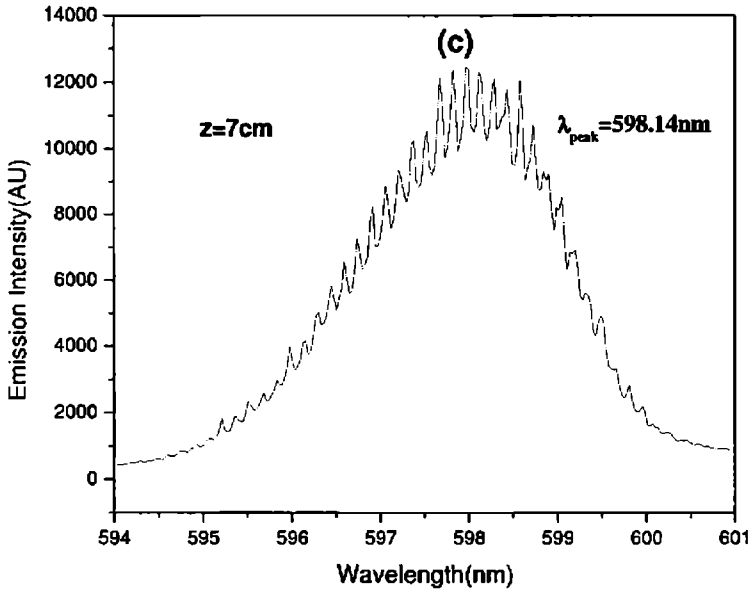
### 3.4.6 Length dependent wavelength tuning of multimode laser emission peak

Fig 3.9 shows the emission spectra from Rh 6G (0.25 mM) and Rh B (0.11 mM) doped POF having different lengths at a pump energy of 1.37 mJ/pulse.

*Multimode laser emission*

---







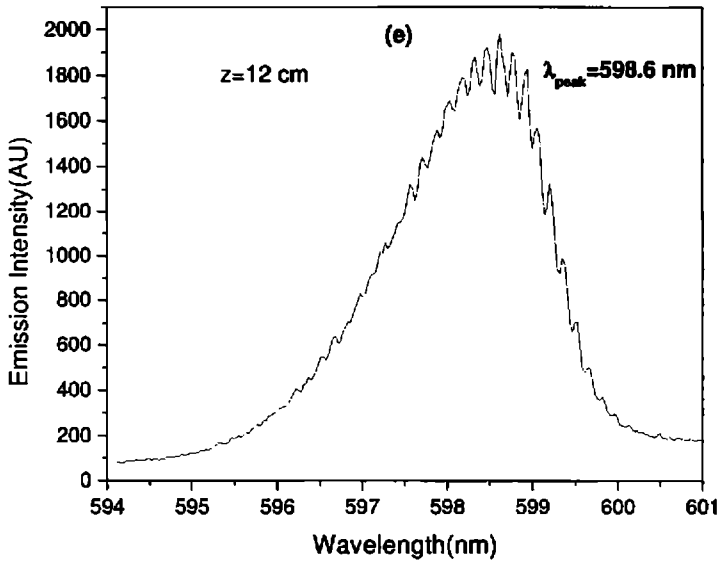


Fig 3.9: Multimode laser emission from 510  $\mu\text{m}$  diameter dye doped POF at a pump energy of 1.37 mJ/pulse. a)  $z=2$  cm (b)  $z=4.5$  cm, (c)  $z=7$  cm, (d)  $z=9$  cm, e)  $z=12$  cm.

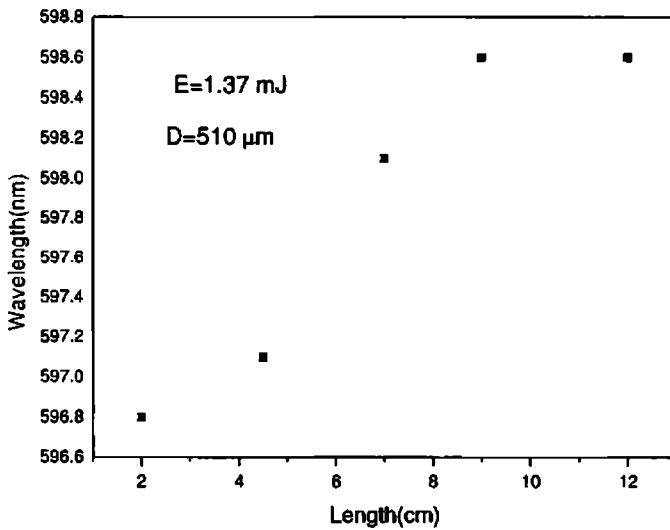


Fig 3.10: Variation of multimode laser emission peak with length of the fiber having a diameter of 510  $\mu\text{m}$  at a pump energy of 1.37 mJ/pulse.

When the fiber length is increased, the multimode structure is observed to be superposed over the amplified spontaneous emission (ASE) upto a length of 9 cm for a fiber having 510  $\mu$  m diameter. When the fiber length is 12 cm the fine structure degrades and laser emission becomes less prominent. Increase in the length of the fiber will result in the enhancement of the propagation loss factor which leads to the reduction of the mode structure as observed in the present case. Also, as the length of the fiber is increased, red shift in the multimode laser emission can be observed due to the re-absorption and re-emission process taking place within the dye doped fiber [40] as shown in Fig 3.10, which shows the length dependent wavelength tunability of multimode laser emission from dye doped fiber.

### **3.5 Conclusions**

Multimode laser emission from a dye doped polymer optical fiber is observed when excited by 532 nm pulsed laser beam from an Nd:YAG laser. Wavelength tuning of multimode laser emission is achieved by using a mixture of dyes utilizing the energy transfer occurring from donor (Rh6G) molecule to acceptor (Rh B) molecule. As the energy of the pump beam is increased, fluorescence spectrum gets narrowed due to amplified spontaneous emission and at a threshold pump energy, laser emission with a multimode structure emerges. Mode competition is observed with increase in pump energy and a particular mode at the centre of the spectrum becomes more prominent compared to the other modes. When the diameter of the fiber is increased the mode spacing is found to decrease correspondingly confirming our proposition that the observed modes are the resonant modes of a number of serially connected micro-disc type cavities formed by the dye doped POF. As the length of the fiber is increased, red shift in the multimode laser emission is observed due to the re-absorption and re-emission processes taking place within the dye doped fiber. Thus one can achieve multimode laser emission over a broad range of wavelengths by suitably selecting the concentration of the dyes and by varying the length of the POF.

---

**References**

1. P.P. Sorokin and J R Lankard, "Stimulated emission observed from an organic dye chloro-aluminum Phthalocyanine," IBM J.of Res. And Dev. **10**,162-163(1966).
2. P.P.Sorokin,W H Culver,E C Hammond and J R Lankard,"End pumped stimulated emission from a Thiocarbocyanine dye," IBM J.of Res and Dev.**10**, 401-403(1966).
3. F P Schafer, W Schmidt and J Volze, "Organic Dye solution laser," Appl.Phys.Letters **9**,306-309(1966).
4. M R Spaeth and D P Bortfeld, "Stimulated emission from polymethine dyes," Appl.Phys.Lett.**9**, 179-181(1966).
5. B B McFarland, "Laser second -harmonic induced stimulated emission of organic dyes," Appl.Phys.Lett.**10**, 208-209(1967).
6. B H Soffer and B B McFarland, "Continuously tunable, narrow band organic dye lasers,"Appl.Phys.Lett.**10**, 266-267(1967).
7. O G Peterson and B B Snavely, "Stimulated emission from flashlamp-excited organic dyes in poly methylmethacrylate," Appl.Phys.Lett.**12**, 238-240(1968).
8. G D Peng,P K Chu ,Z Xiong,T Whitebread and R P Chaplin, " Dye doped step index polymer optical fiber for broad band optical amplification,"J Lightwave Technol. **14**,2215-2223(1996).
9. A Tagaya ,Y Koike ,T Kinoshita ,E Nihei ,T Yamamoto and K Sasaki, "Polymer optical fiber amplifier,"Appl Phys Lett. **63**,883-884(1993).
10. G Somasundaram and A Ramalingam, "Gain studies of coumarin 307 dye doped polymer laser," Opt. Laser Technol **31**,351-358(1999).
11. Soren Balslev, Andrej Mironov, Daniel Nilsson and Anders Kristensen, "Micro-fabricated single mode polymer dye laser," Opt. Express **14**, 2170-2177(2006).
12. Yuhua Huang, Tsung-Hsien Lin, Ying Zhou and Shin-Tson Wu, "Enhancing the laser power by stacking multiple dye-doped chiral polymer films," Opt. Express **14**, 11299-11303(2006).

13. Mohammad Ahmad, Terence A. King, Do-Kyeong Ko, Byung Heon Cha and Jongmin Lee, "Highly photostable laser solution and solid-state media based on mixed pyromethene and coumarin," *Opt. Laser Technol* **34**, 445-448(2002).
14. K Kuriki, Y Koike, Y Okamoto, "Plastic optical fiber lasers and amplifiers containing Lanthanide Complexes," *Chem Rev* **102**, 2347-2356(2002).
15. J Zubia and J Arrue, "Plastic optical fibers: An introduction to their technological processes and applications," *Opt Fiber Technol* **7**, 101-140(2001).
16. Q J Zhang, P Wang, X F Sun, Y Zhai and P Dai, "Amplified spontaneous emission of an Nd<sup>3+</sup> doped poly methyl methacrylate optical fiber at ambient temperature," *Appl Phys Lett.* **72**, 407-409(1998).
17. M Rajesh Sheeba, K Geetha, C P G Vallabhan, P Radhakrishnan and V P N Nampoore, "Fabrication and characterization of dye doped polymer optical fiber as a light amplifier," *Appl. Opt.* **46**, 106-112 (2007).
18. S Muto, A Ando, O Yoda, T Hanawa T and H Ito, "Tunable laser by sheet of dye doped plastic fibers," *Trans. IEICE, J70-C*, 1479-1482(1987).
19. R Gvishi, G Ruland and P N Prasad, "New laser medium: dye-doped sol-gel fiber," *Opt. Commun.* **126**, 66-72(1996).
20. K. Kuriki, T Kobayashi, N Imai, T Tamura, S Nishihara, Y Nishizawa, A Tagaya and Y Koike, "High efficiency organic dye doped polymer optical fiber lasers," *Appl. Phys. Lett.* **77**, 331-333(2000).
21. K Kuriki, T Kobayashi, N Imai, T Tamura, Y Koike and Y Okamoto, "Organic dye doped polymer optical fiber laser," *Polym. Adv. Technol.* **11**, 612-616(2000).
22. K Geetha, M Rajesh, VPN Nampoore, CPG Vallabhan, P Radhakrishnan, "Laser emission from transversely pumped dye-doped free-standing polymer film," *J. Opt. A: Pure Appl. Opt.* **8**, 189-193(2006).
23. M Kuwata-Gonokami, R H Jordan, A Dodabalapur, H E Katz, M L Schilling and R E Slusher and S Ozawa, "Polymer microdisc and microring lasers," *Opt. Lett.* **20**, 2093-2095(1995).

24. A Otomo, S Yokoyama, T Nakahama and S Mashiko, "Super narrowing mirrorless laser emission in dendrimer doped polymer waveguides," *Appl. Phys. Lett.* **77**, 3881-3883(2000).
25. M Fakis, I Polyzos, G Tsigaridas, V Giannetas, P Persephonis, I Spiliopoulos and J Mikroyannidis, "Laser action of two conjugated polymers in solution and in solid matrix: The effect of aggregates on spontaneous and stimulated emission," *Phys Rev B.* **65**, 195203-195210(2002).
26. Rallabandi Sailaja and Prem B. Bisht, "Tunable multiline distributed feedback dye laser based on the phenomenon of excitation energy transfer," *Organic Electronics* **8**, 175-183(2007).
27. Yu Yang, Guannan Lin, Juan Zou, Zhiyu Wang, Minquan Wang and Guodong Qian "Enhanced laser performances based on energy transfer in multi-dyes co-doped solid media," *Opt. Commun.* **277**, 138-142(2007).
28. B E A Saleh and M C Tech, *Fundamentals of photonics* (Wiley Interscience, 1991).
29. A Yariv, *Optical electronics* (Saunders college publishing, 1971).
30. SV Frolov and Z V Vardeny, "Plastic Microring lasers on fibers and wires," *Appl Phys Lett* **72**, 1802-1804(1998).
31. R C Polson, G Levina and Z V Vardeny, "Spectral Analysis of polymer micro ring lasers," *Appl. Phys. Lett.* **76**, 3858-3860(2000).
32. S V Frolov, M Shkunov, Z V Vardeny and K Yoshino, "Ring microlasers from conducting polymers," *Phy. Rev B* **56**, 4363-4366(1997).
33. H Becker and R H Friend, "Light emission from wavelength-tunable microcavities", *Appl. Phys. Lett* **72**, 1266-1268(1998).
34. G D Chern, A W Poon, R K Chang and S Y Kuo "Direct evidence of open ray orbits in a square two-dimensional resonator of dye-doped polymers", *Opt. Lett* **29**, 1674-1676 (2004).
35. Y Kawabe, Ch Spiegelberg, A Schulgen, M F Nabor, B Kippelen and N Peyghambarian "Whispering-gallery-mode microring laser using a conjugated polymer", *Appl. Phys. Lett.* **72**, 141-143(1998).

### *Multimode laser emission*

---

36. N Tsujimoto, T Takashima, T Nakao, K Masuyama and M Ozaki “ Laser emission from spiral-shaped microdisc with waveguide of conducting polymer”, *J.Phys. D. Appl.Phys.* **40**, 1669-1672(2007).
37. N Tessler, G J Denton and R H Friend“Lasing from conjugated polymer microcavities”, *Nature* **382**,695-697(1996).
38. Ritty J Nedumpara,K Geetha,V J Dann,C P G Vallabhan,V P N Nampoore and P Radhakrishnan,“Light Amplification in dye doped polymer films,” *J.Opt.A: Pure Appl.Opt.* **9**,174-179(2007).
39. S Yokoyama, A Otomo A and S Mashiko, “Laser emission from high-gain media of dye doped dendrimer,” *Appl.Phys.Lett* **80**, 7-9(2002).
40. M Rajesh,K Geetha,M Sheeba, C P G Vallabhan,P Radhakrishnan and V P N Nampoore, “Characterisation of rhodamine 6G doped polymer optical fiber by side illumination fluorescence,” *Optical Engineering*, **45**,075003-075007(2006).

*Two photon excited fluorescence studies in dye doped polymer optical fibers.*

*Two photon excited position dependent tuning of side illumination fluorescence in Rh 6G-RhB dye mixture doped polymer optical fiber by pumping it with an 800 nm, femtosecond laser and the effect of energy transfer on the attenuation coefficient is reported in this chapter. The attenuation coefficient is found to be lower at longer propagation distances compared to shorter distances because of the re-absorption and re-emission process taking place within the dye doped fiber.*



#### **4.1 Introduction**

In the previous two chapters, fluorescence studies are carried out in the dye doped POF under one-photon excitation where the dye molecule gets excited to higher energy state by absorbing a single photon from the exciting radiation field and the subsequent emission of fluorescence. If the exciting laser intensity is high, a fluorophore can simultaneously absorb two long wavelength photons to reach the first singlet state by a process called two-photon absorption (TPA) and then the usual fluorescence emission can occur [1]. This process depends strongly on the light intensity and occurs mainly at the focal point of the laser beam where the intensity is high. Two-photon excited (TPE) frequency upconversion lasing and two-photon fluorescence imaging are subjects of intensive research in recent years [2-4]. Multiphoton transitions involving the simultaneous absorption of more than one photon were first predicted by Goppert Mayer [5] in 1931 and were demonstrated in the laboratory in 1961 by Kaiser and Garret [6].

Compact, lightweight and inexpensive lasers operating in the short wavelength visible region are desired for use in such diverse applications as medical diagnostics, surgery, high-capacity optical storage and high-resolution scanning and printing. Methods of generating these shorter wavelengths include optical harmonic generation and sum frequency mixing techniques that require phase matching in expensive inorganic crystals. An excellent alternative to generate these shorter wavelengths is the frequency upconversion by two-photon absorption by pumping in the infrared.

There have been two important technical approaches to achieve frequency upconversion lasing. 1) Simultaneous absorption of two photons by the gain medium (two-photon pumped) [7-12] and 2) Sequential stepwise multiphoton

excitation (multistep one- photon pumped) [13, 14]. Considering that the two-photon excitation cross section is much smaller than the corresponding one photon cross section, a higher pump intensity and longer gain length are required for TPE lasing processes. Advantages of using waveguide or fiber configurations to achieve upconversion lasing are 1) a higher local pump intensity and 2) longer effective gain length. There are earlier reports of upconversion lasing in dye doped polymer waveguide and dye doped polymer fiber [11, 12].

The two- photon excited fluorescence studies in Rh6G, Rh B and Rh6G-Rh B dye mixture doped POF, are reported in this chapter. Our studies illustrate that the combination of a well designed mixture of organic chromophores incorporated into a fiber geometry is appealing for the development of an upconversion polymer fiber laser which is tunable over a broader wavelength region. The optical attenuation in polymer optical fiber (POF) is an important parameter of interest. It is also important to study the successful fabrication of upconversion dye doped polymer fiber laser, frequency upconverted emission and the propagation loss mechanisms in the dye doped POF.

Usually the propagation loss in fibers and planar waveguide structures is measured by the cutback technique, where the transmitted signal is measured at the end of the fiber as a function of length. The disadvantage of the cutback technique is that it is a destructive method [15, 16]. A non-destructive side illumination fluorescence technique for measuring the optical attenuation in dye doped fibers has been developed by Kruhlak et al [17, 18]. The use of this technique to investigate the two-photon excited fluorescence emission, energy transfer process and its effect on the attenuation coefficient in single dye and dye mixture doped POF are also presented in this chapter.

#### 4.2 Two-photon absorption (TPA)

Fluorescence is usually excited by absorption of a single photon with a wavelength within the absorption band of the fluorophore. If the laser intensity is high, as from a picosecond or femtosecond laser pulse, a fluorophore can simultaneously absorb two long wavelength photons to reach the first singlet state. Two possible situations are illustrated in Fig 4.1[19]. In the first case, two photons from the same optical field oscillating at a frequency  $\omega$  are absorbed to make a transition which is approximately resonant at  $2\omega$  (single beam TPA). In the second situation, called two-beam two-photon absorption, two optical fields at frequencies  $\omega_e$  and  $\omega_p$  are present and one photon from each field is absorbed for the transition which is approximately resonant at  $\omega_e + \omega_p$ . In both the cases, the intermediate (or virtual) state is not real, ie, it doesn't involve a real stationary state of the system. Hence the system must absorb the two photons simultaneously. This makes the process sensitive to the instantaneous optical intensity.

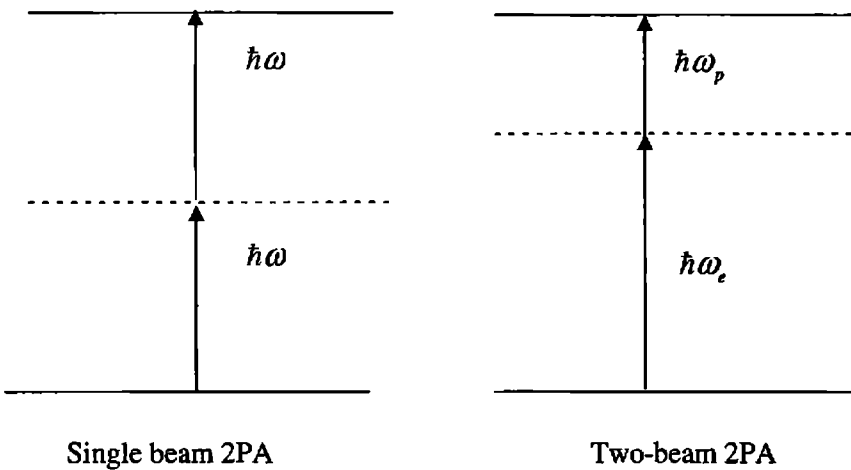


Fig 4.1: Schematic diagram showing single beam and two- beam two-photon absorption.

### 4.3 Single beam two-photon absorption

Single beam two-photon absorption is employed in the present work. The nonlinear absorption in this case is proportional to the square of the instantaneous intensity. The differential equation describing the optical loss is given by

$$\frac{dI}{dz} = -\alpha I - \beta I^2 \quad (4.1)$$

where  $\alpha$  is the linear absorption coefficient and  $\beta$  is the two-photon absorption coefficient.

The TPA coefficient  $\beta$  is a macroscopic parameter characterizing the material. The individual molecular TPA property is described by the TPA cross-section  $\sigma_2$ . The TPA coefficient is also related to the third order susceptibility. It is the imaginary part of  $\chi^{(3)}$  that determines the strength of the non linear absorption [19].

$$\text{Two-photon absorption coefficient, } \beta = \frac{3\pi}{\epsilon_0 n^2 c \lambda} \text{Im } \chi^3 \quad (4.2)$$

$$\text{Two-photon absorption cross section, } \sigma_2 = \frac{\hbar \omega \beta}{N} \quad (4.3)$$

where  $N$  is the number density of molecules in the system,  $n$  is the refractive index of the medium,  $\lambda$  is the free space wavelength and  $c$  is the velocity of light in vacuum.

### 4.4 Jablonski diagram

The processes that occur between the absorption and emission of light are usually illustrated by the Jablonski diagram [1]. Fig 4.2 shows the Jablonski

### TPE fluorescence in dye doped POF

diagram for one-photon and two-photon absorption and the subsequent fluorescence emission. In the one-photon case, a single photon of energy  $h\nu_1$  is absorbed by the molecule and gets excited to a higher energy state. Molecule decays nonradiatively to some lower energy state and from there fluorescence occurs by emitting a photon of energy  $h\nu_f$ . The emitted photon will be of lower energy compared to the absorbed photon. In the two-photon case, two photons of energy  $h\nu_2$  ( $h\nu_2 < h\nu_1$ ) is absorbed and fluorescence occurs by emitting a photon of energy  $h\nu_f$ . The emitted photon will be of higher energy compared to the absorbed photon. Therefore it is called 'upconverted' emission.

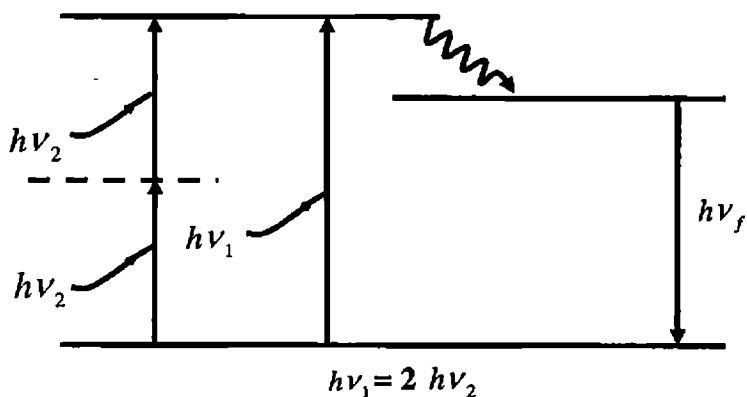
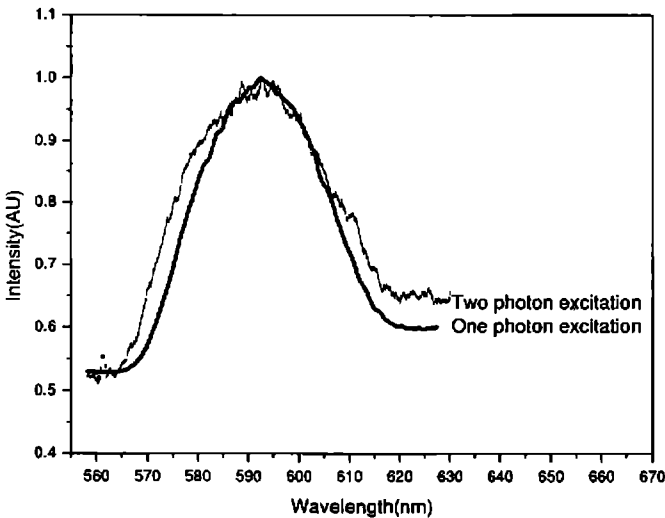


Fig 4.2: Jablonski diagram for one photon and two photon absorption

#### 4.5 One-photon and two-photon excited fluorescence spectra

Two-photon induced fluorescence spectra excited by 800 nm, 70 fs laser beam for a typical sample of Rh 6G doped POF is shown in Fig 4.3. For comparison, one-photon induced fluorescence spectrum excited by 532nm laser beam is also shown in the figure. As is clear from the plots, the one and two-photon induced fluorescence spectra are very similar, which suggests

that the induced fluorescence is emitted from the same excited singlet state ( $S_1$ ) irrespective of one-photon or two-photon excitation. That is, both the one and two-photon excitations (OPE and TPE) ultimately result in the same lowest excited singlet state  $S_1$  via internal conversion from the higher excited states, although the mechanism and the selection rules of the two-photon process differ from that of one-photon process. As a result, the fluorescence emitted from the same excited state leads to similar fluorescence spectral behavior from both OPE and TPE [20, 21].



**Fig 4.3:** One photon and two photon excited fluorescence spectra from Rh 6G dye doped POF.

#### 4.6 Square-law dependence of fluorescence intensity

The excitation intensity dependence of the two-photon fluorescence is investigated by plotting the logarithm of fluorescence intensity versus the logarithm of incident laser power as shown in Fig 4.4. It is clear from the plot that the two-photon excited fluorescence obeys the square-law dependence,

## *TPE fluorescence in dye doped POF*

---

where the slope is about 1.8. This confirms that the excitation is a typical two-photon process at the excitation wavelength of 800 nm [20-21].

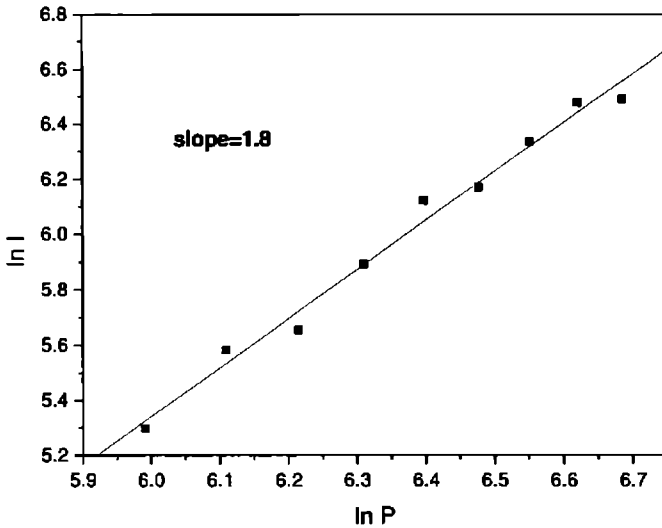


**Fig 4.4:** The log-log plot of the fluorescence intensity versus the incident laser power at the excitation wavelength 800nm.

### **4.7 Side illumination fluorescence (SIF) measurement technique.**

Typically, the propagation loss in a polymer fiber is measured by the successive cut and measure (cut back) technique at a specific wavelength. A nondestructive SIF measurement is used for the loss measurement in the present study. In the SIF measurement, the fluorescence generated from the dye doped POF, when it is excited from the side by a monochromatic light source, is used as a broad-wavelength light source to measure the linear absorption in the fibers.

## 4.8 Experiment

The dye doped polymer optical fiber for the present study is fabricated as described in the chapter 2. For investigating the TPE fluorescence emission, energy transfer process and its effect on the attenuation coefficient in dye doped POF, four fiber samples with a diameter of  $400\ \mu\text{m}$  are fabricated having the following dye concentrations. *a)* Rh6G (0.25 mM) *b)* Rh6G (0.25 mM) and Rh B (0.11 mM) *c)* Rh6G (0.25 mM) and RhB(0.25 mM) *d)* Rh B(0.25 mM).

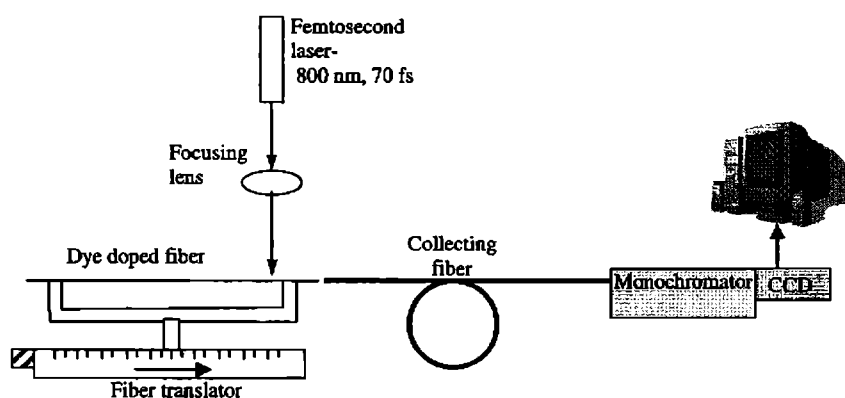


**Fig 4.5:** Experimental set up to record the two photon excited SIF emission from the dye doped POF.

A schematic of the experimental set up for the two-photon excited SIF studies from dye doped polymer optical fiber is shown in Fig 4.5. A mode-locked Ti:sapphire laser (Tsunami, Spectra Physics) is used as the pump source which has an output wavelength of 800 nm, pulse width of 70 fs and an average power of 0.4 W at a repetition rate of 80 MHz. The fiber is mounted normally on a translation stage with respect to the incident pump beam. Pump beam is focused on the fiber using a convex lens of appropriate focal length. When the femtosecond laser pulse is focused, very high peak power is produced at the focal volume leading to simultaneous absorption of two



## *TPE fluorescence in dye doped POF*

photons. It can be noted that though there is no linear absorption for the dyes Rh6G and Rh B at 800 nm, the two-photon energy of 800 nm just falls within the linear absorption band, 400-550 nm, of these dyes and can lead to two-photon absorption.

C.Xu et al have reported that the two-photon excitation (TPE) peak wavelength appear blue shifted relative to twice the one-photon absorption (OPA) peak wavelength in the case of rhodamine dyes and the TPE peak wavelength is observed to be around 800 nm[22]. Therefore, 800 nm pump source is quite suitable for recording the TPE fluorescence spectrum in the case of rhodamine dyes.

The side illumination of the dye doped fiber generates two-photon excited fluorescence emission at the focal point. Light emission is collected from one end of the dye doped fiber using a collecting optical fiber coupled to a monochromator-CCD system (Acton Spectrapro). To measure the transmitted fluorescence as a function of propagation distance through the fiber, the illumination point on the fiber is varied by translating the fiber horizontally across the laser source.

## **4.9 Results and Discussion**

### **4.9.1 Energy Transfer**

Two types of energy transfer processes which figure in our investigations are discussed in the following sections.

#### **Case 1**

First one is the energy transfer occurring from the dye Rh 6G to Rh B. There is a strong overlap between the emission spectrum of Rh 6G and absorption spectrum of Rh B as explained in chapter 2 (Fig 2.7 chapter 2), which clearly indicates the possibility of energy transfer from Rh 6G to Rh B. Energy

transfer of Rh 6G: Rh B dye mixtures in a PMMA matrix is well studied and it is shown that energy transfer is occurring from Rh 6G to Rh B [23-24]. Here, in the two-photon excitation process also, a clear energy transfer is observed from Rh 6G to Rh B.

Fig 4.6 shows a comparison of the two-photon excited side illumination fluorescence emission from POF doped with Rh 6G, Rh 6G- Rh B dye mixture system and Rh B. The propagation distance of the transmitted fluorescence emission through the fiber is 26 mm.

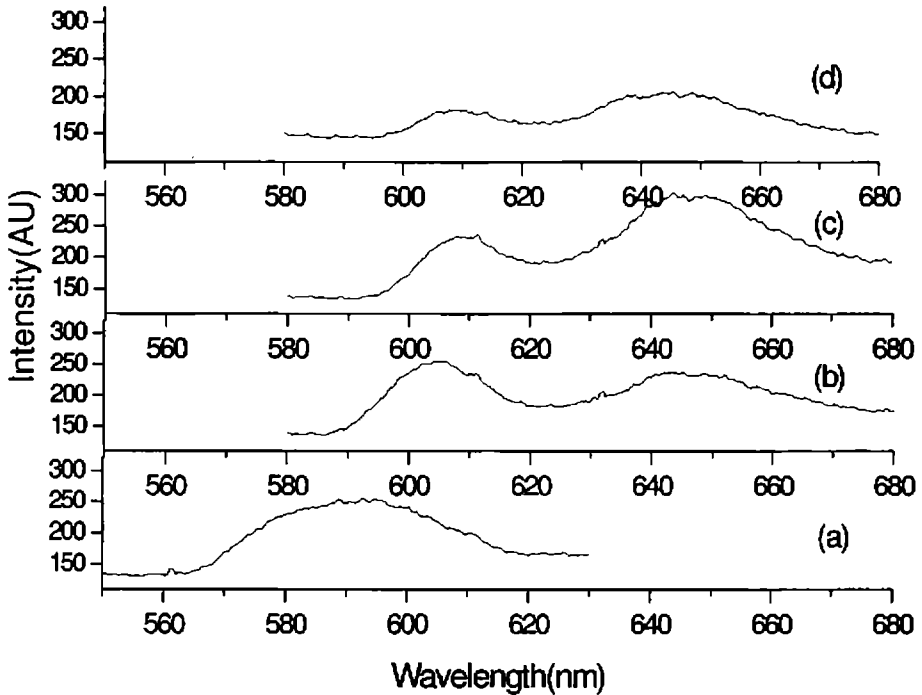


**Fig 4.6:** Shift of fluorescence emission peak due to energy transfer process in dye mixture doped POF *a)* Rh 6G (0.25mM) *b)* Rh 6G (0.25mM) and Rh B (0.11mM) *c)* Rh 6G (0.25mM) and Rh B (0.25mM) *d)* Rh B (0.25mM).

### *TPE fluorescence in dye doped POF*

In the case of Rh 6G (0.25 mM) doped POF, fluorescence emission peak is observed to be at 590 nm (Fig 4.6 a). Consider the case of Rh 6G (0.25 mM) and Rh B (0.11 mM) doped POF (Fig 4.6 b). It is to be noted that both the dyes Rh 6G and Rh B can get excited by two-photon absorption and exhibit their own fluorescence in the dye mixture system since the quantum yield of fluorescence is almost equal for both the dyes. But as a result of the strong overlap between Rh 6G emission and Rh B absorption, energy transfer also occurs from Rh 6G to Rh B through radiative (shorter wavelength part of the fluorescence emission of Rh 6G gets re-absorbed and re-emitted by the Rh B molecules) and non-radiative (FRET) paths. Therefore, Rh B molecules in the dye mixture system are excited both by direct two-photon excitation at 800 nm and by reabsorbing the energy transferred from the Rh 6G molecules, which initially absorb the pump photons.

Thus, in Fig 4.6b the fluorescence spectral peak is observed to be red shifted to 604 nm because of the energy transfer from Rh 6G to Rh B. Also a second peak is observed at 647 nm which is the characteristic peak of Rh B. In the case of Rh 6G (0.25 mM) and Rh B(0.25 mM) doped POF(Fig 4.6c), intensity of the first peak in the fluorescence emission becomes less compared to the prominent peak at 647 nm. In this case the energy transfer from Rh 6G to Rh B is maximum and the spectrum appears to be the same as that of Rh B (0.25 mM) doped POF (Fig 4.6d). This is because of the fact that maximum energy transfer occurs when both dyes are taken in equal concentration. Fig 4.6d represents the fluorescence spectrum corresponding to RhB (0.25 mM) alone.

It is to be noted here that the two-photon excited fluorescence emission spectra of the dye doped POF samples as shown in Fig 4.6 are showing the same spectral behavior as in the one-photon case ( Fig 2.11, chapter 2). The

spectral peak wavelength is slightly different in the two cases because of the difference in the length of the samples used for recording the spectrum. The length of the fiber samples used in the one-photon case is longer (7 cm) compared to that in the two-photon case (2.6 cm). Hence, as a result of the re-absorption- re-emission effect observed in the dye doped POF, the fluorescence peak wavelength is redshifted in the case of one- photon case compared to that of the two-photon case.

Again, consider the fluorescence intensity of the three samples *b*, *c* and *d* in Fig 4.6. Compared to Rh B (0.25 mM) doped sample, the fluorescence intensity (for example at 647 nm) is slightly more in the case of Rh 6G(0.25mM) and Rh B(0.11 mM) doped mixture sample as a result of the energy transfer from Rh 6G to Rh B. For Rh 6G (0.25 mM) and Rh B(0.25 mM) doped sample, the fluorescence intensity is maximum compared to that of the samples *b* and *d* because of the maximum energy transfer in this case. Table 4.1 summarizes the above observations.

Concentration of samples.	Fluorescence intensity (at 647nm) A.U
Rh B(0.25 mM)	200
Rh6G(0.25 mM) &RhB(0.11 mM)	231
Rh 6G(0.25 mM)& Rh B(0.25 mM)	293

**Table 4.1:** Enhancement in Rh B fluorescence intensity as a result of the energy transfer from Rh6G to Rh B

## TPE fluorescence in dye doped POF

It is to be noted here that the fluorescence spectra from the dye doped fiber samples and the energy transfer phenomenon discussed above are similar to that of one-photon excited fluorescence described in chapters 2 and 3. This again confirms that irrespective of one-photon or two-photon excitation, the fluorescence emission is taking place from the same excited singlet level[20,21].

### **Case2**

There is an overlap between the absorption and fluorescence emission from the dye molecules as explained in chapter 2. Thus, as the propagation distance increases, the propagating fluorescence light gets re-absorbed and re-emitted at a longer wavelength causing red shift in the emitted fluorescence spectrum. In effect, this re-absorption: re-emission process causes a radiative energy transfer from shorter wavelength part of the fluorescence spectrum to the longer wavelength part, as the propagation distance is increased. This will be discussed in detail in the following sections.

### **4.9.2 SIF spectra with propagation distance**

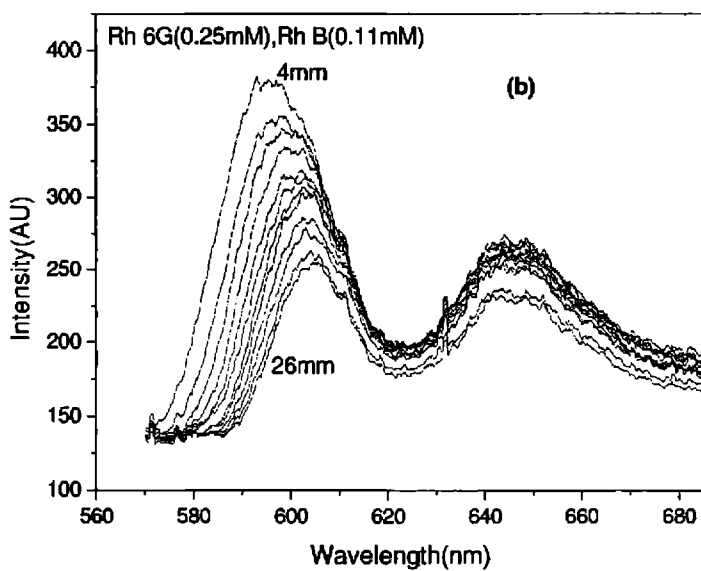
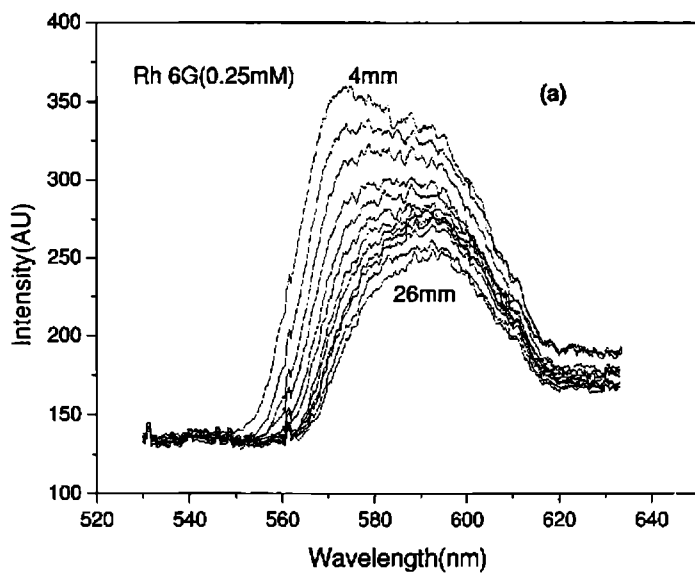
Fig 4.7 shows the two-photon excited side illumination fluorescence spectra for different propagation distances (4 mm-26 mm) through the fiber in the case of the above mentioned four samples *a*, *b*, *c* and *d*. Three important observations can be deduced from these plots.

#### **1) *Decrease in fluorescence intensity:***

As the propagation distance increases, the overall magnitude of the fluorescence intensity decreases in all the cases due to loss mechanisms such as absorption and scattering of the fluorescence emission.

#### **2) *Redshift in fluorescence peak with propagation distance:***

There is a red shift for the peak fluorescence emission in all the four cases as the illumination distance from the collecting end of the fiber is increased.



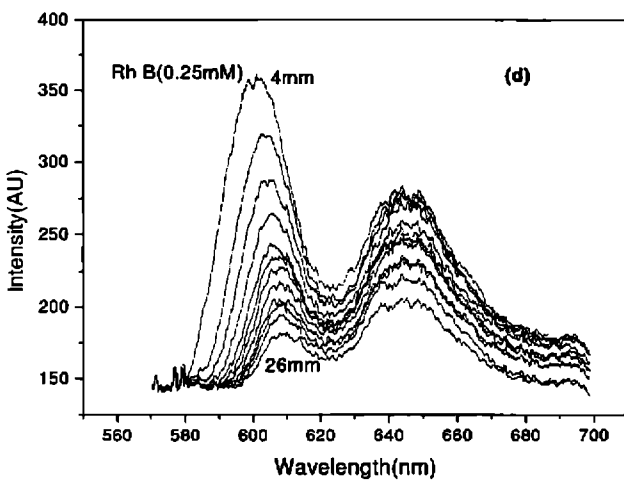
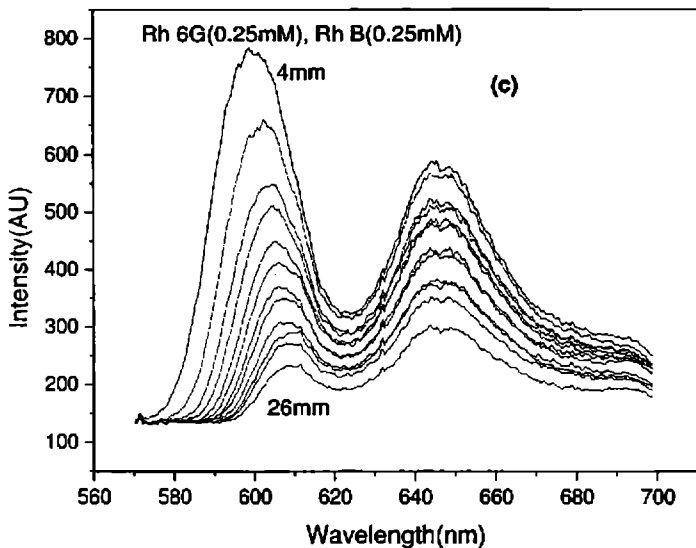


**Fig 4.7:** Two photon excited SIF spectra for different propagation distances (4 mm-26 mm) through the fiber. *a)* Rh 6G(0.25mM) *b)* Rh 6G(0.25mM) and Rh B(0.11mM) *c)* Rh 6G(0.25mM) and Rh B(0.25mM) *d)* Rh B(0.25mM).

Fig 4.8 shows the variation of the peak fluorescence emission with propagation distance through the fiber for the four samples. A clear red shift in the peak fluorescence emission wavelength is observed for the first peak as the propagation distance is increased from 4 mm to 26 mm. This red shift is 581-592 nm in the case of Rh 6G(0.25mM) doped POF(Fig 4.8a), 595-605nm for Rh 6G(0.25mM) and Rh B(0.11mM) doped POF(Fig 4.8b), 599-609nm for Rh 6G(0.25mM) and Rh B(0.25mM) doped POF(Fig 4.8c) and 600-608 nm for Rh B(0.25mM) doped POF(Fig 4.8d). The observed red shift of the first peak is due to the re-absorption and re-emission process (radiative energy transfer) taking place within the dye doped fiber as the propagation distance increases (case 2). Re-absorption process occurs only at the shorter wavelength part of the fluorescence signal. Therefore no red shift is observed for the second peak at the longer wavelength part in the case of the samples *b*, *c* and *d*.

It is to be noted here that in the case of the dye mixture doped samples *b* and *c*, the propagating fluorescence light gets absorbed mainly by the Rh B molecule and there is only a slight chance of absorption by Rh 6G molecule. As is obvious from the absorption spectrum (Fig 2.5:chapter 2), the absorption band of Rh 6G ends at 570nm and the fluorescence light from the dye mixture system is beyond that wavelength.

### 3) *Energy transfer from the first peak to the second peak:*

An energy transfer is observed from the first peak region of the fluorescence spectrum to the second peak region in the case of the samples *b*, *c* and *d* as the propagation distance is increased from 4 mm to 26 mm. For getting a clear picture of this energy transfer, the intensity ratio of the first peak to the second peak ( $I_1/I_2$ ) versus propagation distance is plotted in the case of the last three fiber samples *b*, *c* & *d* (Fig 4.9).



**TPE fluorescence in dye doped POF**

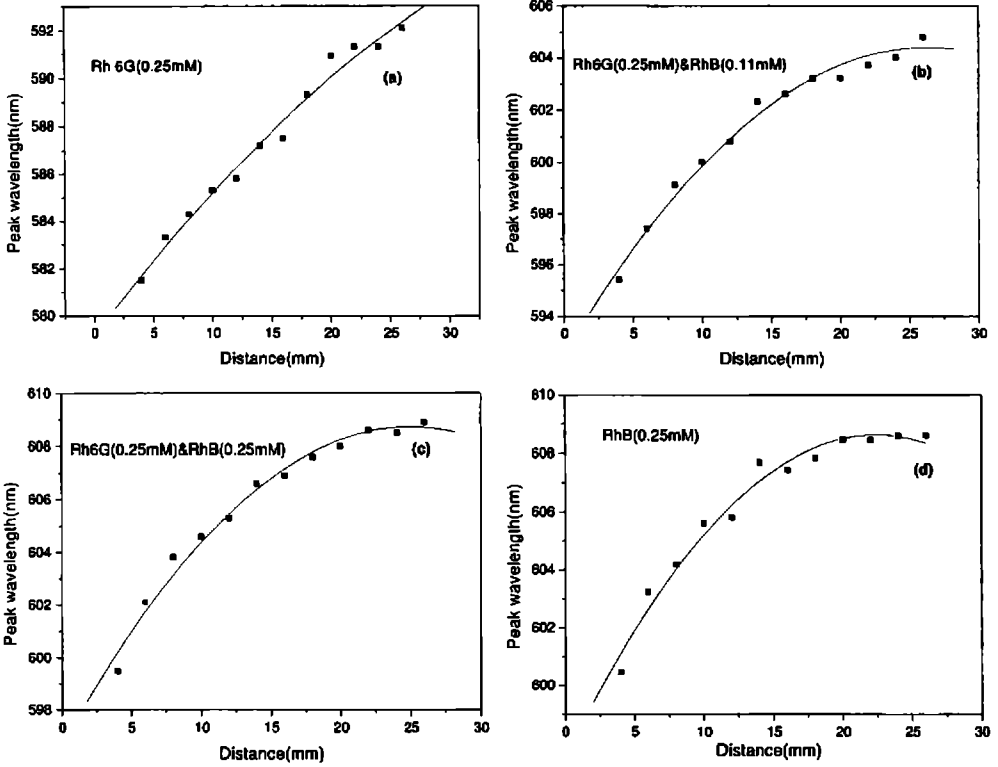


**Fig 4.8:** Redshift of the peak fluorescence emission with propagation distance (4mm-26mm) through the fiber. *a)* Rh 6G(0.25mM) *b)* Rh 6G(0.25mM) and Rh B(0.11mM) *c)* Rh 6G(0.25mM) and Rh B(0.25mM) *d)* Rh B(0.25mM).

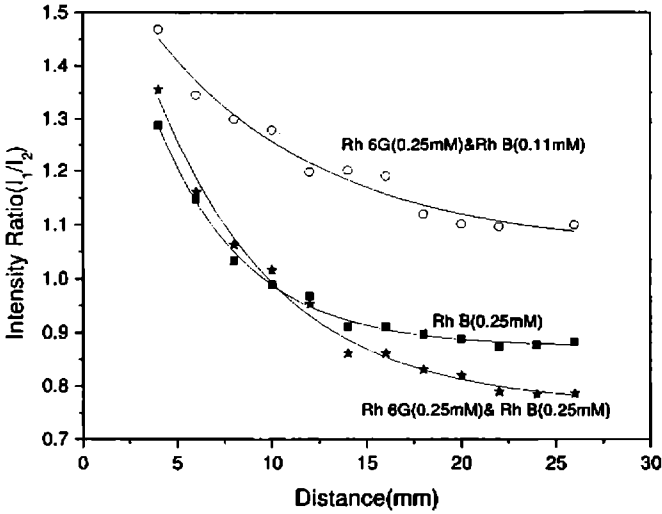


**Fig 4.9:** Intensity ratio of the first peak to the second peak ( $I_1/I_2$ ) versus propagation distance.

In all the three plots,  $(I_1/I_2)$  decreases with propagation distance. The decrease in the value of intensity ratio is a clear indication of the existence of an energy transfer from the first peak to the second peak. As mentioned earlier, the shorter wavelength part of the fluorescence spectrum corresponding to the first peak gets re-absorbed by the Rh B molecule and is re-emitted at longer wavelength as the propagation distance is increased. This causes relatively more loss in the first peak region and a net gain in the second peak region. Thus in effect, energy transfer of radiative type occurs from the first peak region to the second peak region of the fluorescence spectrum as propagation distance increases.

Considering the samples *c* and *d*, the energy transfer effect is almost at the same rate as a result of the same Rh B concentration (0.25 mM) in both the cases. For Rh 6G(0.25 mM) and Rh B(0.11 mM) doped sample, the effect is less prominent as expected because of the lower Rh B concentration which is the main component of this energy transfer process.

#### ***Energy transfer coefficient***

We can define a transfer coefficient,  $\beta$ , which can be deduced from the  $\ln(I_1/I_2)$  versus distance plot (Fig 4.10), such that,

$$Y_{(z)} = Y_{(0)} e^{-\beta z}, \quad (4.4)$$

where  $Y = I_1/I_2$

$Y_{(z)}$  is the intensity ratio value after a propagation distance  $z$ ,  $Y_{(0)}$  is the initial intensity ratio value and  $\beta$  is the transfer coefficient.

It is observed that the plots in Fig 4.10 cannot be fitted to a single straight line. But it can be peeled off to two straight lines using the peeling the curve method [25, 26] corresponding to two transfer coefficients  $\beta_1$  and  $\beta_2$  such that,

***TPE fluorescence in dye doped POF***

$$Y_{(z)} = Y_{(01)} e^{-\beta_1 Z} , \text{ for shorter propagation distances} \quad (4.5)$$

$$Y_{(z)} = Y_{(02)} e^{-\beta_2 Z} , \text{ for longer propagation distances} \quad (4.6)$$

The above equations can be expressed as

$$Y_{(z)} = Y_{01} H(Z_c - Z) e^{-\beta_1 Z} + Y_{02} H(Z - Z_c) e^{-\beta_2 Z} \quad (4.7)$$

where  $H(x)$  is the Heaviside step function such that

$$H(x) = 1, \quad x > 0$$

$$= 0, \quad x < 0.$$

$Z_c$  is a critical length below which the intensity ratio varies according to the first component in equation (4.7) with an energy transfer coefficient  $\beta_1$  and above which it varies according to the second component with an energy transfer coefficient  $\beta_2$ .

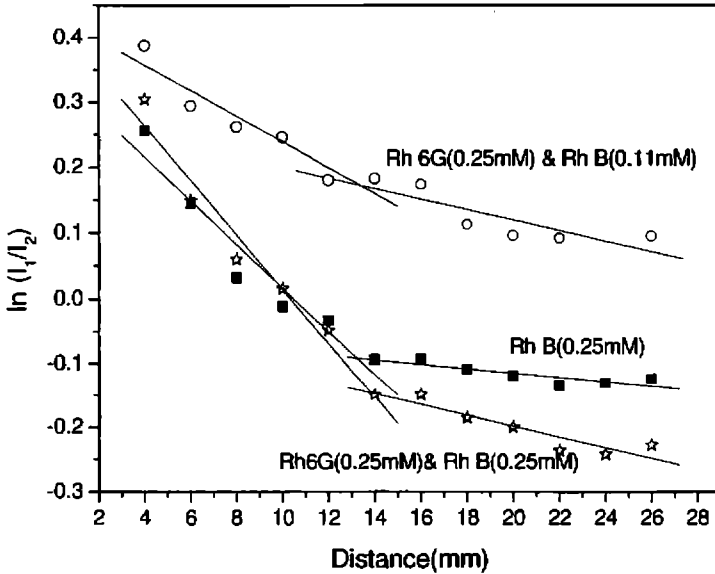


**Fig 4.10:** Natural logarithm of  $(I_1/I_2)$  versus propagation distance.

It is observed that the transfer coefficient values obtained from the slopes of the peeled off straight lines, for shorter propagation distances,  $\beta_1$ , is higher

than the longer propagation distance value,  $\beta_2$ , in all the three cases. Therefore it is evident that the energy transfer is more at shorter propagation distances and it saturates at longer propagation distances. As the propagation distance increases the fluorescence spectrum shows a red shift as shown in Fig 4.7. As a result, the extent of spectral overlap between the absorption and fluorescence emission, which is the main cause of this energy transfer process, goes on decreasing as the propagation distance increases. This decrease in the extent of spectral overlap causes the reduction in energy transfer process at longer propagation distances compared to shorter propagation distances.

In the case of Rh B doped POF, the transfer coefficient value,  $\beta_1$ , is 0.03 which is higher than the value 0.01 for longer propagation distances and similar behavior is observed for the other two samples (*b* and *c*) also. Again, the transfer coefficient,  $\beta_1=0.02$ , for Rh6G (0.25 mM) and RhB (0.11 mM) doped POF is lower than the corresponding transfer coefficient,  $\beta_1=0.04$ , for Rh6G (0.25 mM) and RhB (0.25 mM) doped POF as expected because of the lesser number of Rh B molecules and hence less energy transfer.

### 4.9.3 Attenuation coefficient

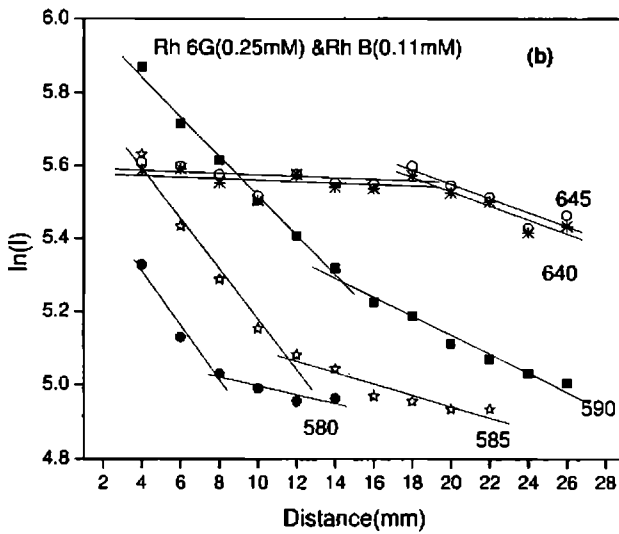
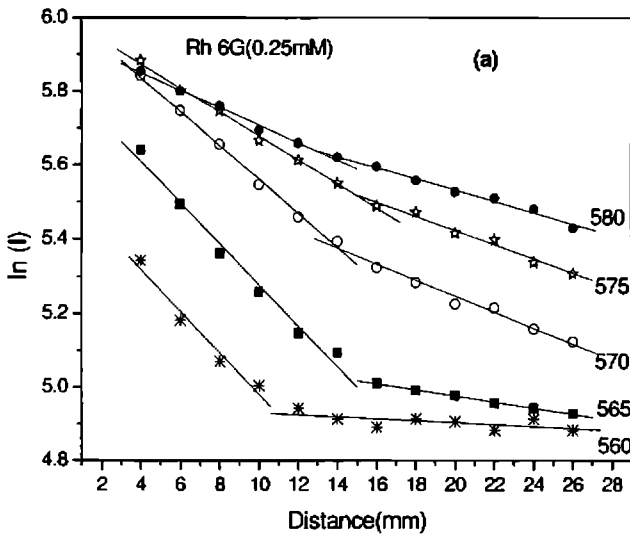
Fluorescence emission collected from the dye doped fiber has a spectral width of about 100 nm and that itself can be used as a broad-wavelength light source to characterize the attenuation coefficient in the dye doped POF. The transmitted fluorescence is measured as a function of propagation distance so as to characterize the attenuation in the fiber.

### TPE fluorescence in dye doped POF

From Beer-Lambert's law for linear optical attenuation in a medium,

$$I(\lambda, z) = I_0(\lambda) \exp(-\alpha(\lambda) z) \quad (4.8)$$

where  $I(\lambda, z)$  and  $I_0(\lambda)$  represent the intensity of the transmitted light at wavelength  $\lambda$  for propagation distances  $z$  and  $z=0$  respectively and  $\alpha(\lambda)$  is the linear attenuation coefficient. Fig 4.11 shows the natural logarithm of the transmitted intensity versus propagation distance (data taken from Fig 4.7) for different wavelengths in the case of the above mentioned four samples.



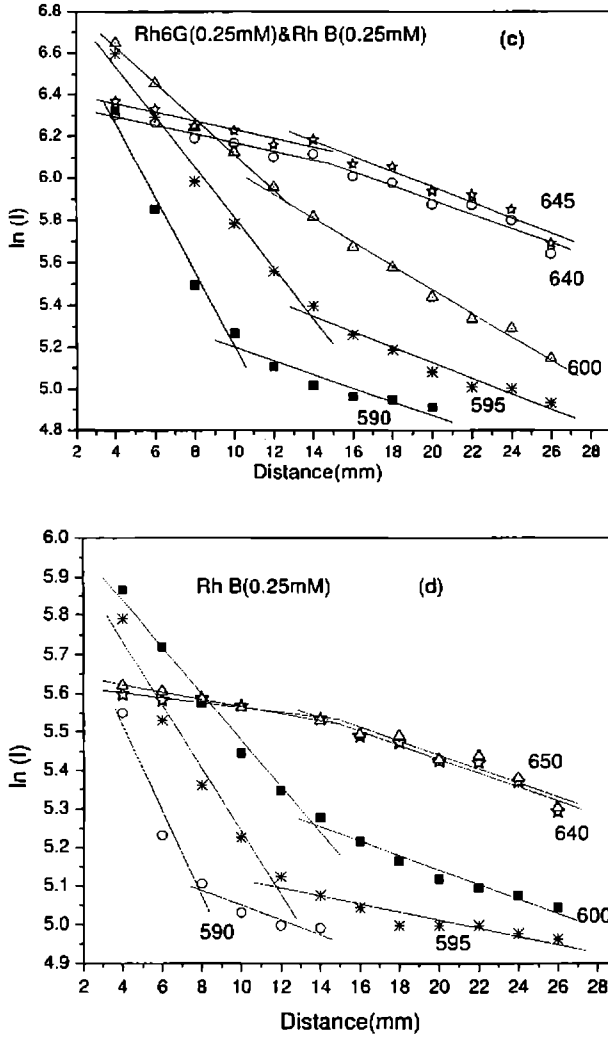


**Fig 4.11:** Natural logarithm of the transmitted intensity versus propagation distance through the fiber for different wavelengths. *a)* Rh 6G(0.25mM) *b)* Rh 6G(0.25mM) and Rh B(0.11mM) *c)* Rh 6G(0.25mM) and Rh B(0.25mM) *d)* Rh B(0.25mM).

## TPE fluorescence in dye doped POF

An interesting observation is the nonlinear behavior of the  $\ln I$  versus distance plot, which suggests that the attenuation coefficient is not a constant for the total length of propagation through the fiber. The non linear plot of  $\ln I$  versus  $z$  can be fitted to a minimum number of straight lines which will provide the corresponding attenuation coefficients [25, 26]. The plots can be peeled off to two straight lines corresponding to two different attenuation coefficients  $\alpha_1$  and  $\alpha_2$  for shorter and longer propagation distances respectively.

The spatial dependence of intensity variation along the length of the fiber can be represented by the following equation using the Heaviside step function,

$$I_z = I_{01}H(Z_0 - Z)e^{-\alpha_1 z} + I_{02}H(Z - Z_0)e^{-\alpha_2 z} \quad (4.9)$$

where  $Z_0$  is a critical length below which the intensity decreases according to the first component in equation (4.9) with the attenuation coefficient  $\alpha_1$  and above which according to the second component with the attenuation coefficient  $\alpha_2$ .

It is observed that there is a decrease in the attenuation coefficient for longer propagation distances compared to shorter propagation distances in all the four cases corresponding to the first peak wavelengths (say 560,570,580,590,600 nm etc) as depicted in Table 4.2a-d. This is because of the re-absorption and re-emission effect observed in the dye molecules as the propagation distance is increased. As propagation distance increases, the propagating light interacts with more number of dye molecules which results in enhanced emission and thereby reduction in loss. This result is in accordance with the higher transfer coefficient  $\beta_1$  at shorter propagation distances which leads to an increase in the attenuation coefficient at shorter distances compared to longer propagation distances.

When short distance of propagation is considered, the attenuation coefficient is found to be larger for shorter wavelengths compared to longer wavelengths in all the samples (Table 4.2 a-d). The re-absorption of propagating fluorescence light by dye molecules is more at the shorter wavelength side of the fluorescent emission spectrum due to the overlap between the absorption spectrum and the shorter wavelength part of the fluorescent spectrum of dye molecules. This re-absorbed light gets emitted at a longer wavelength. So the emission intensity at longer wavelength side is larger and attenuation is less compared to shorter wavelength region.

Wavelength(nm) Rh 6G(0.25 mM)	Attenuation coefficient(mm <sup>-1</sup> )	
	shorter distance	Longer distance
560	0.06	0.01
565	0.06	0.01
570	0.05	0.02
575	0.03	0.02
580	0.02	0.02
590	0.02	0.01
595	0.02	0.01
605	0.01	0.01

Table 4.2 a



*TPE fluorescence in dye doped POF*

---

Wavelength(nm) Rh6G(0.25 mM) RhB(0.11 mM)	Attenuation coefficient(mm <sup>-1</sup> )	
	shorter distance	longer distance
First peak		
580	0.07	0.01
585	0.07	0.01
590	0.05	0.03
Second peak		
640	0.01	0.01
645	0.01	0.02

Table 4.2 b

Wavelength(nm) Rh6G(0.25 mM) RhB(0.25 mM)	Attenuation coefficient(mm <sup>-1</sup> )	
	shorter distance	longer distance
First peak		
590	0.18	0.03
595	0.12	0.04
600	0.09	0.06
605	0.07	0.05
Second peak		
640	0.02	0.03
645	0.02	0.04

Table 4.2 c

Wavelength(nm) Rh B(0.25 mM)	Attenuation coefficient(mm <sup>-1</sup> )	
	shorter distance	longer distance
<b>First peak</b>		
590	0.11	0.02
595	0.08	0.01
600	0.06	0.02
605	0.04	0.02
<b>Second peak</b>		
640	0.01	0.02
650	0.01	0.02

Table 4.2 d

Table 4.2: Variation of attenuation coefficient for different wavelengths and different propagation distances for the four samples under study. *a)* Rh 6G (0.25mM) *b)* Rh 6G (0.25mM) and Rh B (0.11mM) *c)* Rh 6G (0.25mM) and Rh B (0.25mM) *d)* Rh B (0.25mM).

The attenuation coefficient for wavelengths (say 640 nm, 645 nm, 650 nm) corresponding to the second peak region is found to be very less compared to the attenuation for shorter wavelengths corresponding to the first peak region (Fig 4.11 b, c & d and Table 4.2b-d). This is because of the energy gain achieved by the second peak region due to the energy transfer occurring from first peak to the second peak.

Another observation is that the attenuation coefficient for wavelength corresponding to the second peak region is found to be slightly lower at shorter propagation distances than at longer distances. This is in accordance with the result that  $\beta$ , the transfer coefficient, is higher at shorter propagation

*TPE fluorescence in dye doped POF*

---

distances than at longer distances. This results in maximum energy transfer leading to reduction in loss at shorter propagation distances for the second peak region.

#### **4.10 Conclusions**

Two-photon excited SIF spectrum from Rh 6G: Rh B dye mixture doped POF is found to be redshifted compared to that of Rh 6G doped POF due to the energy transfer occurring from Rh 6G to Rh B. The fluorescence intensity of Rh B doped POF gets enhanced in the presence of Rh 6G as a result of this energy transfer. Position dependent tuning of two-photon excited SIF spectra is investigated for different dye doped POF samples. As a result of the re-absorption and re-emission process in dye molecules, an effective energy transfer is observed from the shorter wavelength part of the fluorescence spectrum to the longer wavelength part as the propagation distance is increased in dye doped POF. Energy transfer coefficient is found to be higher at shorter propagation distances compared to longer distances. Two-photon excited fluorescence signal is used to characterize the optical attenuation coefficient in dye doped POF. The attenuation coefficient is lower at longer propagation distances compared to shorter distances. This is due to the re-absorption and re-emission process taking place within the dye doped fiber as the propagation distance is increased. The attenuation coefficient is found to be larger for shorter wavelengths compared to longer wavelengths due to the enhanced re-absorption of fluorescent light at shorter wavelength side. The attenuation coefficient for wavelengths corresponding to the second peak region is found to be very less compared to the loss at shorter wavelengths corresponding to the first peak region due to the energy gain achieved in the second peak. These results on energy transfer and the attenuation coefficient is useful for the appropriate selection of specific combinations of dyes for efficient upconverted lasing in dye doped POF.

## References

1. Joseph R Lakowicz, *Principles of fluorescence spectroscopy* (Springer, 2006).
2. K Svoboda and R Yasuda, "Principles of two-photon excitation microscopy and its applications to neuroscience," *Neuron* **50**, 823-839(2006).
3. E Heumann, S Bar, K Rademaker, G Huber, S Butterworth, A Diening and W Seelert, " Semiconductor- laser- pumped high-power upconversion laser," *Appl.Phys.Lett* **88**, 061108-061111(2006).
4. G.Qin, S Huang, Y Feng, A Shirakawa, M Musha and K I Ueda, "Power scaling of Tm<sup>3+</sup> doped ZBLAN blue upconversion fiber lasers: modeling and experiments," *Appl.Phys B:Lasers and Optics* **82**, 65-70(2006).
5. M.Goppert-Mayer, *Ann.Phys.* **9**,273-294 (1931).
6. W K Kaiser and C G B Garrett, " Two-Photon Excitation in CaF<sub>2</sub>:Eu<sup>2+</sup>," *Phys.Rev.Lett* **7**,229-231 (1961) .
7. X H Yang,J M Hays,W Shan and J J Song, " Two-photon pumped blue lasing in bulk ZnSe and ZnSSe," *Appl.Phys.Lett* **62**,1071-1073 (1993).
8. G S He,L Yuan, P N Prasad,A Abbotto,A Facchetti and G A Pagani, " Two photon pumped frequency upconversion lasing of a new blue green dye material," *Opt.Commun* **140** ,49-52(1997).
9. A S Kwok,A Serpenguzel,W F Hsieh and R K Chang, "Two-photon-pumped lasing in microdroplets," *Opt.Lett* **17**,1435-1437(1992).
10. G S He,C F Zhao,J D Bhawalkar and P N Prasad, "Two-photon pumped cavity lasing in novel dye doped bulk matrix rods," *Appl.Phys.Lett* **67**, 3703-3705 (1995).
11. Guang S He, J D Bhawalkar, C F Zhao, C K Park and P N Prasad,"Upconversion dye-doped polymer fiber laser," *Appl.Phys.Lett.***68**, 3549-3551(1996).
12. A Mukherjee,"Two photon pumped upconverted lasing in dye doped polymer waveguides," *Appl.Phys.Lett.***62**, 3423-3425(1993).
13. D C Nguyen,G E Faulkner and M Dulick, " Blue-green (450nm) upconversion Tm<sup>3+</sup>:YLF laser," *Appl.Opt.* **28**, 3553-3555 (1989).

14. Y Mita, Y Wang and S Shionoya, "High brightness blue and green light sources pumped with a 980nm emitting laser diode," *Appl.Phys.Lett* **62**, 802-804(1993).
15. D W Garwey, K Zimmerman, P Young, J Tostenrude, J S Townsend, Z Zhou, M Lobel, M Dayton, R Wittorf and M G Kuzyk, "Single mode nonlinear optical polymer fibers," *J.Opt.Soc.Am B* **13**, 2017-2023(1996).
16. T Kaino, "Waveguide fabrication using organic nonlinear optical materials," *J.Opt.A: Pure Appl.Opt* **2**, R1-7(2000).
17. R J Kruhlak and M G Kuzyk, "Side-illumination fluorescence spectroscopy. I.Principles," *J.Opt.Soc.Am.B* **16**, 1749-1755(1999).
18. R J Kruhlak and M G Kuzyk, "Side-illumination fluorescence spectroscopy.II. Applications to squarine dye-doped polymer optical fibers", *J.Opt.Soc.Am.B* **16**,1756-1767(1999).
19. Richard L Sutherland, *Handbook of non-linear optics* (Marcel Decker,1996).
20. Z Yang, Z K Wu, J S Ma, A D Xia and YQ Li , "One and two-photon induced fluorescence from novel compounds formed by self-assembly of pyrrol-2-yl-methyleneamines with zinc(II)," *Colloids and surfaces A: Physicochem. Eng. Aspects* **257-258**, 515-519(2005).
21. P D Zhao, P Chen, G Q Tang, G L Zhang and W J Chen, "Two-photon spectroscopic properties of a new chlorin derivative photosensitizer," *Chem.Phy.Lett.* **390**,41-44(2004).
22. C.Xu and Watt.W.Webb,"Measurement of two photon excitation cross sections of molecular fluorophores with data from 690 to 1050nm," *J.Opt.Soc.Am.B* **13**, 481-491(1996).
23. G A Kumar, Vinoy Thomas, Gijo Thomas, N V Unnikrishnan, and V P N Nampoori,"Energy Transfer in Rh 6G: Rh B system in PMMA matrix under CW laser excitation," *J.Photochem.Photobiol A: Chemistry* **153**,145-151(2002).
24. N V Unnikrishnan, H S Bhatti and R D Singh, "Energy transfer in dye mixtures studied by laser fluorimetry,"*Journal of Modern Optics.***31**, 983-987(1984).

25. M Rajesh, K Geetha, M Sheeba, C P G Vallabhan, P Radhakrishnan and V P N Nampoore, "Characterisation of rhodamine 6G doped polymer optical fiber by side illumination fluorescence," *Optical Engineering* **45**,075003-075007 (2006).
26. K Geetha,M Rajesh,V P N Nampoore,C P G Vallabhan and P Radhakrishnan, "Loss characterisation in rhodamine 6G doped polymer film waveguide by side illumination fluorescence," *J.Opt. A, Pure. Appl.Opt* **6**, 379-383(2004).

*Fiber optic sensor for the  
detection of adulterant traces in  
coconut oil*

*The design and development of a fiber optic sensor for the detection of trace amounts of paraffin oil and palm oil in coconut oil are presented. This sensor is based on a side polished multimode polymer optical fiber.*



## **5.1 Introduction**

Many advances have been made in recent years in the use of optical fibers as sensors [1-9]. Fiber optic sensor is a device in which variations in the transmitted power or the rate of transmission of light in an optical fiber are the means of measurement or control. The advantages of optical fiber based sensors are well known which include high sensitivity, insensitivity to electromagnetic radiation, spark free, light weight and minimal intrusiveness due to their relatively small size and deployment in harsh and hostile environments. Out of a range of optical fiber sensors reported in the literature, intensity based optical fiber sensors represent one of the earliest and perhaps the most basic type of optical fiber sensor [10-17]. But the main drawback of these types of sensors is that the source fluctuations will affect the output intensity which can be overcome to an extent using a reference signal. The flexibility and sensitivity of fiber optic based sensors permit the monitoring of a variety of parameters, including temperature, pressure, strain, degree of cure, chemical content, viscosity, acoustic waves, magnetic fields, degree of rotation etc.

The use of optical fiber sensors for contaminant detection in food stuffs has been a field of great interest. Edible oil like coconut oil finds an important role in the day- to-day life of ordinary people of south Asia. Because of its high demand and good price, it is very much prone to adulteration. The most commonly used adulterants are paraffin oil, which is a relatively cheap petroleum by- product, and palm oil. These oils are very good candidates for adulteration because of their odourless, colourless and tasteless properties. Since paraffin oil is not an edible oil, its detection plays an important role in determining the quality of coconut oil. Consumption of paraffin oil causes many health hazards. Petroleum, paraffin, paraffin oil and propylene glycol are all derivatives of mineral oil which dissolve the natural oil of skin making

it more dehydrated. It is indigestible and prolonged use may cause leukemia. Hence it is very important to check the purity of coconut oil. Palm oil, due to its low cost and availability, is considered as an inexpensive adulterant option. Palm oil doesn't have all the good qualities of coconut oil. Therefore adding palm oil into coconut oil is not a faithful practice to follow, even though it doesn't cause any serious harm to health.

In many applications like sensors it is often necessary to interact with fields that are guided by a fiber. To gain access to guided waves one must normally remove portions of the fiber cladding. The fibers with cladding partially removed on one side are referred to as side polished fibers [18-24]. They are the building blocks of many fiber optic components such as fiber directional couplers, polarisers, modulators, switches, amplifiers and filters [25-28].

In this chapter, we describe a side polished polymer optical fiber based sensor for the detection of trace amounts of paraffin oil and palm oil in coconut oil. The sensing head is basically a multimode side polished polymer optical fiber [18-24]. Polymer optical fiber has the advantage of low cost, high degree of mechanical flexibility, tensile strength and breaking strength compared to silica fiber [8]. The fiber is polished in such a manner that a large number of guided modes get coupled to the surrounding medium. This increases the sensitivity of the sensor to a great extent. Further increase in sensitivity is achieved by bending the side polished sensor head. The main advantage of this type of sensor is that it is very rugged, washable and reusable. Also, in the case of side polished fiber based sensor, very small amount of sample is needed for analysis. This is important when the procurement of the sample in large quantity is not possible.

## 5.2 Theory of operation

When light propagates in an optical fiber, a fraction of the radiation extends a short distance from the guiding region into the medium of lower refractive index that surrounds it. This is the evanescent field. This evanescent energy may interact with non-absorbing /non-scattering analytes that attenuate the evanescent field by means of refractive index changes, given by [9]

$$P_{out} = P_{in} \frac{(n_1^2 - n_s^2)}{(n_1^2 - n_2^2)} \quad (5.1)$$

where  $n_1$  is the refractive index of the core,  $n_2$  is the refractive index of the cladding,  $n_s$  is the refractive index of the sample surrounding the core,  $P_{in}$  represents the total power injected into the guided modes of the fiber from the source and  $P_{out}$  represents the power coupled to the fiber end in the presence of the sample. It is evident from this equation that power coupled to the fiber after the sensing region decreases with increase in the refractive index of the surrounding medium [9]. Here, this result is exploited to construct a fiber optic refractive index based sensor to detect adulterants in coconut oil.

The amplitude  $E(x)$  of evanescent field decreases exponentially with distance,  $x$  from the core-cladding interface according to the equation

$$E(x) = E_0 \exp(-x/d_p) \quad (5.2)$$

where  $d_p$  is the penetration depth.

The penetration depth describes the distance from the interface where the evanescent field decreases to  $\frac{1}{e}$  of its initial value  $E_0$ .

The magnitude of the penetration depth is given by

$$d_p = \frac{\lambda}{2\pi n_1 \left[ \sin^2 \theta - \left( \frac{n_2}{n_1} \right)^2 \right]^{1/2}} \quad (5.3)$$

where  $\lambda$  = vacuum wavelength,

$\theta$  = angle of incidence to the normal at the interface,

$n_1, n_2$  refractive index values of the core and the cladding.

From equation (5.3), it is clear that the penetration depth  $d_p$  increases with cladding refractive index, indicating an increase in the magnitude of the electric field present in the cladding medium and thus a reduction in the electric field within the core.

The normalized frequency (fiber V-parameter) is given by [29, 11]

$$V = \frac{2\pi a}{\lambda} \sqrt{n_1^2 - n_2^2} \quad (5.4)$$

where  $a$  = core radius.

This equation shows that the  $V$  parameter decreases when cladding refractive index increases. Since the number of modes  $N$  propagating within the fiber is proportional to the square of the normalized frequency it can be inferred that increasing the refractive index of the cladding reduces the number of modes propagating within the fiber.

It is to be noted here in the theoretical treatment that the core refractive index is fixed and the cladding refractive index is less than the core refractive index.

### *Side polished POF sensor*

---

The behavior of side polished fibers with variation in the refractive index of the adjacent medium has been well established in the existing literature [18]. The propagation of light through a side polished fiber is viewed as a perturbed one compared to that of the unpolished fiber. At the side polished region, the cylindrical symmetry of the fiber is altered and the guiding condition, ie, the total internal reflection condition is not satisfied and the propagating rays leaks out. When an external medium like oil is placed at the polished region, it acts as a new cladding there. Depending on the refractive index of the external medium at the polished region, the transmitted optical power output changes according to the theory discussed above. Adulteration of coconut oil with paraffin oil/palm oil increases the refractive index of the resulting sample mixture, which is the cladding at the polished region and the transmitted optical power output reduces accordingly.

### **5.3 Experimental setup**

The experimental arrangement used to determine the adulterant traces in coconut oil is shown in Fig 5.1. The setup consists of a laser source, a side polished fiber sensor head and a detector. The contact area of the bent portion of the fiber with the sample is 7 mmx0.5 mm. Laser source used for the investigation is an intensity stabilized 4mW diode laser emitting at 670 nm. The laser beam is focused onto the sensor head. The output is measured from the other end of the sensor head using an optical power meter (Newport 1825C, accuracy 0.1%). The step index multimode polymer optical fiber used (Super ESKA, SK-40) has a core diameter of 980  $\mu\text{m}$  and a numerical aperture of 0.5. The core and the cladding refractive indices are 1.49 and 1.41 respectively. The core material is polymethylmethacrylate (PMMA) and the cladding is a thin layer of fluorinated polymer. The test samples for this investigation are prepared by changing the concentration of paraffin oil in a fixed volume of coconut oil. Studies are also carried out by mixing palm oil

in a fixed volume of coconut oil. Here, paraffin oil and palm oil are used as adulterants. Sample mixtures of increasing refractive indices are prepared by separately taking increasing concentrations of paraffin oil or palm oil in coconut oil. The refractive indices of samples are measured using a multi-wavelength Abbe refractometer (ATAGO DRM2). The refractive indices of pure coconut oil, paraffin oil and palm oil are found to be 1.449, 1.476, and 1.454 respectively. The accuracy of measurement of refractive index is better than 0.1%.

#### **5.4 Fabrication of the sensor head**

For the fabrication of the sensor head, a few centimeters of a multimode step index polymer optical fiber is used. Fibers to be polished are commonly held in a host-block which allows polishing and prevents the fiber from breaking. Host materials reported in the literature for this purpose are fused silica, etched silicon V-grooves and epoxy resin [18-24]. Epoxy resin is used in the present studies. To begin with, an epoxy resin block is made and the fiber is inserted into the block. The resin block is fabricated in such a manner that the fiber sits inside it in a bent fashion. The bending provides added sensitivity to the sensing head by allowing more modes to get coupled to the sample placed on it. After the fiber is placed inside the resin block, the top portion of it is polished by using abrasives. The abrasive used is aluminum oxide powder of progressively decreasing grain size (10, 5 and 1  $\mu\text{m}$ ). The polishing is continued until the top portion along with a portion of the cladding is peeled off. It is again polished by using finer abrasives. The polishing is done until a flat surface is obtained and enough power is coupled to the outside region. Glass plates are fixed at the sides of the sensing region to hold the sample over the sensing region. The whole assembly is made very compact so that only 0.5 ml of the sample is needed for the whole experimental investigation.

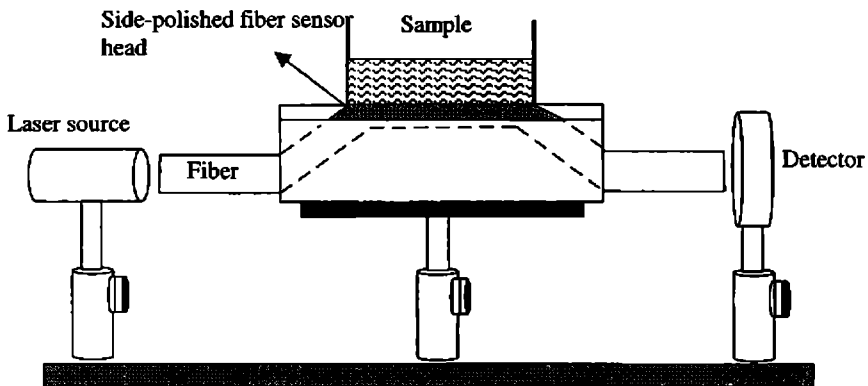


**Fig 5.1:** Side-polished fiber optic sensor for the detection of adulterant traces in coconut oil.

## **5.5 Results and discussion**

To characterize the side polished POF based sensor, samples of different concentrations are placed at the centre of the polished surface of the sensor head using a syringe and the corresponding output power is measured. The results obtained on the basis of the experimental data are shown in Fig 5.2. To improve the reliability of our measurements the readings are noted before and after the sample is added. The normalized output is plotted by taking the ratio of these readings. Fig 5.2a shows the normalized output power as a function of the square of the refractive index of the test samples of paraffin oil in coconut oil. The graph shows a linear decrease in transmitted power at the output as expected from equation (5.1). Fig 5.2b shows the variation in refractive index with volume percentage of adulterants in coconut oil. Fig 5.2c shows the plot of the normalized output power as a function of different concentrations of test samples of paraffin oil / palm oil in coconut oil.

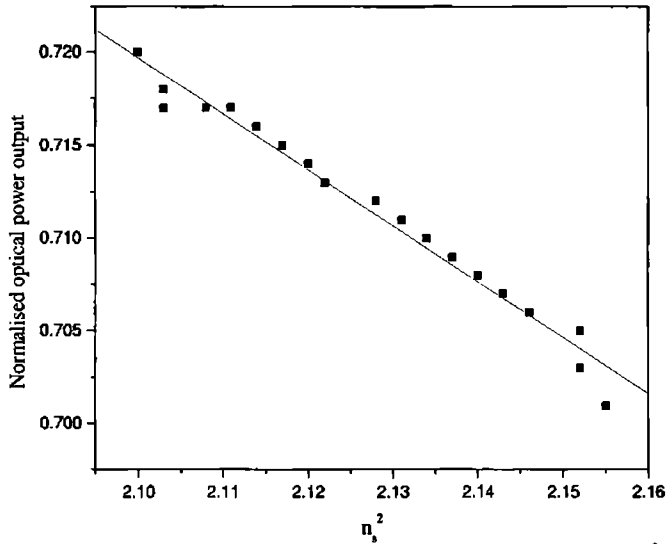


**Fig 5.2a:** Variation of normalized output power  $P$  with  $n_s^2$  of test samples of paraffin oil in coconut oil.

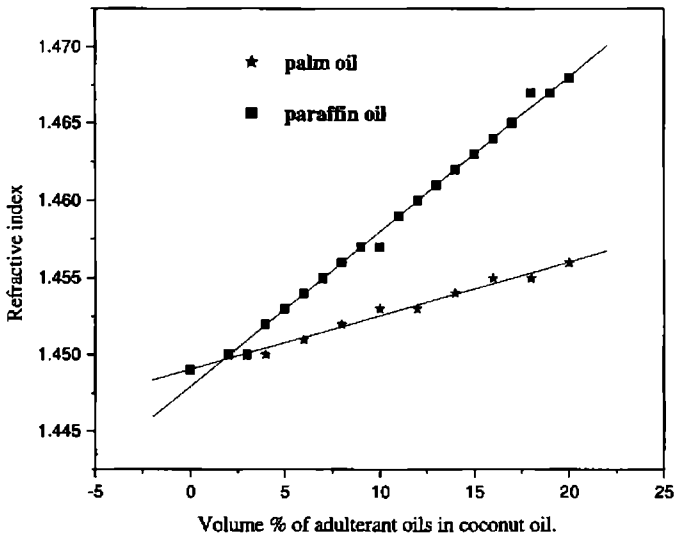


**Fig 5.2b:** Refractive index of the samples against the volume percentage of paraffin oil /palm oil in coconut oil.



### Side polished POF sensor

From the plot it is evident that a decrease in output intensity is observed with increase in the amount of adulterants. Since the adulterant oils used are colourless (low absorbance) at the wavelength of the light at 670 nm (Fig 5.3), the reduction in transmitted light intensity is only due to the refractive index variation. As the concentration of paraffin oil or palm oil increases, refractive index of the medium surrounding the sensor head increases which results in a reduction of output power as illustrated by the theory. Slope of the graph 5.2c gives the sensitivity of the sensor. From the plot it is clear that we can detect a minimum of 2 % paraffin oil / palm oil in the test sample. To find the response time of the sensor, the output of the power meter is connected to a digital multimeter (HP 34401A) which in turn is interfaced to a computer using LabVIEW-7 software. Typical value of the response time is found to be 7 seconds as shown in Fig 5.4.

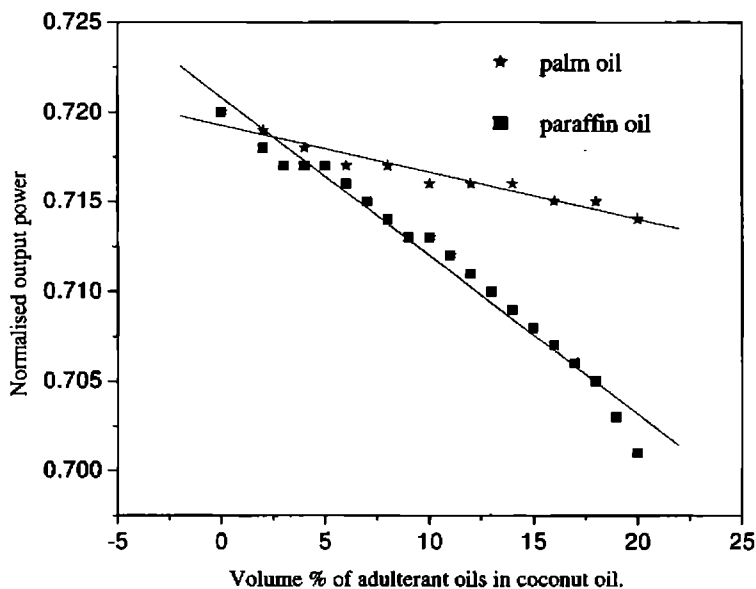


**Fig 5.2c:** Normalized output power against the volume percentage of paraffin oil /palm oil in coconut oil.

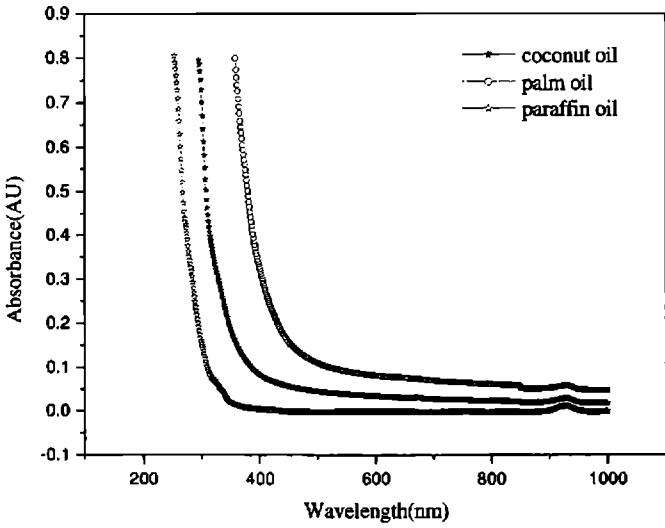


Fig 5.3: Absorption spectra of coconut oil, palm oil and paraffin oil showing negligible absorbance at 670 nm.

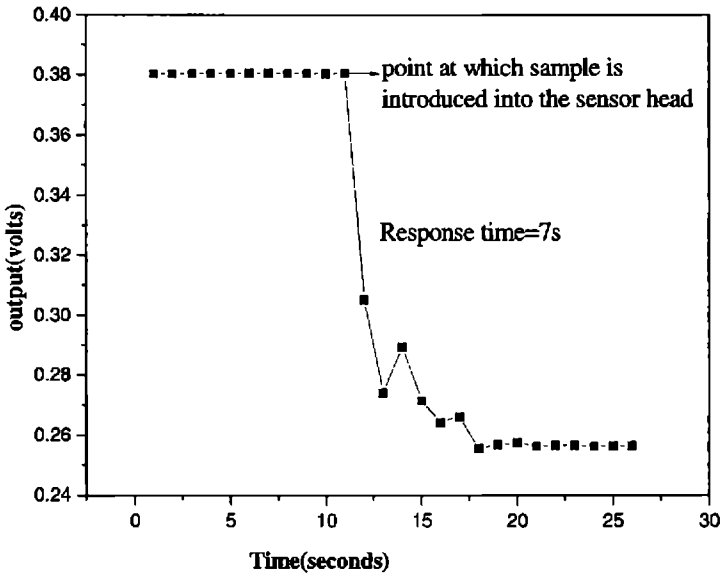


Fig 5.4: Response time of the sensor plotted using a digital multimeter and LabVIEW-7 interface.

## **5.6 Conclusions**

Sensitive and versatile side polished polymer optical fiber based sensor design is developed for the detection of trace amounts of adulterants in coconut oil, which is one of the most commonly used edible oils in south Asia. The sensor exploits refractive index dependent intensity variation. This side polished fiber based device which acts as a refractometer can not only differentiate chemicals based on their refractive index, such as palm oil / paraffin oil, but it can also act as a concentration indicator of a particular colorless chemical solution. The observed sensitivity is almost linear and the detection limit is 2 %( by volume) paraffin oil /palm oil in coconut oil. The developed sensor is user friendly and reusable allowing instantaneous determination of the presence of adulterant traces in a coconut oil sample without involving any chemical analysis.

---

**References**

1. Anna Grazia Mignani and Francesco Baldini, "In -Vivo Biomedical Monitoring by Fiber Optic Systems", *Journal of lightwave technology* **13**, 1396-1406(1995).
2. D J Monk and D R Walt, "Optical fiber- based biosensor", *Anal Bioanal Chem* **379** ,931-945(2004).
3. P V Preejith, C S Lim, A Kishen, M S John and A Asundi , "Total protein measurement using a fiber optic evanescent wave based biosensor", *Biotechnology Lett.* **25**,105-110(2003).
4. G D Peng and P L Chu , "Polymer optical fiber photosensitivities and highly tunable fiber gratings" ,*Fiber and Integrated optics* **19**, 277-293(2000).
5. X Chen, K Zhou, L Zhang and Ian Bennion, "Optical chemsensor based on etched tilted Bragg grating structures in multimode fiber", *IEEE Phot.Tech. Lett.* **17**, 864-866 (2005).
6. J Zubia, G Garitaonandia and J Arrue, "Passive device based on plastic optical fibers to determine the indices of refraction of liquids", *Appl.Opt* **39**, 941-946 (2000).
7. R J Bartlett, R P Chandy, P Eldridge, D F Merchant, R Morgan and P J Scully, "Plastic optical fiber sensors and devices", *Transactions of the institute of measurement and control* **22**, 431-457(2000).
8. Mark G Kuzyk, *Polymer fiber optics-Materials,Physics and Applications*(Taylor &Francis group,2007).
9. B.P.Pal ed, *Fundamentals of fiber optics in telecommunication and sensor systems* (John Wiley& Sons,Newyork, 1992).
10. Anna Grazia Mignani and Andrea Azelio Mencaglia, "Direct and chemically- mediated absorption spectroscopy using optical fiber instrumentation", *IEEE Sensors journal* **2**,52-57 (2002).
11. R.Philip-chandy,PatriciaJ.Scully,PiersEldridge,H.J.kadim and M.Gerard Grapin "An optical fiber sensor for biofilm measurement using intensity modulation and image analysis", *IEEE Journal on selected topics in quantum electronics* **6**, 764-772 (2000).

12. J.Villatoro, D.Monzon-Hernandez and D.Talavera, "High resolution refractive index sensing with cladded multimode tapered optical fiber, *Electronic letters* **40**, 106-107(2004).
13. David Monzon-Hernandez, Joel Villatoro, and Donato Luna-Moreno, "Miniature optical fiber refractometer using cladded multimode tapered fiber tips", *Sensors and Actuators B* **110**, 36-40(2005).
14. A.Kumar,T.V.B.Subrahmanyam,A.D.Sharma,K.Thyagarajan,B.P.Pal and I.C.Goyal, "Novel refractometer using a tapered optical fiber ", *Electronics letters* **20**, 534-535(1984).
15. L.M.bali,Atul Srivastava,R.K.Shukla, and Anchal Srivastava "Optical sensor for determining adulteration in a liquid sample," *Optical engineering* **38**, 1715-1721(1999).
16. K.Cherif, S.hleli, A.Abdelghani, N.Jaffrezic-Renault and V.Matejee: "Chemical detection in liquid media with a refractometric sensor based on a multimode optical fiber", *Sensors* **2**,195-204 (2002).
17. Jan Turan, Edward F.Carome and L'ubos Ovsenik: "Fiber optic refractometer for liquid index of refraction measurements".*IEEE Proceedings of the 5th International conference on Telecommunications in Modern Satellite, Cable and Broadcasting Service, TELSIKS 2001* **2**, 489 – 492 (2001).
18. R M Ribeiro, J L canedo, M M Werneck and L R Kawase, "An evanescent-coupling plastic optical fiber refractometer and absorptionmeter based on surface light scattering", *Sensors and Actuators A :Physical* **101**, 69-76(2002).
19. Alberto, Alvarez-Herrero, Hector Guerrero, and David Levy, "High-sensitivity sensor of low relative humidity based on overlay on side-polished fibers", *IEEE Sensors journal* **4**, 52-56(2004).
20. Ssu-Pin Ma and Shaio-Min Tseng, " High performance side polished fibers and applications as liquid crystal clad fiber polarizers", *Journal of light wave technology* **15**,1554-1558 (1997).

21. Alberto Alvarez-Herrero, H Guerrero, T Belenguer and D. Levy, "High sensitivity temperature sensor based on overlay on side polished fibers", *IEEE photonics technology letters* **12**, 1043-1045(2000).
22. N K Sharma and B D Guptha "Fabrication and characterization of pH sensor based on side polished single mode optical fiber" *Opt. Communications* **216**, 299-303(2003).
23. W Johnstone, G Thursby, D Moodie, and K McCallion "Fiber optic refractometer that utilizes multimode waveguide overlay devices" *Opt.Lett* **17**, 1538-1540(1992).
24. D.G.Moodie and W.Johnstone, "Wavelength tunability of components based on the evanescent coupling from a side -polished fiber to a high – index- overlay waveguide", *Optics letters* **18**,1025-1028(1993).
25. R A Bergh, G Kotler and H J Shaw "Single mode fiber optic directional coupler", *Elec. Lett* **16**, 260-261(1980)
26. W V Sorin, K P Jackson and H J Shaw "Evanescent amplification in a single mode optical fiber" *Elec. Lett* **19**,820-822(1983).
27. C Miller, M Brierley and S Mallinson "Exposed-core single mode fiber channel dropping filter using a high index overlay waveguide" *Opt.Lett* **12**, 284-287(1987).
28. S.G.Lee, J.P.Sokoloff, B.P.McGinnis and H Sasabe, "Fabrication of a side polished fiber polarizer with a birefringent polymer overlay", *Optics letters* **22**,606-608 (1997).
29. B D MacCraith, "Enhanced evanescent wave sensors based on sol-gel derived porous glass coatings" *Sensors and Actuators B* **11**, 29-34(1993).

*General conclusions and  
future prospects*

*General conclusions and future prospects are discussed in this chapter.*

## **6.1 General conclusions**

Polymer optical fiber based systems are gaining much popularity due to their inherent advantages such as low weight, low processing temperature, economical viability, ease of fabrication and so on. It has got tremendous potential in automobile, space, aircraft and lighting industries along with short haul communication systems. Optical amplifiers operating in the visible communication spectrum is very much needed in short haul communication systems using polymer optical fibers. Polymer optical fiber based sensors have found wide range of applications because of their definite edge over their counterparts. The five chapters of this thesis discuss the fabrication and characterisation of polymer optical fibers for some photonic device applications.

Rh 6G and Rh B based dye mixture and single dye doped PMMA polymer optical fibers are fabricated successfully by the preform method using the fiber drawing station developed in our laboratory. Absorption and emission characteristics of these fibers are investigated. It is observed that there is a clear overlap between the shorter wavelength part of the emission band and the longer wavelength tail of the absorption band leading to the re-absorption of fluorescence emission by the dye molecules and re-emission at a longer wavelength. As a result of this, length dependent wavelength tunability is achieved in the dye doped POF system. Also there is an overlap between the Rh 6G emission and RhB absorption bands giving rise to both radiative and non-radiative (FRET) energy transfer from Rh 6G to Rh B in the Rh 6G-RhB dye mixture doped POF.



### ***Conclusion and future prospects***

---

A broad wavelength optical amplifier is successfully fabricated from Rh 6G: RhB dye mixture doped POF. An increased gain bandwidth of about 60 nm is obtained in dye mixture doped POF. Tunable operation of amplifier is achieved by mixing different ratio of dyes. The amplifier gain increases with pump energy and a tendency of gain saturation occurs at higher pump energies. There exists an optimum length for the amplifier at which the gain is maximum. It is observed that a relatively high gain of 22 dB can be achieved from a short length of dye doped POFA. This property has got a very high potential in making the amplifier unit very compact for application level designs. Also, the photostability of the dye doped POF is investigated and is found to be stable upto 180000 shots of pump pulse.

Multimode laser emission from a dye doped POF is observed when excited with 532 nm pulsed laser beam. When mixtures of laser dyes are used, wavelength tunability of these emissions is achieved by utilizing the energy transfer occurring between the dye molecules. At higher pump energies mode competition is also observed. The observed modes are attributed to the resonant modes of a number of serially connected micro-disc type cavities formed by the dye doped POF. A careful selection of laser dye concentration is done to suitably select the wavelength range required for these lasing modes. Length dependent wavelength tunability of the multimode laser emission is also achieved.

Two-photon excited fluorescence emission from dye doped POF is recorded using an 800 nm, 70 fs laser beam. One-photon and two-photon excited fluorescence spectra are exhibiting the same spectral behaviour. The excitation intensity dependence of the two photon fluorescence is investigated and found that it obeys the square law dependence. Position dependent wavelength tuning